Protein lipidation by a ubiquitin-like system is essential for autophagy

Yoshinobu Ichimura

Department of Molecular Biomechanics
Graduate Program in School of Life Science
The Graduate University for Advanced Studies

Contents

List of Figures and Tables

Summary

Autophagy is a dynamic membrane phenomenon for bulk protein degradation in the lysosome/vacuole. When cells face starvation conditions, the cytoplasmic components are nonselectively enclosed by a double-membrane structure, autophagosome and delivered to the lysosome/vacuole to be degraded (Fig. 1). Autophagy is ubiquitous in eukaryotes and is essential for survival during starvation and cell differentiation. However, the molecular basis of each process in autophagy is still poorly characterized. Taking advantage of yeast genetics, autophagy defective mutants (*apg*) have been isolated (Tsukada and Ohsumi, 1993), and so far 15 *APG* genes have been cloned.

Apg8 is the first molecule found to be localized to the intermediate structures of the autophagosome, and is necessary for autophagosome formation (Kirisako et al., 1999). Our recent studies revealed that the carboxy-terminal arginine of newly synthesized Apg8 is removed by Apg4 protease, leaving a glycine residue at the C terminus (Kirisako et al., 2000). This cleavage reaction is essential for production of tightly bound form of Apg8 to unidentified membrane. Interestingly, the membrane bound form of Apg8 is covalently conjugated to phosphatidylethanolamine (PE) through an amide bond between the C-terminal glycine and the amino group of phosphatidylethanolamine.

The biochemical analysis of the mechanism for Apg8-PE conjugation revealed that the Apg8-PE was formed by sequential enzyme reactions, similar to ubiquitination-like system. The C-terminal glycine of processed Apg8 (called as Apg8FG in this thesis) was activated in ATP dependent manner by Apg7 (E1 enzyme), and linked to a cysteine residue of Apg7 via a high-energy thioester bond. Through a transthioester reaction, Apg8FG conjugated with a novel identified E2 enzyme, Apg3. Finally, Apg8FG covalently conjugated with the PE. Notably, Apg7 is a unique E1-like enzyme, activates two different proteins, Apg12 and Apg8, and assigns them to specific E2 enzymes, Apg10 and Apg3, respectively.

The reactions of Apg8-PE conjugation system were reconstituted *in vitro* by purified Apg7, Apg3, Apg8FG, and PE only, under the presence of ATP. These *in vitro* reconstitution studies demonstrated that the PE content of membrane affects the

production of Apg8-PE. Apg8-PE conjugation of the *in vitro* reconstitution was enhanced by high amounts of Apg7 and Apg3. On the other hand, excessive Apg8FG inhibited their PE conjugation in a cell-free system. Apg8-PE conjugation directly occurs from Apg8-Apg3. However, some specific mechanisms seem to be required for the catalytic reactions in the system of Apg8-PE conjugation. The detailed mechanism of Apg8-PE conjugation step and its intracellular localization in yeast might be elucidated by the *in vitro* reconstitution study of Apg8-PE.

Ubiquitination and Ubiquitination-like system generally mediates a covalent conjugation of modifier to its target protein. However, the target of Apg8 turned out to be a PE. This thesis is the first report that ubiquitination-like system mediates protein lipidation.

Introduction

Protein degradation

Proteins are the principal constituents of cells and determine not only their structure but also their functions. Intracellular proteins are maintained in the living cells by the harmony both their synthesis and degradation. The synthesis from DNA to protein occurs at each second in every cell, by the flow of genetic information from DNA to RNA to protein. This transcription from DNA to RNA and translation from RNA to protein have been termed the central dogma of molecular biology. On the other hand, the field of protein degradation had many unsolved problems compared with protein synthesis. Two major pathways for degradation, ubiquitin-proteasome and autophagy, are well conserved among eukaryotes. These degradative pathways are particularly important during development and under certain environmentally stressed conditions. Newly synthesized proteins have a life span according to their role. For instance, within eukaryotes, the various regulatory factors related to progress of a cell cycle are short-lived proteins whose selective degradation is carried out by ubiquitin-proteasome at each stage of the cell cycle (Ciechanover, 1998) (Hochstrasser, 1996) (Hershko and Ciechanover, 1998). The ubiquitin-proteasome-dependent proteolytic system is needed also in the regulation of various cellular events such as signal transduction, transcriptional regulation, quality control of cellular proteins, immune responses, biogenesis of organelles and apoptosis. Generally, one function of ubiquitin-proteasome-dependent proteolytic system is to degrade those proteins whose lifetimes must be short. Another is to recognize and eliminate proteins that are damaged or misfolded. Living cells require supply of a large amount of amino acids for the protein synthesis. This amino acids pool is established by degradation of intracellular proteins more than the amino acid taken from external nutrients. The degradation of long-lived proteins is mainly performed by the lysosome/vacuole via autophagy (Klionsky and Ohsumi, 1999) (Klionsky and Emr, 2000). In addition, autophagy, the bulk degradation process is an only system for the turnover of organelles. Autophagy seems to be one of the most important systems for the life of cells under starvation conditions. Therefore, protein degradation is necessary for the normal development and viability of cells.

Ubiquitin-proteasome

The intracellular protein degradation is the work which requires careful control and strict specificity. The selectivity of protein degradation in prokaryotes is performed with ATP-dependent proteases (Goldberg, 1992) (Gottesman and Maurizi, 1992). The energy requirement of protein degradation in eukaryotes had been also reported in early studies, however, the observed manner of ATP-dependent proteolysis was obviously different mechanism from prokaryote's. Hershko, Ciechanover, and co-workers discovered ATP-dependent proteolysis factor, ubiquitin, and provided the conceptual framework for our current understanding of the mechanism on ubiquitin proteasome-dependent proteolytic pathway (Ciechanover et al., 1980) (Wilkinson et al., 1980).

Ubiquitin is a 76 amino acid protein that is highly conserved in eukaryotes, and it presents a degradation signal by carrying out a covalent attachment to a target protein (Hochstrasser, 1996) (Ciechanover, 1998) (Hershko and Ciechanover, 1998). Ubiquitination requires the sequential action of three enzymes. First, the C-terminal glycine residue of ubiquitin is activated in ATP dependence by a ubiquitin activating enzyme, E1. This step consists of an intermediate formation of ubiquitin adenylate, followed by the binding of ubiquitin to a cysteine residue of E1 in a thioester bond, with the liberation of AMP. Secondly, activated ubiquitin is transferred to an active site cysteine residue of a ubiquitin conjugating enzyme, E2 by transthioester reaction. Thirdly, the ubiquitin is catalyzed by a ubiquitin ligase, E3, and linked its C-terminus glycine in an isopeptide bond to an ε-amino group of lysine residue of the substrates.

Usually there is a single E1, but there are many species of E2s and multiple families of E3s or E3 multiprotein complexes. The E1 of *Saccharomyces cerevisiae*, Uba1 is found to be essential for cell viability, and its homologue is highly conserved in eyukaryotes, and their sequences possess GXGXXG motifs typically associated with nucleotide binding domains (McGrath et al., 1991). The active site cysteine is required for ubiquitin-E1 thioester formation, has been identified through analysis of point mutantation. The domains both adenylation and thioester formation occupy distinct place of the E1 sequences, although these sites might be very close in the protein-fold, since the adenylated ubiquitin attaches to the active cysteine residue of E1 enzyme.

At least 11 species of E2 can be found in the genome of *Saccharomyces cerevisiae* (Over 20 species of E2 are likely to be found in mammals.) (Haas and Siepmann, 1997). Some E2s have overlapping functions, whereas others have more specific roles. Because of the specific effects of mutations in some E2 genes, it was proposed that E2s might participate in the recognition of the substrates, either directly or in combination with an E3 enzyme. However, not much experimental evidence exists for the direct binding of E2s to their substrates. Specific function of some E2s may be the result of their association with specific E3s, which in turn bind their specific substrates. The number of E2s is assumed to be providing their substrate specificity with next E3s.

To date many E3 enzymes have been found (Kornitzer and Ciechanover, 2000). *In vivo* half-life test of a protein revealed that degraded protein was strongly dependent on the identity of its N-termunal residue, called the N-end rule (Varshavsky, 1996). The first discovered E3 (E3α) appeared the N-end rule for the recognition of substrate proteins, and further the N-end rule was found to be present in all eukaryotes (Bachmair et al., 1986) (Varshavsky, 1996). The N-end rule E3 (E3α), its yeast counterpart Ubr1 recognizes either basic (Arg, Lys, and His) or bulky hydrophobic N-terminal (Phe, Leu, Trp, Tyr, and Ile) residues of their substrates (Bartel et al., 1990). Additionally, when the substrates have Asn or Gln at the N-termini, their N-termini are converted to one of destabilized residue, Arg by N-terminal amidohydrolase and arginine transferase (Bachmair et al., 1986). Ubr1 associates with Ubc2, but not with ubiquitin. The function of Ubr1 is likely to facilitate the direct transfer of ubiquitin from Ubc2 to substrates. Whereas the N-end rule recognition mechanism is highly conserved among eukayotes, their rule seems not to be main pathway in ubiquitin-dependent degradation. Because, Ubr1 is not essential for the cell viability, and in some cases, Ubr1 also recognize non-N-end rule substrates.

E6-AP (E6-associated protein) was discovered from ubiquitin-dependent degradation of tumor suppressor, p53 (Huibregtse et al., 1991). The oncoprotein, E6 from papillomavirus associates with p53 and linked to the ligase, E6-AP. Then, ubiquitin is transferred from E2 to E6-AP and subsequently ligated to p53. In contrast to E3α, E6-AP does not bind directly to the substrate (p53) but rather binds indirectly via E6. The C-terminal E6-AP showed similar sequences in several species of E3 and

was named HECT (homologous to E6-AP C-terminus) domain (Huibregtse et al., 1995). Since the HECT domain contains the ubiquitin binding cysteine residue, ubiquitin is transferred from an appropriate E2 to the HECT E3 enzyme via transthioester reaction (Scheffner et al., 1995). The HECT proteins recognize a substrate via associated protein (AP) and transfer ubiquitin to the substrate. Several HECT proteins have now been appeared to be E3s, such as Nedd4, Rsp5, Tom1, Ufd4, Pub1, Smuf1, Smuf2.

In other case, since E3 enzymes tightly bind cognate E2s and they also directly bind their appropriate substrates, ubiquitin can be transferred directly from E2s to their substrates. One of such E3 complexes, cyclosome/APC (anaphase promoting complex) has a ubiquitin ligase activity specific for cell-cycle regulators that contains a nine amino acids motif designated as destruction box and are degraded by ubiquitination during mitosis (Irniger et al., 1995) (King et al., 1995) (Sudakin et al., 1995) (Yamano et al., 1996). Its substrates are mitotic cyclins, some anaphase inhibitors, and spindle-associated proteins, all of which are degraded at the end of mitosis. The APC is a complex composed of at least eight proteins, which are not part of the core complex conferring further substrate specificity and regulation to the complex. Phosphorylation also appears to play a role in regulation of this complex (Shteinberg et al., 1999). For example, the MPF (M-phase promoting factor) complex is consisted with cyclin-B/cyclin-dependent kinase and activated at the start of M-phase by dephosphorylation mediated by Cdc25 phosphatase. At the end of mitosis, the cyclin B and securin are ligated to ubiquitin via cyclosome/APC and followed degradation by proteasome (Hershko, 1999).

Another multi subunit ubiquitin ligase regulates the G1/S phase. Here, phosphorylated substrates are converted to susceptible form for binding ligase complex. Several such ligase complexes are designated as SCFs (Skp1-Cdc53/Cullin-F-box protein ligase complexes) (Feldman et al., 1997) (Skowyra et al., 1997) (Michel and Xiong, 1998). The F-box motif is present in a variety of proteins that binds to Skp1. The ubiquitin conjugated E2, Cdc34 (Ubc3) associates with Cdc53 of SCF, then the ubiquitin is transferred directly from E2 to various phosphorylated F-box substrates on Skp1. Hence, Skp1 plays a role for the adapter to bind to specific substrates.

Recent studies of SCF ligase revealed that the SCFs function with Rbx1/Roc1/Hrt1 (Kamura et al., 1999) (Skowyra et al., 1999) (Ohta et al., 1999) (Tan et

al., 1999). Indeed, Rbx1 linked between E2, Cdc34 and SCFs. The Rbx1/Roc1/Hrt1 contains RING finger motif, which has been defined by consensus sequence of zinc binding residues (Saurin et al., 1996). The previous N-end rule E3 (E3α), Ubr1 and cyclosome/APC component, Apc11 also include RING finger motifs (Kwon et al., 1998). Therefore, the distinct two motifs of E3s present two major groups, Hect and RING finger families. The cyclin-dependent kinase inhibitor, Sic1, G1 cyclins, other cell cycle regulators, and proteins involved in transcriptional regulation are targets for the Rbx1 containing SCFs. The Rbx1 has been also found in the CBC (Rbx1/Cul2/Elongins C and B/SOCS box proteins) complex. The SOCS-box is an analogous to F-box, and its family includes the von Hippel Lindau (VHL) tumor suppressor protein in mammals (Kamura et al., 1998) (Kamizono et al., 2001). VHL mutations prevent the assembly between this E3 and substrates, and lead to malignacies of VHL disease. Other member of RING finger E3, Mdm2 binds p53 through its N terminus region and catalyzes the ubiquitination of p53 by itself not a complex. The number of candidate E3s of ubiquitin has now increased dramatically.

After the linkage of ubiquitin to the substrate protein, a polyubiquitin chain is usually formed, in which the C-terminus glycine of each ubiquitin is linked to a specific lysine residue (commonly Lys48) of the previous ubiquitin (Hochstrasser, 1996) (Ciechanover, 1998) (Hershko and Ciechanover, 1998). The polyubiquitinated proteins are degradated by a 26S proteasome discovered by Rechsteiner and co-workers (Rechsteiner et al., 1993) (Pickart, 1997). The 26S proteasome is composed of the 20S core catalytic complex flanked on both sides by the 19S regulatory complexes/PA700. An important advance in studies of the 26S complex has been the resolution of the crystal structure of the yeast 20S complex at 2.4 Å (Groll et al., 1997). This 20S complex is demonstrated as a stack of four rings, each containing seven different subunits organized as $\alpha_{1\text{-}7}\beta_{1\text{-}7}\beta_{1\text{-}7}\alpha_{1\text{-}7}$. Topological analysis of the location of the subunits has revealed three distinct proteolytic activities: trypsin-like, chymotrypsin-like and post-glutamyl peptidyl hydrolytic-like activities (Baumeister et al., 1998) (Kisselev et al., 1999). The active sites are generated by adjacent pairs of identical β-type subunits residing in different β rings. The crystal structure has also revealed that the catalytically inactive α rings play an essential role in stabilizing the two ring structures of the β subunits. The α rings also act for the binding of the 19S regulatory complexes.

Polyubiquitinated proteins recognition by the 26S proteasome seems to be mediated by the interaction of specific ubiquitin receptor of the 19S complexes. Then, subunits of 19S complexes include ATPase which play unfolding and translocation into 20S catalytic subunit for the substrate proteins in ATP dependence. Hence, the energy consumption in ubiquitin-proteasome system is explained at two steps, the activation by E1 (selection step of substrates) and the translocation of their targets into the proteasome (recognition step of substrates).

In an additional step of ubiquitin pathway, there is a cleavage reaction by de-ubiquitinating enzyme (Dub) (Hochstrasser, 1996) (Ciechanover, 1998) (Hershko and Ciechanover, 1998). Dubs are classified into two types, ubiquitin C-terminal hydrolases (Uchs) and ubiquitin specific proteases (Ubps). They release ubiquitin from lysine residue of target proteins, which are degradation products, disassembled polyubiquitin chains, and mistaken ubiquitinated proteins. Newly synthesized ubiquitin also requires Dubs, because they are synthesized as head to tail linear polyubiquitin chains and ubiquitin-ribosome ligated complexes. These Dub processes are essential for the recycling system of ubiquitin in principle.

Notably, recent studies have revealed that several post-translational modifications in eukaryotes are ubiquitination-like reaction (described below).

Autophagy

The lysosome/vacuole is a major degradative organelle in eukaryotic cells. This compartment contains various hydrolases that become active forms in acidic pH and so an acidic environment inside the lysosome/vacuole is maintained by the lysosomal/vacuolar membrane H^+-ATPase (Nakamura et al., 1997). The primary route of bulk protein degradation to the lysosome/vacuole is known to be autophagy (Kopitz et al., 1990). Autophagy mainly carries out the degradation of long-lived proteins and in some case turnover of organelles such as mitochondria. In order to recruit degradation substrates from the cytosol to the lysosome/vacuole, this system requires the membrane sequestration of cytosol and machinery for the membranous docking and fusion (Fig. 1) (Klionsky and Ohsumi, 1999) (Klionsky and Emr, 2000) (Kim and Klionsky, 2000). Early studies involving autophagy have been developed in mammalian cells (Schworer and Mortimore, 1979). Autophagy is generally induced

by starvation conditions in mammals such as depletion of serum or amino acids. Ohsumi and co-workers have also discovered the induction of autophagy in yeast cells during nutrient starvation (Takeshige et al., 1992). Now, autophagy system seems to be essentially same in all eukaryotes (Klionsky and Ohsumi, 1999) (Klionsky and Emr, 2000) (Kim and Klionsky, 2000). Autophagic process in yeast was shown as follows, cytoplasmic components are enclosed by double (or sometimes multiple in mammalian cells) membrane structure called autophagosome, and the autophagosome directed to the vacuole/lysosome (Takeshige et al., 1992) (Baba et al., 1994). Upon the fusion between outer membrane of the autophagosome and vacuolar membrane, the inner single membrane of autophagosome called autophagic body is released into the vacuolar lumen (Takeshige et al., 1992) (Baba et al., 1994). Consequently, the cytoplasmic components derived from the autophagosome are degraded by lysosomal/vacuolar proteases. This autophagic process sometimes referred to macroautophagy. Different types of autophagy, microautophagy and chaperon-mediated autophagy are known. Microautophagy is a process of incorporation of cytoplasmic components by invagination of the lysosomal/vacuolar membrane. Chaperon-mediated autophagy appears to be directly transport via Hsc73 chaperon and Lamp2-a receptor on the lysosome membrane (Cuervo and Dice, 1996) (Agarraberes et al., 1997). Macroautophagy is distinct from other autophagy in the aspect of membrane topology. The progress of macroautophagy studies in yeast, *Saccharomyces cerevisiae*, have provided us some understanding molecular mechanisms of autophagy process. Using morphologic and genetic methods in yeast, Ohsumi and co-workers in our laboratory first isolated autophagy defective mutants (*apg*) (Tsukada and Ohsumi, 1993). The autophagic process with vacuolar proteinase deficient cells can be easily monitored by light microscope, for the accumulation of autophagic bodies in the vacuole. Autophagy mutant, *apg1* was initially isolated by using this strategy, lacking the accumulation of autophagic bodies inside the vacuole. The *apg1* cells had normal vacuolar proteinases, but still their vacuolar bulk protein degradation was not under starvation conditions. Notably, the loss of viability of *apg1* cells was faster than wild-type during starvation conditions. By using the loss of viability as a first screening, 15 groups of *apg* mutant (*apg1~apg15*) were isolated. Their common phenotypes have been reported as follows. 1) *apg* mutants do not accumulate autophagic bodies in their

vacuole in the presence of vacuolar protease inhibitor (PMSF) under starvation conditions. 2) *apg* mutants show a defect in bulk protein degradation in the vacuole during starvation. 3) Homozygous diploids with *apg* mutation do not sporulate. 4) *apg* mutants lose the viability in starvation. In further studies, *APG16* and *APG17* were isolated by genetical interaction with *APG12* and *APG1* respectively (Mizushima et al., 1999) (Kamada et al., 2000). Among of isolated *apg* mutants, *apg7* and *apg11*, or *apg16* and *apg15* were confirmed as the mutants in the identical gene. Thus, so far our laboratory member has identified 15 *apg* loci, and further originally has cloned all *APG* genes. Cloned *APG* genes were novel genes except *APG6* or *APG2* which was allelic to *VPS30* or *SPO72* (Kametaka et al., 1998) (Shintani et al., 2001). Another group, Thumm and co-workers have also isolated autophagy deficient cells (*aut*) (Thumm et al., 1994). Fatty acid synthase is a cytoplasmic enzyme, is usually degraded inside the vacuole via autophagy (Thumm et al., 1994) (Egner et al., 1993). Taking advantage of this physiological phenomenon, a group of *aut* mutants were isolated by colony immunoblot screening with anti-fatty acid syntase antibody. Genetic analysis and yeast genome database has revealed that several *apgs* are identical to the *auts* (Table 1). The analysis of identified Apg molecules has revealed many molecular mechanisms of autophagy.

Rapamycin, an antifungal antibiotic, inhibits a Tor (phosphatidylinositol kinase-related kinase), and induces a starvation response of yeast cells even under nutrient rich conditions (Noda and Ohsumi, 1998). Initial step of autophagy seems to be negatively regulated by Tor-kinase, because administration of rapamycin also stimulates autophagy in yeast. It has appeared that the association of Apg1-Apg13 depending on starvation signal or rapamycin treatment promotes the autophagy (Matsuura et al., 1997) (Funakoshi et al., 1997) (Kamada et al., 2000) (Klionsky and Emr, 2000) (Stromhaug and Klionsky, 2001). Apg13 is hyperphosphorylated in vegetative conditions, but not in starvation. Apg1 is a serine-threonine kinase, binds to de-phosphorylated Apg13, and the interaction enhances kinase activity of Apg1. High activity of Apg1 kinase has been previously reported essential for autophagy. The target of Apg1 kinase should be an important molecule, but it has been not still identified. Importantly, Apg1 kinase also interacts with two other proteins, Apg17 and Cvt9. Apg17 is required for autophagy, but not for the cytoplasm-to-vacuole targeting

(Cvt) pathway that is used to deliver the resident hydrolase aminopeptidase I (API) under vegetative conditions (described below). In contrast, Cvt9 is required for the Cvt pathway, but not for autophagy. *Saccharomyces cerevisiae* switches between autophagy and the Cvt pathway depending on nutrient conditions. Apg1 kinase complexes will play a role in this regulatory switch.

Morphological studies in mammalian cells have proposed that the membranes of autophagosome were originated from ribosome-free regions of the rough ER, or post-Golgi membrane (Dunn, 1990a) (Dunn, 1990b) (Yamamoto et al., 1990). However, the origin of autophagosome membrane is unclear. Freeze replica electron micrographs of autophagosome in yeast revealed that the density of intramembrane particles is extremely low in this membrane and the inner membrane is especially lacking them (Baba et al., 1994). These observations indicate a specific feature of autophagosome double membranes, different from other organelle membrane, such as vacuole, nucleus, mitochondrion, rough ER and plasma membrane. Apg8 is the first molecule identified as localized on autophagosome membrane and intermediate structure of autophagosome (Kirisako et al., 1999). The immuno electron microscopic observation of Apg8 suggested that the Apg8 participates in autophagosome formation. The amount of Apg8 significantly increased by starvation conditions or rapamycin treatment. These observations indicate that Apg8 plays as a key molecule of autophagosome formation. Apg12 and Apg5 are also involved in autophagosome formation process (Mizushima et al., 2001). Apg12 is post-translationally modificated by Apg5 with covalent bond (Mizushima et al., 1998a) (Mizushima et al., 1998b) (Ohsumi, 2001). This modification resembles to the ubiquitination conjugation system which depending on Apg7 (E1) and Apg10 (E2) (described below section). Recent morphological analysis using green fluorescent protein tagged Apg5 in mammalian autophagy revealed that the cup-shaped isolation membrane is developed from a small crescent-shaped compartment through elongation process in Apg12-Apg5 conjugation dependence (Mizushima et al., 2001). This result indicated that autophagosome membrane is maturated from the small compartment, not simply derived from large preexisting organelle membranes. The Apg5 localizes on isolation membrane (precursor of autophagosome), and then the conjugate of Apg12-Apg5 is required for the elongation of the isolation membrane. In addition, analysis of yeast autophagy

showed that Apg16 interacts with Apg12-Apg5 conjugate, forms a homo-oligomer, and results in Apg12-Apg5-Apg16 multi-complexes (Mizushima et al., 1999). The Apg16 will be essential for the function of Apg12-Apg5 conjugate in autophagy.

Other Apgs will be also required for autophagosome formation in the initial or late step. Apg6 is identical to Vps30 involved in vacuolar protein sorting. Therefore, the *apg6* mutants show the defect of both autophagy and sorting of CPY (carboxypeptidase Y) (Kametaka et al., 1998). Apg6/Vps30 interacts with Apg14, in which further forms a complex with both Vps34, a phosphatidylinositol 3-kinase, and Vps15, an activator of Vps34 (Kihara et al., 2001a) (Kihara et al., 2001b) (Stromhaug and Klionsky, 2001). The phosphorylation of Vps34 is mediated by Vps15 depending on the Apg6-Apg14 complex. These complexes, Vps34-Vps15-Apg6-Apg14 functions in autophagy. On the other hand, another complexes, Vps34-Vps15-Apg6-Vps38 is known to be essential for CPY sorting. Apg2 co-localizes with Apg8, that structure is a dot-like and exists close to vacuole (Shintani et al., 2001). The punctate structure of Apg2 depends on Apg1, Apg6-Apg14 phosphatidylinositol 3-kinase complex, and Apg9, but not Apg8. Apg9 is a putative integral membrane protein, and localizes on perivacuolar membrane compartment (Noda et al., 2000). Recent findings suggest that Apg2 localizes to the Apg9 compartment (Wang et al., 2001).

The cytoplasm to vacuole targeting (Cvt) pathway

The cytoplasm to vacuole targeting (Cvt) pathway is a selective transport for aminopeptidase I (API), and occurs constitutively in *Saccharomyces cerevisiae*. D.J. Klionsky and co-workers initially isolated the complementation genes of *cvt* mutants (Harding et al., 1995) (Klionsky and Ohsumi, 1999). Some of the *CVT* overlaps to *APG* (see Table. 1). API is synthesized as precursor form in the cytosol, after which the precursor API assembles to an oligomer (Kim et al., 1997). The oligomerized API further forms a homododecamer, and they are specifically enwrapped by the Cvt vesicle, and delivered to the vacuole (Fig. 1). Consequently, the precursor API is processed to the mature form by the removal of its N-terminal propeptide region depending on vacuolar proteinase B. The morphological studies of the Cvt pathway using electron microscopy showed that the Cvt complex is enclosed by autophagosome-like membrane, and the Cvt body inside the vacuole was detected in vacuolar proteinase deficient cells.

The membrane topology between autophagosome and the Cvt vesicles is quite similar, although they are made in different sizes. The size of autophagosome is 300-900 nm, whereas that of the Cvt vesicle is 140-160nm (Baba et al., 1997). Under starvation conditions, since the Cvt complex is enriched in the autophagosome, the autophagy carries out the transport of precursor API. Most of *APG* genes are also required for the Cvt pathway (Scott et al., 1996). This substantial genetic overlap between autophagy and the Cvt pathway suggests a mechanistic similarity between them.

Ubiquitination-like system

Recently, several ubiquitin-like proteins (Ubls) are discovered, such as SUMO-1/Smt3, NEDD8/Rub1 and Urm1 (Hochstrasser, 2000) (Yeh et al., 2000). Their protein modification mechanism is similar to ubiquitination system. SUMO (small ubiquitin-related modifier) conjugation system is known to catalyze modification of a few substrates (Kretz-Remy and Tanguay, 1999). The nucleocytoplasmic transport protein, RanGAP1 localizes to nuclear-pore complexes depending on SUMO-modification, which is required for its nuclear import activity. In other case, SUMO-modification blocks ubiquitination and degradation of the inflammatory response regulatory protein, IκBα by being attachment at its major ubiquitination site. The set of known substrates for SUMO-modification includes proteins participating in transcriptional regulation, signal transduction, inflamation, and control of cell growth. Smt3 is a yeast homolog of SUMO. Smt3 is activated by Uba2-Aos1 heterodimer (E1-like), and after transferred to Ubc9 (E2-like), then linked to substrates in a manner analogous to ubiquitination (Johnson et al., 1997) (Johnson and Blobel, 1997). There are also specific proteases Ulp1 and Ulp2/Smt4 (Dub-like) that cleave Smt3-substrate isopeptide bonds (Takahashi et al., 2000) (Li and Hochstrasser, 2000). NEDD8 (neural precursor cell expressed development down-regulation gene 8) and its yeast homolog Rub1 modify a cullin family via ubiquitination-like pathway with Uba3-Ula1 (E1-like), Ubc12 (E2-like), and whose modification results in activation of ubiquitin ligases, SCFs (Osaka et al., 1998) (Gong and Yeh, 1999). More recently, Urm1 (ubiquitin-related modifier) is discovered (Furukawa et al., 2000). Urm1 requires a Uba4 (E1-like) for the activation, and then covalently attached to an unidentified target protein. A number of ubiquitin-like proteins are highly conserved among eukaryotic

cells.

Mizushima et al. discovered a protein conjugation system that is essential for autophagy (Mizushima et al., 1998a). Apg12 is post-translationally modificated by Apg5 with covalent bond. This modification resembles to the ubiquitination system. The modifier, Apg12 is activated by Apg7, an activating enzyme (E1-like) depending on ATP (Tanida et al., 1999). The activated Apg12 is transferred from Apg7 to Apg10, conjugating enzyme (E2-like) (Shintani et al., 1999). Finally, the C-terminal glycine of Apg12 is conjugated to a lysine residue of Apg5 via an amide bond. Interestingly, Apg12 has no significant homology to ubiquitin and has a single ending glycine residue at the C-terminus.

Analysis of autophagy

As previous described, a lot of questions have been still remained regarding autophagy. Autophagosome formation demonstrates a dynamic membrane movement such as membrane expansion, sequestering of cytoplasmic components, and fusion to the vacuole. How do Apgs carry out those steps? Further, what is the origin of autophagosome membrane? In my study, I started to characterize Apg3, of which function is unknown. As a result, I found novel mechanism of protein lipidation involving Apg8 and Apg7, Apg3. This mechanism resembles with a ubiquitination-like system. Apg8 is modified with phosphatidylethanolamine in a totally different manner from the other lipidation.

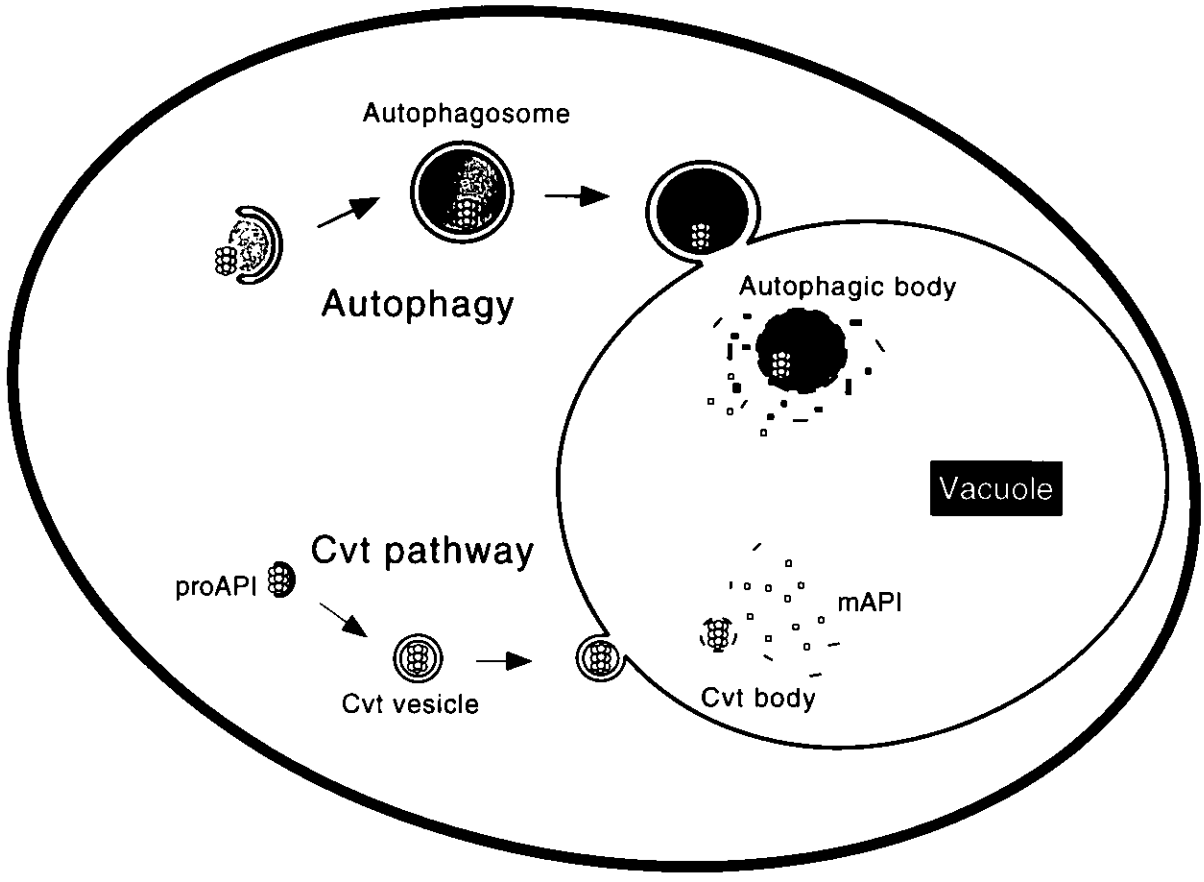

Figure 1. Membrane dynamics in autophagy and the Cvt pathway. prAPI; Precursor form of aminopeptidase I, mAPI; Mature form of aminopeptidase I.

ORF No.	*APG*	*CVT*	*AUT*
YGL180w	1	10	3
YNL242w	2		8
YNR007c	3		1
YNL223w	4		2
YPL149w	5		
YPL120w	6		
YHR171w	7	2	
YBL078c	8	5	7
YDL149w	9	7	9
YLL042c	10		
YBR217c	12		
YPR185w	13		
YBR128c	14	12	
YMR159c	16	11	
YLR423c	17		

Table. 1 Genetic overlap of *APG* and *CVT*.

Abbreviations

ADH, alcohol dehydrogenase

ALP, alkaline phosphatase

API, aminopeptidase I

BSA, bovine serum albumin

CBB, coomassie brilliant blue

Cvt, cytoplasm to vacuole targeting pathway

DOPE, dioleoylphosphatidylethanolamine

DTT, dithiothreitol

DUB, deubiquitinating enzyme

EDTA, ethylenediamine tetraacetic acid

ER, endoplasmic reticulum

GST, glutathione S-transferase

HA, hemagglutinin

HSP, high speed pellet

HSS, high speed supernatant

IPTG, isopropylthio-β-D-galactopyranoside

LSP, low speed pellet

mAPI, mature form of API

ORF, open reading frame

PAGE, polyacrylamine gel electrophoresis

PBS, phosphate-buffered saline

PCR, polymerase chain reaction

PE, phosphatidylethanolamine

PMSF, phenylmethylsulfonylfluoride

POPC, 1-palmitoyl-2-oleoylphoshatidylcholine

PrAPI, precursor form of API

SD, synthetic dextrose medium

SDS, sodium dodecyl sulfate

STRE, stress response elements

TBS Tris-buffered saline

TCA, trichloroacetic acid

Material and Methods

Strains media and standard molecular genetical methods

The strains used in this study are listed in Table 2. *Eschericia coli* strain, XL1Blue was used as a host for the various plasmids. All recombinant proteins were expressed in XL1Blue. Cell-free system and liposome preparation were performed by XL1Blue, W3110, and GN10 (*ΔpssA10:: cm*^{r} derivative of W3110). *E. coli* cells were grown in Luria-Bertani broth (LB) at 37℃. Transformant of *E. coli* was grown in LB supplemented appropriate antibiotics (ampicillin (Amp) (50 μg/ml), chloramphenicol (Cm) (25 μg/ml)). PE-deficient strain, GN10 was grown in LB containing 50 mM $MgCl_2$ at 37℃. W3011 was a gift from Dr. Hidaka (NIBB). GN10 was a gift from Dr. Matsumoto (Saitama Univ.) (Kikuchi et al., 2000).

Saccharomyces cerevisiae, YW5-1B and SEY6210 were used as hosts for the various plasmids. For the cloning of *APG3* gene, MT38-4-3 was used (Tsukada and Ohsumi, 1993). ALP assay was performed with Tn125 and Tn125Δ*apg3*. Strain, Δ*apg3* was constructed in this study as described below. Yeast cells were grown in YEPD (1% yeast extract, 2% polypepton, 2% glucose), or SD (0.67% yeast nitrogen base without amino acids and ammonium sulfate, 0.5% ammmonium sulfate, 2% glucose and appropriate amino acids) at 30℃. SD(-N) (0.67% yeast nitrogen base without amino acids and ammonium sulfate, 2% glucose) was used for the nitrogen starvation culture. 2% Bacto agar was added to each solid medium.

Molecular biological methods generally followed standard procedures (Rose et al., 1990).

Cloning of the *APG3* gene

The *APG3* gene was cloned by complementation of the loss of viability of *apg3* mutant under nitrogen starvation conditions. The *apg3* mutant, MT38-4-3 (*MAT***a** *ura3 leu2 apg3-1*) was transformed with yeast genomic library based on centromeric vector YCp50. Resulted transformants were replica-plated onto SD(-N) plates containing phloxine B (20 μg/ml) and incubated for 2 days at 30℃. These plates showed the stained red and white colonies, in which red colony indicated dead cells. White colonies were selected and their complemented phenotype was checked by

morphological change of vacuoles during autophagy, as described in below section (Assay of autophagy). The plasmid (YcpApg3) was rescued from the candidates. Subsequently, inserted ORF (*No. YNR007C*) to cloning site on Ycp50 was determined as *APG3*. Subcloning Apg3 was performed as following, an HpaI-SalI fragment (3 kb) from YCpApg3 was introduced into SmaI-SalI site of pRS series plasmid (pRS–Apg3) and pBlueScript II KS$^-$ plasmid (pBSApg3). To construct the *APG3* gene disruption plasmids (pAPG3::TRP1, pAPG3::LEU2), BglII-PstI region into *APG3* ORF on pBS-Apg3 was replaced with *LEU2* and *TRP1* gene from pJJ282, pJJ252 respectively.

Construction of plasmids

C-terminal 3x Myc tagged Apg7 plasmids, pYO324Apg7-Myc and pYO324Apg7G333A-Myc (Gly333 in Apg7 replaced by arginine) were gifted from Dr. Tanida (Tanida et al., 1999). The *APG7-MYC* and *APG7G333A-MYC* were cloned into BamHI site either in pRS424 or in pRS314. Apg7G333A contains single amino acid substitution from Gly333 to Ala333 at the ATP binding site on Apg7. pRS424 (or 314) Apg7C507S-Myc plasmid, which contains site replacement from Cys507 to Ser507 at the active center on Apg7, was constructed by using QuikChange site-directed mutagenesis kit (Stratagene) and following mutagenesis oligonucleotides; (*APG7C507S*) Fw, 5'ACTTTGGATCAAATGTCGACAGTAACTAGACC-3', Rv, 5'-GGGTCTAGTTACTGTCGACATTTGATCCAAAGT-3'. pRS425 (or 315) Apg3C234S or pRS425 (or 315) Apg3C234A plasmids, which contains single amino acid substitution from Cys to Ser or Ala at the active center on Apg3, was constructed by using QuikChange site-directed mutagenesis kit (Stratagene) and following mutagenesis oligonucleotides; (*APG3C234A*) Fw, 5'-GTTTCCATTCATTCATCCAGCTAAGCATGCATGCTAATGT A-3', Rv, 5'-TACATTAGCATGCTTAGCTGGATGAATGGAAAC-3'. (*APG3C234S*) Fw, 5'-GTTTCCATTCATCCAAGCAAGCATGCTAATGTA-3', Rv, 5'-TACATTA GCATGCTTGCTTGGATGAATGGAAAC-3'. N-terminal 3x HA tagged Apg8 plasmid (pRS426-HA-Apg8), its C-terminal amino acid deletion series (-HA-Apg8FG and -HA-Apg8F), and N-terminal 3x Myc tagged Apg8 plasmid (pRS426-Myc-Apg8) were gifted by Kirisako (Kirisako et al., 2000). C-terminal 3x HA tagged Apg10 plasmid (pRS425-Apg10-HA) was gifted by Shintani (Shintani et al., 1999). N-

terminal 3x Myc tagged Apg12 plasmid (pRS426-Myc-Apg12) was gifted by Mizushima (Mizushima et al., 1998). For the construction of expressing vector of Apg7-Myc, Apg3, and Apg8FG in *E. coli*, each gene was amplified by PCR and introduced into pUC18 and pBAD plasmids (pBAD18 and pBAD33). PCR was performed with using following primer; (*APG7-MYC*) KpnI-SD(Fw), 5'-GGGGTACC CCAGGAGGAATTCACCATG TCGTCAGA-3', SmaI(Rv), 5'-TCCCCCGGGGGAA TGCAAAATATTA-3', (*APG3*) SmaISD(Fw), 5'-TCCCCCGGGGGAAGGAGGAAT TCACCATGTTAGATC-3', BamHI(Rv), 5'-CGGGATCCCGTTACCAACCTTCC-3', (*APG8FG*) BglII-SD(Fw), 5'-GAAGATCTTCAGGAGGAATTCACCATGAAGTCTA C-3', XbaI(Rv), 5'-GCTCTAGAGCCTAGCCAAATGTATTTTC-3'. The resulting PCR products contain a Shine-Dalgarno sequence (SD) upstream of start codon so as to be translated. Each fragment was subcloned into pUC18, and then used for insertion to multi cloning sites on arabinose inducible plasmids, pBAD18 or pBAD33. pBAD18 encodes P_{BAD} promoter, AraC, Amp^r (ampicillin resistance), and pBR origin. pBAD33 encodes P_{BAD} promoter, AraC, Cm^r (chloramphenicol resistance), and pACYC origin. pBAD33 was gifted by Dr. Yasuda (Nat. Ins. Genetics). General molecular biological techniques were done in accordance with standard procedures (Sambrook et al., 1989).

Disruption of *APG3*

The deletion of chromosomal *APG3* was done by homologous recombination. Disruption vector (pAPG3::TRP1 or pAPG3::LEU2) was digested with KpnI/SacI or BamHI/NcoI, and resulting fragments (1.8 or 2.5 kb) were transformed into YW5-1B, SEY6210, and Tn125. The deletion of *APG3* in transformed cells was confirmed with genomic PCR and immunoblot using anti-Apg3 antibody.

Preparation of cell lysates and subcellular fractionation

Yeast cell lysates were prepared according to the previously reported methods as follows, alkali lysis, osmotic lysis, or glass beads disruption (Rose et al., 1990). For the alkaline lysis, cells were suspended in alkaline solution (0.2 N NaOH, 0.5% 2-mercaptoethanol) at 5.0 OD_{600} unit per 100 μl, and incubated on ice for 5 min. Resultant proteins were precipitated with cold acetone, and collected by centrifugation

at 15,000 rpm for 10 min at 4℃. The precipitate was washed twice with cold acetone, and suspended in SDS-PAGE sample buffer (50 mM Tris-HCl, pH 6.8, 2% SDS, 10% glycerol, 0.002% bromophenol blue, and 100 mM DTT) (5.0 OD_{600} unit/ 100 μl). SDS-PAGE sample was boiled for 5 min and subjected to immunoblot.

Subcellular fractionation of yeast lysate was performed by spheroplasts lysis. Yeast cells were grown in YEPD until OD_{600} =1.0. Starved cells were shifted to SD(-N), then further grown for 4.5 h. Harvested cells were suspended in 0.1 M Tris-HCl, pH 9.0, 40 mM 2-mercaptoethanol at room temperature for 5 min. The cells were harvested, and converted to spheroplasts by incubation for 30 min in medium containing 50 mM Tris-HCl, pH 7.5, 1.2 M sorbitol, and Zymolyase 200T (10 U/ml). The spheroplasts were collected by centrifugation at 2000 rpm for 5 min at 4℃, and washed with 1.2 M sorbitol. Spheroplasts were suspended in lysis buffer (0.2 M sorbitol, 20 mM 1,4-piperazinediethanesulfonic acid (PIPES)-KOH, pH 6.8, 1 mM phenylmethylsulfonyl fluoride (PMSF), and protease inhibitor cocktail (Roche Molecular Biochemical)) and lysed osmotically on ice for 5 min. To remove the debris, the lysate was centrifuged by 2,000 rpm for 5 min at 4℃. Resulting lysate (Total) was fractionated by centrifugation at 13 k *g* for 15 min (LSP, LSS). The supernatant (LSS) was recentrifuged at 100 k *g* for 1 h at 4℃ (HSP, HSS). Each fraction was subjected to SDS-PAGE and analyzed by immunoblotting.

Glass beads disruption of yeast cells was used usually for immunoprecipitation experiments and in ALP assay as described below section.

E. coli cells were suspended in lysis buffer (50 mM Tris-HCl, pH 7.5, 150 mM NaCl, 5 mM EDTA, 1 mM PMSF, protease inhibitor cocktail) at 1.0 OD_{600} unit per 100 μl, and sonicated for 6 times with interval for 30 sec on ice. Unbroken cells and debris were removed by centrifugation at 5,000 rpm for 5 min. Resulted lysate (Total) was separated by centrifugation at 100 k *g* for 1 h, to the simple fractionation (P100 and S100). Obtained lysate was suspended in SDS-PAGE sample buffer and boiled for 5 min. SDS-PAGE sample was subjected to SDS-PAGE, and analyzed by immunoblotting.

Antibodies and immunoblotting

For preparation of polyclonal antibodies against Apg3, coding region of *APG3*

(933 bp) was amplified by PCR. The amplified full-length *APG3* fragments were inserted to pQE9 (Qiagen) (pQE-Apg3). Plasmid, pQE-Apg3 was introduced to *E. coli*, XL1-Blue, and then recombinant Apg3 was induced by 0.5 mM IPTG (isopropylthio-β-galactoside). For the purification of recombinant Apg3, expressed Apg3 was subjected to SDS-PAGE and stained by 0.025% CBB (Coomassie Brilliant Blue G-250) in 50% methanol. Then, 36 kDa band of Apg3 appeared on SDS-PAGE gel. The Apg3 band was excised, and its containing Apg3 eluted to the elution buffer (100 mM Tris-HCl, pH 6.8, 0.05% SDS) by gentry shaking at 4℃ for 12 h. The purified Apg3 was used for immunization of rabbit by Shibayagi Co., and anti-Apg3 antibody was obtained.

Anti-Apg8 peptide antibody was generated by synthetic 14 amino acid peptide. The synthesized peptide including N-terminal sequence of Apg8, MKSTFKSEYPFEHC, was immunized to a rabbit by Shibayagi Co., and anti-Apg8 peptide antibody was obtained (Kirisako et al., 1999).

In this study, I also used other primary antibodies as follows; anti-Apg1, anti-Apg6, anti-Apg9, anti-Apg12, anti-ADH, anti-ALP, anti-Kex2, anti-Myc, anti-HA, and anti-API antibodies. Anti-Myc (9E10) and anti-HA (16B12) antibodies were purchased from Babco. Anti-API antibody was a gift from D.J Klionsky (Univ. Michigan, Annarbor). Other antibodies were laboratory stock.

Protein concentration was assayed by using biocinchoninic acid kit (BCA assay kit, Pierce) and bovine serum albumin as a standard. Proteins in SDS-PAGE sample buffer were boiled for 5 min prior to being loaded on SDS-PAGE gel. SDS-PAGE was carried out by Laemmli's method. The sample was subjected to SDS-PAGE (SDS-PAGE containing 6 M urea gel used to detect Apg8-PE), and separated proteins were transferred to polyvinylidene difluoride (PVDF) membrane (Millipore). Immunoblotting was carried out by primary antibodies and peroxidase conjugated secondry antibodies, and then imunoblotted proteins were visualized by ECL system (Amersham Pharmacia Biotech). As described previously, rabbit or mouse antibodies against respective proteins were used as primary antibodies, and peroxidase conjugated goat anti-rabbit IgG or rabbit anti-mouse IgG used as secondary antibodies. Blocking reagent used for immunoblotting was 0.5% skim milk in TBST (0.1 M Tris-HCl, pH 7.5, 0.15 M NaCl, 0.5% Tween20)

Assay of autophagy

To detect the morphological change of vacuoles during autophagy, cells were grown in SD(-N) containing 1 mM phenylmethylsulfonyl (PMSF). Under these conditions, accumulation of autophagic bodies in the vacuole could be observed under light microscope (Tsukada and Ohsumi, 1993).

For the biochemical assay of autophagy, alkaline phosphatase (ALP) activity was measured by using Tn125 (*pho8::pho8Δ60*) background cells (Noda et al., 1995). The principle of ALP assay system; ALP is transported to the vacuole from ER via secretory pathway, and then processed an active form by proteinase A into the vacuole. Tn125 has an artificial defect of the ALP transport, subsequently remains proform of ALP (pro-ALP) in the cytosol. During starvation, the pro-ALP in Tn125 is transported to the vacuole depend on autophagy. Hence, ALP activity in Tn125 indicates the autophagic activity. To take advantage this assay system, autophagic activity was measured. Cells were grown in YEPD to log phase (OD_{600} =0.8) (Growing cells), and then the cells were shifted to SD(-N) for 4.5 h (Starved cells). Harvested growing and starvation cells were washed with distilled water and suspended in ALP assay buffer (50 mM Tris-HCl, pH 9.0, 5 mM $MgCl_2$, 1 mM PMSF, and protease inhibitor cocktail). The cells in ALP assay buffer were disrupted by vortexing with glass beads and centrifuged by 100 k *g* for 5 min to remove the debris. Resulting lysate was used for ALP assay, and its protein concentration was measured by BCA assay kit (described in above). The lysate was mixed with α-naphthyl phosphate and incubated at 30℃ for 20 min. The reaction was terminated by the addition of stop buffer (2 M glycine, NaOH, pH 11.0). ALP activity was measured by fluorescence spectrometer (excitation at 345 nm and emission at 472 nm), and autophagic activity was expressed by unit (ΔF_{472}/min/mg protein/10.7).

Sucrose density gradient centrifugation

Linear sucrose density gradient ranging from 5 to 20% was made by gradient maker at 4℃. Yeast lysates were prepared with spheroplasts lysis as described above and layered on top of the gradient. Fractionation was performed with centrifugation at 100 k *g* for 16 h at 4℃, and then separated fraction was collected by fraction collector. Proteins of each fraction were precipitated by trichloroacetic acid (TCA) (10% final

concentration) and suspended in SDS-PAGE sample buffer. Each sample was analyzed with immunoblotting.

Immunoprecipitation

Cells were suspended in immunoprecipitation buffer (50 mM Tris-HCl, pH 7.5, 150 mM NaCl, 5 mM EDTA, 1 mM PMSF, 1% NP-40, protease inhibitor cocktail) and disrupted physically by vortexing with glass beads for 5 min at 4℃. The cell lysate was centrifuged at 8,000 rpm for 5 min. Resulting supernatant was pretreated by 5 μl of protein G-Sepharose (or protein A-Sepharose) (50% slurry in immunoprecipitation buffer) (Amersham Pharmacia Biotech) for 30 min at 4℃, followed recentrifugation at 5,000 rpm for 1 min to remove the non-specific binding to protein G (or A)-Sepharose. Appropriate antibody was added in the lysate and incubated for 2 h at 4℃. The sample was mixed with 20 μl of protein G (or A)-Sepharose for 2 h at 4℃. Bound proteins to the sepharose beads were collected and washed three times with immunoprecipitation buffer by centrifugation at 3,000 rpm for 10 sec. The immunoprecipitates were eluted from the sepharose beads with SDS-PAGE sample buffer, and subjected to SDS-PAGE. In some cases, SDS-PAGE sample buffer without DTT was used for the elution to non-reducing condition analysis.

Purification of Apg7-Myc, Apg3, and Apg8FG

For the purification of respective components of Apg8 system, glutathione-S-transferase (GST) fused Apgs were prepared (GST-Apg7-Myc, GST-Apg3, and GST-Apg8FG). To construct the expressing plasmid, each *APG* was amplified by PCR using subcloned plasmid (pBADApg7-Myc, pUCSDApg3, and pBADApg8FG) as template. The oligonucleotides primer used for the PCR were (*APG7-MYC*) BamHI-(Fw), 5'-CAGGAGGAATTCACCATGGGATCCTCGTCAGAAAGGGTC-3', (Rv), 5'-TCCCCCGGGGGAATGCAAAATATTA-3', (*APG3*) BamHI- (Fw), 5'-AAGGAGGAA TTCACCATGGGATCCATTAGATCTACACTA-3' (Rv), 5'-CGGGATCCCGTTACC AACCTTCC-3', (*APG8FG*) BamHI- (Fw), CAGGAGGAATTCACCATGGGATCCA AGTCTACATTTAAG-3', (Rv), 5'-GCTCTAGAGCCTAGCCAAATGTATTTTC-3', respectively. Amplified genes were inserted to the cloning site (BamHI/SalI) in pGEX4-T-1. The resulting plasmids (pGEXApg7-Myc, pGEXApg3, and

pGEXApg8FG) contain *GST-APG* fusion genes, in which initiation codon of Apg is replaced from Met to Gly, respectively. The constructed plasmids were introduced to *E. coli*, XL1Blue, and their expression was induced by 0.5 mM IPTG.

For the expression and purification of each Apg, transformed cells were grown in LB (50 ml) supplemented with 50 μg/ml ampicillin (amp) at 37℃ for 12 h. The cells were shifted to LB amp (1 l) and cultured at 30℃ to OD_{600} =0.5, then 0.5 mM IPTG was added to each culture. Then, expressed Apg7-Myc cells were incubated at 20℃ for 15 h, and expressed Apg3 or Apg8FG cells were incubated at 30℃ for 6 h. The cells were harvested and suspended in 40 ml lysis buffer (PBST) (NaCl/ 8 g, KCl/ 0.2 g, $Na_2HPO_4 12H_2O$/ 2.9 g, KH_2PO_4/ 0.2 g, 1% Triton X-100) and disrupted by sonication with 4 times interval for 30 sec on ice. After removed cell debris by centrifugation at 10,000 rpm for 10 min, cell lysate was obtained. Recombinant protein was recovered by incubation with 200 μl glutathione Sepharose 4B (50% slurry in PBST) (Amersham Pharmacia Biotech) at 4℃ for 30 min. The bound proteins to sepharose beads were washed with PBST and suspended in 450 μl TB buffer (50 mM Tris-HCl, pH 8.0, 150 mM NaCl, 2.5 mM $CaCl_2$). Each GST fused Apg was treated with thrombin (5 U) at 37℃ for 1 h, and then glutathione Sepharose 4B/ GST complexes were removed by centrifugation to obtain the purified Apg. Resulted purified Apg was confirmed by CBB staining SDS-PAGE, and the protein concentration was measured by BCA protein assay (Apg7-Myc: 0.27 mg/ml, Apg3: 0.08 mg/ml, Apg8FG: 0.19 mg/ml). Finally, each protein concentration was estimated as follows; Apg7-Myc: 0.05 mg/ml, Apg3: 0.07 mg/ml, Apg8FG: 0.17 mg/ml.

Reconstitution of Apg8-PE conjugation system *in vitro*

Plasmids, pBAD-Apg7-Myc (Apg7-Myc in pBAD18), pBADC-Apg3 (Apg3 in pBAD33), and pBADC-Apg8FG (Apg8FG in pBAD33), respectively were introduced in *E. coli* (XL1Blue), and then transformed cells were grown in appropriate medium at 37℃ to OD_{600} =0.5. After the addition of 0.2% arabinose, each Apg was induced at 37℃ for 3-6 h (Guzman et al., 1995). Harvested cells were suspended in lysis buffer (20 mM Tris-HCl (pH 7.5), 50 mM NaCl, 0.2 mM DTT, 1 mM PMSF, and protease inhibitor cocktail) (20 OD_{600} unit/ml), and then the cells were disrupted by using sonication on ice. Resulting lysate was centrifuged at 8,000 rpm for 5 min to remove

the debris, and then total lysate was obtained. Equivalent amount of lysate (7 μl) was mixed and incubated at 30℃ for 15 h, in the presence of ATP regeneration system (0.5 mM ATP, 10 mM $MgCl_2$, 10 mM phosphocreatine, and 5 μg creatine kinase) or ATP depletion system (20 mM 2-deoxyglucose, 0.2 mg hexokinase), then the total volume of reaction mixture was adjusted to 25 μl. SDS-PAGE sample buffer (6x) (5μl) was added to the reaction mixture, and cell free reaction was terminated by boiling for 5 min. The sample (3 μl) was subjected to SDS-PAGE containing 6 M urea and analyzed by immunoblotting with anti-Myc, anti-Apg3, or anti-Apg8 antibody.

The activity of purified Apg was confirmed by using cell-free system. Total lysates were prepared from the cells, in which co-expressing either Apg7-Myc/Apg3, Apg7-Myc/Apg8FG, or Apg3/Apg8FG. Each total lysate (10 μl) was mixed with ATP regeneration system or ATP depletion system, and reacted to 1-5 μl of each purified Apg (Apg7-Myc, Apg3, and Apg8FG) at 30℃ for the indicated time, then the total volume of reaction mixture was adjusted to 20 μl. SDS-PAGE sample buffer (6x) (5 μl) was added to the reaction mixture, and cell free reaction was terminated by boiling for 5 min. 2.5 μl of the sample was subjected to SDS-PAGE containing 6 M urea and analyzed by immunoblotting with anti-Apg8 antibody.

In vitro reconstitution of Apg8 system was performed with each purified Apg and liposome. The liposome (5 μl) (total phospholipids: 5 nmoles) was mixed with Apg7-Myc (1 μl: ca. 0.64 pmoles), Apg3 (0.5 μl: ca. 1.0 pmol), and Apg8FG (0.07 μl: ca. 0.9 pmoles), then the total volume of reaction mixture was 20 μl. The reaction was done at 30℃ for 15 h under the presence of ATP regeneration system. SDS-PAGE sample buffer (6x) (5 μl) was added to the reaction mixture, and *in vitro* reaction was terminated by boiling for 5 min. The sample (2.5 μl) was subjected to SDS-PAGE containing 6 M urea and analyzed by immunoblotting with anti-Apg8 antibody.

Extraction of total lipids and preparation of liposome

Cellular lipids were extracted by Bligh and Dyer's method with a slight modification (Renkonen, 1967). *E. coli* and yeast cells were grown in appropriate medium to stationary phase. The cells were harvested by centrifugation and washed with distilled water (cells wet-weight 10 g). The cells were suspended in chloroform/methanol/distilled water (1/2/0.8) (190 ml), and the suspension was

incubated with strong agitation every 10 minutes at room temperature for 1h. Then, chloroform (50 ml) and distilled water (50 ml) was added to the suspension. After vigorous shaking, the layer of chloroform containing total lipids was separated by centrifugation at 2,000 rpm for 10 min. Obtained lipids in chloroform were recovered to a round-bottomed flask and the chloroform removed by rotary evaporation. Resulting lipid film was suspended in 19 ml chloroform/methanol/distilled water (1/2/0.8). Then, chloroform (5 ml) further added to the suspension, and it was centrifuged at 2500 rpm for 5 min to remove the contaminated proteins. The lipids in chloroform were transferred to 15 ml glass tube and dried under stream of nitrogen. Resulted lipids were suspended in chloroform (10 ml).

The concentration of total phospholipids was quantified by phosphorus assay using phospho-molybdate reaction and 3 mM KH_2PO_4 as a standard (W3110: 6.8 mM, GN10: 4.34 mM, SEY6210: 1.63 mM). Individual phospholipids were separated by two-dimensional thin-layer chromatography by using chloroform/methanol/acetic acid (13/5/2) as first and chloroform/methanol/formic acid (13/5/2) as second developing solvent. The phospholipids were visualized on thin-layer chromatography plate by staining with iodine vapor. Each stained phospholipid was scraped from the thin-layer chromatography plate, and the composition of phospholipids was detemined by phosphorus assay (W3110; PE : PG : CL : PA (75.4 : 16.6 : 8.59 : 3.57), GN10; PE : PG : CL : PA (< 0.01 : 52.6 : 33.6 : 11.4), SEY6210; PE : PC : PS : PI (16.6 : 51.7 : 13.7 : 18.0) (Bartlett, 1958).

For the preparation of liposome, 1 μmol phospholipids in chlorohorm was transferred to a new glass tube, and chloroform removed by rotary evaporation. *E. coli* phosphatidylethanolamine (PE), dioleoylphosphatidylethanolamine (DOPE), and 1-palmitoyl-2-oleoylphoshatidylcholine (POPC) were purchased from Avanti Polar Lipids, Inc. Resulted lipid film was further dried in desiccator under vacuum for 20 min. The lipid film was suspended in 1 ml TBS (10 mM Tris-HCl (pH 7.4), 150 mM NaCl) by vortex to form multilamellar liposome (1 mM). Unilamellar liposome was prepared from the multilamellar liposome by sonication on ice for 5 min. The liposome was stored at 4℃ and used within two weeks.

Strain	Genotype	Source
YW5-1B	*MATa leu2-3,112 trp1 ura3-52*	Tsukada and Ohsumi, 1993
NNY20	YW5-1BΔ*apg1::LEU2*	Matsuura et al., 1997
ICHW-3T	YW5-1BΔ*apg3::TRP1*	this study
TID4-2D	YW5-1BΔ*apg4::LEU2*	Kirisako et al., 2000
SKD5-1D	YW5-1BΔ*apg5::LEU2*	Kametaka et al., 1996
ICHW-7L	YW5-1BΔ*apg7::LEU2*	this study
TK405	YW5-1BΔ*apg8::LEU2*	Kirisako et al., 1999
TFD10-L1	YW5-1BΔ*apg10::LEU2*	Shintani et al., 2001
GYS13	YW5-1BΔ*apg12::TRP1*	Suzuki et al., 2001
SEY6210	*MATα leu2-3 112 ura3-52 trp1-Δ901 his3-Δ200 ade2-101 lys2-801 suc2-Δ9*	Darsow et al., 1997
ICHY-3T	SEY6210Δ*apg3::TRP1*	this study
YTS12	SEY6210Δ*apg7::HIS3*	this study
ICHY-8L	SEY6210Δ*apg8::LEU2*	Shintani et al., 2001
IS38-TH	SEY6210Δ*apg3::TRP1* Δ*apg8::HIS3*	this study
IS78-HT	SEY6210Δ*apg7::HIS3* Δ*apg8::TRP1*	this study
Tn125	*MATa leu2–Δ1 ura3-52 trp1-Δ1 his3-Δ200 ade2-101 lys2-801*	Noda et al., 1995
TND3	Tn125Δ*apg3::TRP1*	this study
XL1-Blue	F'::Tn*10 proA+B+* lacIq *Δ(lacZ) M15/recA1 endA1 gyrA96*(Nalr)*thi hsdR17* (rK-mK+) *glnV44 relA1 lac*	Lab. stock
W3110	F- IN(*rrnD-rrnE*)*1*	Saha et al., 1996
GN10	W3110 *ΔpssA10::cam*	Saha et al., 1996

Plasmid name	Replicon	Selectable makers
pRS314	pMB1, CEN6, ARS	Amp^r, TRP1
pRS424	pMB1, 2μ,	Amp^r, TRP1
pRS315	pMB1, CEN6, ARS	Amp^r, LEU2
pRS425	pMB1, 2μ,	Amp^r, LEU2
pRS316	pMB1, CEN6, ARS	Amp^r, URA3
pRS426	pMB1, 2μ,	Amp^r, URA3
pBAD18	pMB1	Amp^r
pBAD33	p15A	Cm^r

Table. 2 Strains and Plasmids used in this study.

Results

Analysis on *Δapg3* cells

Autophagy deficient cells show loss of viability phenotype under starvation conditions by the impediment of their bulk degradation. By the previous studies in our laboratory, 15 genes (*APG*) essential for autophagy have been cloned and identified in yeast, *Saccharomyces cerevisiae*. Among of these *APG* genes, *APG3* was cloned from yeast genomic library by complementing mutation *apg3-1* (Tsukada and Ohsumi, 1993). Sequence analysis revealed that *APG3* is identical to *AUT1* (ORF *YNR007c*) (Fig. 2). *AUT1* has been reported as an essential gene for autophagy, however its detailed function was unknown (Schlumpberger et al., 1997). The *APG3* encodes 310 amino acids, and its calculated molecular size was 36 kDa. The *APG3* gene product Apg3 seems to be quite hydrophilic with clusters of charged amino acids and a predicted isoelectric point is 4.55. Amino acid sequence of yeast Apg3 also showed its homologues in several other species (Fig. 2). To elucidate the function of Apg3 in autophagy, I first constructed Apg3 disrupted cells. *Δapg3* cells were made by homologous recombination to chromosomal *APG3* using the disrupted genes by *TRP1* marker. The resulting *Δapg3* cells were checked by immunoblotting with anti-Apg3 antibody. This immunoblot showed that *Δapg3* cells lost a 36 kDa band corresponding to Apg3 (Fig. 3 and 4). Next, morphological change of *Δapg3* during starvation was checked. Cells were grown in nitrogen starvation medium (SD (-N)) containing 1 mM PMSF for 4.5 h, then the accumulation of autophagic bodies in the vacuole was observed under a light microscope. During starvation the autophagic bodies in the vacuole could be detected in the wild-type, but not in *Δapg3* cells. By introducing Apg3 plasmids into *Δapg3*, the autophagic activity was recovered.

To examine the effect of *Δapg3* on localization of other Apgs, I carried out subcellular fractionation of lysate from *Δapg3*. Logarithmically growing *Δapg3* cells in YEPD were harvested and converted to spheroplasts. Total lysate was prepared from the spheroplasts by osmotic lysis, and separated to LSP and LSS by centrifugation at 13 k *g* for 15 min. LSS was further separated to HSP and HSS by centrifugation at 100 k *g* for 60 min. Each fraction was subjected to SDS-PAGE and immunoblotted with antibodies against Apg1, Apg3, Apg6, Apg8, Apg9, Apg12 (Fig. 3). There was

no significant difference of distribution of Apg proteins except Apg8, when *Δapg3* was compared to wild-type (Fig. 3). In wild-type cells, Apg8 appeared partly in the LSP, while it was not recovered in the LSP of *Δapg3* (Fig. 3). I confirmed the subcellular distribution of the Apg8 in wild-type, *Δapg1*, and *Δapg3*. Subcellular fractionation was performed as described above. Each fraction was subjected to SDS-PAGE and immunoblotted with anti-Apg3, anti-Apg8, anti-ADH, and anti-ALP antibodies. Apg3 distributed in HSS fraction in wild-type and *Δapg1* similar to ADH, cytosolic marker (Fig. 4). A vacuolar enzyme, ALP is transported from Golgi to vacuole by vesicular transport, and localizes on the vacuolar membrane. The ALP was detected normally in the LSP from each strain (Fig. 4). Apg8 was significantly recovered in the LSP in wild-type and *Δapg1* cells, but not in *Δapg3* cells (Fig. 4). These results indicated that the distribution change of Apg8 in *Δapg3* is not due to the general defect of autophagy. Apg3 would be required for the localization of Apg8 to LSP.

Apg3 increases during starvation conditions

It is known that the amount of Apg8 increases during starvation conditions. I examined expression of Apg3 under starvation conditions. Wild-type cells were grown in YEPD to OD_{600} =1.0, then shifted to nitrogen starvation medium (SD (-N)). Cells were harvested at 0.5, 1.0, and 3.0 h of starvation, and broken by vortexing with glass beads. Debris and glass beads were removed by centrifugation at 12 k *g* for 3 min to generate total lysate. Total lysate was suspended in SDS-PAGE sample buffer at a concentration of 2 mg/ml, and 20 μg protein sample was subjected to SDS-PAGE, and immunoblotted using anti-Apg3 and anti-Apg8 antibodies. As shown in Fig. 5 the amount of Apg3 increased during starvation conditions, but it was less intensive than that of Apg8 (Fig. 5). Next, I examined the amount of Apg3 in late-log phase cells. Wild-type cells were grown from early-log to late-log phase in YEPD. At the indicated time, cells were harvested and suspended in alkaline solution (0.2 N NaOH, 0.5% 2-mercaptoethanol) (Fig. 6). Total proteins of the lysed cells by the alkali treatment on ice for 5 min were precipitated with cold acetone, and collected by centrifugation at 15 k rpm for 10 min at 4℃. The precipitated extracts were washed twice with cold acetone and suspended in SDS-PAGE sample buffer at a concentration of 50 OD_{600} unit/ml. The equal volume of samples was subjected to SDS-PAGE and

immunoblotted with anti-Apg3, anti-Apg8 and anti-ADH antibodies. Signal of the Apg3 in blot gradually increased to late-log phase, but that of ADH not changed (Fig. 6). This expression of Apg3 also suggested that the function of Apg3 be related to that of Apg8.

Apg3 interacts to Apg8 depending on the C-terminal Gly of Apg8

To examine the above possibility, physical interaction of Apg3 and Apg8 was analyzed. Apg3 and/or Myc-Apg8 were introduced to Δ*apg3* via multicopy plasmids, pRS425Apg3 and pRS426Myc-Apg8, respectively. The resultant transformants were grown in YEPD to mid-log phase, and harvested by centrifugation. Total cell lysates were prepared by glass beads disruption in IP buffer. The obtained lysates were immunoprecipitated with anti-Apg3 antibody. Immunocomplexes bound to Protein Sepharose A were suspended in SDS-PAGE sample buffer, and eluted by boiling for 5 min. Eluted proteins were subjected to SDS-PAGE and immunoblotted with anti-Apg3 and anti-Myc antibodies. Immunodetection using each antibody revealed that immunoprecipitated proteins with anti-Apg3 antibody contained both Apg3 and Myc-Apg8, when the cells co-expressing them (Fig. 7). Cells harboring pRS426HA-Apg8 were examined by immunoprecipitation using anti-HA antibody. The resulting immunocomplexes bound to Protein Sepharose G were eluted into SDS-PAGE sample buffer by boiling for 5 min, and subjected to immunoblotting with anti-Apg3 and anti-HA antibodies. This immunoblotting showed both signals of Apg3 and HA-Apg8 (Fig. 8). The association of HA-Apg8 to endogeneous Apg3 was clearly detected in wild-type (Fig. 8). Hence, I concluded that Apg3 forms a complex with Apg8.

The physical interaction between Apg8 and Apg4 has been reported (Lang et al., 1998). Moreover, Kirisako et al. reported Apg4 is a novel cysteine protease and cleaves carboxy terminal arginine of Apg8 and exposes a glycine at the carboxy terminal of Apg8 (Kirisako et al., 2000). Next, I examined the interaction between Apg3 and Apg8 in Δ*apg4*. The lysates from cells harboring pRS426HA-Apg8 were immunoprecipitated by using anti-HA antibody. Resulting precipitates were subjected to SDS-PAGE and immunoblotted with anti-Apg3 or anti-HA antibody. Immunoblotting with anti-Apg3 antibody showed that in Δ*apg1* cells lysate, Apg3 and HA-Apg8 were co-precipitated by anti-HA antibody, as the case of wild-type (Fig. 8).

On the other hand, using the Δ*apg4* cells lysate, the immunoprecipitation by anti-HA antibody did not show the co-precipitated Apg3 with HA-Apg8 (Fig. 8). Thus, Δ*apg4* lost the physical interaction between Apg8 and Apg3. Next, I used the HA-tagged series of C-terminal mutant Apg8 plasmids. The series of pRS426HA-Apg8 yields the N-terminal HA-tagged Apg8 as follows, Apg8FGR is nascent Apg8, Apg8FG lacks the C-terminal Arg, and Apg8F lacks the C-terminal Gly-Arg (Fig. 9). Δ*apg4* cells were transformed with these plasmids. Cell lysates of these transformants were immunoprecipitated with anti-HA antibody. Resultant immunoprecipitates were subjected to SDS-PAGE, and immunoblotted with anti-Apg3 and anti-HA antibodies. The immunoblotting showed the signal of both endogeneous Apg3 and HA-Apg8FG in the immunoprecipitates with anti-HA antibody of HA-Apg8FG expressing cells (Fig. 9). Although HA-Apg8FGR and HA-Apg8F were shown in the immunoprecipitates with anti-HA antibody of their expressed cells, the signal of Apg3 was not detected (Fig. 9). These results indicated that the C-terminal Gly of Apg8 is essential for the interaction between Apg3 and Apg8.

The interaction between Apg3 and Apg8 requires Cys133 residue of Apg3

I found that the interaction between Apg3 and Apg8 requires the C-terminal Gly of Apg8. Ubiquitin is well known post-translational modification, in which ubiquitin sequentially conjugates to activating enzyme (E1) and conjugating enzyme (E2), and in many case ligase (E3) via its C-terminal Gly. Finally the Gly residue of ubiquitin forms an isopeptide bond with a Lys residue of target molecules. I assumed that Apg8 is modified through ubiquitination like reaction and conjugated to some molecule via its C-terminal Gly. This assumption was partly supported by sequence analysis between Apg3 and Apg10. Apg10 is known as the conjugating enzyme (E2) for Apg12, and its Cys^{133} residue is identified as the active site for its conjugation (Shintani et al., 1999). When the amino acid sequence of Apg10 was compared with that of Apg3, the region around Cys^{133} of Apg10 exhibited partial homology to the region around Cys^{234} of Apg3 (Fig. 10). This similarity suggested that Apg3 may be a conjugating enzyme for Apg8. To confirm this idea, I constructed site direct amino acids replacement Apg3, $Apg3^{C234A}$ and $Apg3^{C234S}$, in which Cys^{234} was substituted to Ala or Ser, respectively by Quik Change mutagenesis kit (Fig. 11). Mutant form $Apg3^{C234A}$

or $Apg3^{C234S}$ was expressed by multicopy plasmids (pRS425) in *Δapg3* harboring pRS426Myc-Apg8. These transformed cell lysates were analyzed by immunoprecipitation using anti-Myc antibody. Immunoprecipitation with anti-Myc antibody showed the co-precipitated Apg3 with Myc-Apg8 in wild-type cell lysate (Fig. 11). However, when the transformed cells expressing either $Apg3^{C234A}$ or $Apg3^{C234S}$, the immunoprecipitation with anti-Myc antibody showed only Myc-Apg8, no $Apg3^{C234A}$ and $Apg3^{C234S}$ (Fig. 11). $Apg3^{C234A}$ and $Apg3^{C234S}$ did not have the physical interaction with Apg8-Myc. These results suggested that the Cys^{234} of Apg3 is necessary to interact with Apg8.

C-terminal Gly of Apg8 is necessary to interact with Apg7

If Apg3 is a conjugating enzyme (E2) for Apg8, the Apg8 should be activated by an activating enzyme (E1). The interaction of Apg8-Apg3 was examined by other *Δapg* cells. The immunoprecipitation analysis revealed that the interaction of Apg8-Apg3 was abolished in *Δapg7* (Fig. 12). Apg7 is known as an E1 for Apg12 (Tanida et al., 1999). *Δapg7* cells can not form the Apg12-Apg5 conjugation. Apg7 also participates in the interaction of Apg8-Apg3, because other mutants for Apg12-Apg5 conjugation system, such as *Δapg5*, *Δapg10*, *Δapg12* cells show the interaction Apg8-Apg3 normally (Fig. 12).

I tested a physical interaction of Apg8 with Apg7 by immunoprecipitation. *Δapg7Δapg8* cells were co-transformed with pRS424Apg7-Myc and/or pRS425Apg8. Resulting transformants were grown in YEPD to mid-log phase, and then harvested by centrifugation. Total cell lysates were obtained by disruption with glass beads in IP buffer, then subjected to immunoprecipitation with anti-Myc antibody. Immunocomplexes bound to Protein Sepharose G were suspended in SDS-PAGE sample buffer, and eluted by boiling for 5 min. Obtained proteins were subjected to SDS-PAGE and analyzed by immunoblotting with anti-Myc and anti-Apg8 antibodies. This immunoblotting revealed that co-precipitated proteins by anti-Myc antibody contained both Myc-Apg7 and Apg8 (Fig. 13). To further confirm the dependency of Apg8 C-terminus glycine for the interaction of Apg8-Apg7, the HA tagged Apg8 and its C-terminal variant plasmids (HA-Apg8FGR, -Apg8FG, or -Apg8F described above) was introduced into *Δapg4* carrying Apg7-Myc cells. The lysates from resulted

transformants were immunoprecipitated by using anti-HA antibody. Immunoprecipitates were subjected to SDS-PAGE and analyzed by immunoblotting with anti-Myc or anti-HA antibody. The immunodetection by anti-Myc or anti-HA antibody showed that the interaction between Apg7-Myc and HA-Apg8FG in *Δapg4*, however the interaction disappeared in *Δapg4* harboring either HA-Apg8FGR or HA-Apg8F cells (Fig. 14). Thus, Apg8 C-terminus Gly is also essential for the interaction of Apg8-Apg7.

Apg8 binds to Apg7 via a thioester bond

Ubiquitin and ubiquitin-like proteins are activated by E1 in an ATP dependent manner. In this reaction, the modifier forms a thioester linkage with E1 after adenylation. For activation of Apg12, the ATP binding domain and the active center in Apg7 are shown to be essential (Fig. 15) (Tanida et al., 1999). I tested the E1 activity of Apg7 for the interaction between Apg8 and Apg7 by Apg7 mutants. By using Quik Change mutagenesis kit, the Gly^{333} of Apg7-My was replaced by Ala^{333}, and the Cys^{507} of Apg7-Myc by either Ala or Ser, on a single copy plasmid (pRS314). Constructed Apg7-Myc mutants denoted as follows, Apg7G333A-Myc; replacement from Gly^{333} to Ala^{333} at the ATP binding site, Apg7C507A-Myc; replacement from Cys^{507} to Ala^{507} at the active site, Apg7C507S-Myc; replacement from Cys^{507} to Ser^{507} at the active site (Fig. 15) were introduced into *Δapg7* cells expressing HA-Apg8. The lysates were prepared from resultant transformants, and examined by immunoprecipitation using anti-HA antibody. Co-precipitated proteins by anti-HA antibody were subjected to SDS-PAGE, and analyzed by immunoblotting with anti-HA and anti-Myc antibodies. As shown Fig. 15, immunoblot by anti-HA antibody showed the signal of HA-Apg8 in all cell lysates. When the cells expressed both wild-type Apg7-Myc and HA-Apg8, wild-type Apg7-Myc was co-precipitated with HA-Apg8. Further, the immunoblot by anti-Myc antibody showed that the mutant series of Apg7-Myc did not co-precipitated with HA-Apg8 (Fig. 15). Thus, Apg7-Myc mutant (G333A, C507A, or C507S, respectively) cells failed to interact with HA-Apg8 (Fig. 15). These results indicated that the interaction of Apg8-Apg7 requires the E1 activity of Apg7, and which functioned exactly at the same residues for activating Apg12.

Next I examined whether Apg7 actually activates Apg8 by determination of a

linkage between Apg7 and Apg8. Cell lysate of *Δapg8Δapg7* co-expressing both Apg7-Myc and HA-Apg8 was immunoprecipitated with anti-HA antibody. The immunocomplexes bound to Protein Sepharose G was collected, and eluted into SDS-PAGE sample buffer with or without 100 mM DTT, at 65℃ for 15 min. Each sample was subjected to SDS-PAGE and immunoblotted with anti-Myc or anti-Apg8 antibody. HA-Apg8-Apg7-Myc conjugates were detected by immunoblotting with anti-Myc or anti-Apg8 antibody under non-reducing conditions (Fig. 16). The conjugates disappeared in the presence of 100 mM DTT (Fig. 16). I concluded from these results that C-terminal Gly of Apg8 conjugates to the Cys^{507} of Apg7 via a thioester bond.

Apg8 interacts with Apg3 via a thioester bond

I confirmed the E2 function of Apg3 for Apg8. First, the interaction between Apg3 and Apg8 in cells expressing Apg7-Myc mutant (G333A, C507A, or C507S, respectively) was analyzed by immunoprecipitation experiments. The mutant series of Apg7-Myc and HA-Apg8 plasmids were introduced to *Δapg7* cells. The resulting transformants were disrupted in IP buffer by glass beads, and generated lysates were immunoprecipitated with anti-HA antibody. Co-precipitated proteins by anti-HA antibody were subjected to SDS-PAGE and examined by immunoblotting with anti-Apg3 and anti-HA antibodies. In expressed both Apg7-Myc and HA-Apg8 cells, Apg3 was co-precipitated with HA-Apg8 by anti-HA antibody (Fig. 17). Apg3 did not co-precipitated with HA-Apg8 in the cell lysates which expressed both Apg7-Myc mutant and HA-Apg8 (Fig. 17). As expectedly, the interaction of Apg8-Apg3 could not be detected in all cells expressing mutant forms of Apg7 (Fig. 17). These results indicated that the interaction of Apg8-Apg3 must be followed by the activation of Apg8 via Apg7. I examined characteristics of interaction between Apg8 and Apg3. Complex of Myc-Apg8-Apg3 was taken from cell lysate co-expressing Myc-Apg8 and Apg3 by immunoprecipitation using anti-Myc antibody. The immunocomplexes, Myc-Apg8-Apg3 were eluted from Protein Sepharose G at 65℃ for 15 min into SDS-PAGE sample buffer with or without 100 mM DTT. Immunoblot by using anti-Apg8 and anti-Apg3 antibodies showed that Myc-Apg8-Apg3 conjugates were detected by each antibody under non-reducing conditions, and disappeared in reducing conditions (Fig. 18). Accordingly, I concluded that Apg8 and Apg3 are conjugated via a thioester

bond. The thioester conjugate was completely diminished in Δ*apg7*, and was not affected by the absence of Apg10 (Fig. 18).

Apg8 is modified by sequential biochemical reaction (Apg8 system)

Here, I indicated the thioester linkage in both Apg8-Apg7 and Apg8-Apg3 (Fig. 16 and 18). The C-terminal Gly of Apg8 is essential for both conjugates (Fig. 9 and 14). Then, the interaction of Apg8 with Apg7 mutants (G333A, C507A and C507S) or Apg3 mutants (C507A, C507S) could not be detected (Fig. 11 and 15). In addition, the Apg8-Apg3 interaction also disappeared in the cells expressed Apg7 mutants (G333A, C507A and C507S) (Fig. 17). From these observations, the physical interaction of both Apg8-Apg7 and Apg8-Apg3 mostly explained as their thioester linkage. Altogether, the C-terminal Gly of Apg8 is adenylated at the ATP binding domain including Gly^{333} on Apg7, and then binds to the Cys^{507} on Apg7 via a thioester bond (Fig. 19). Subsequently, activated Apg8FG on Apg7 is transferred to Apg3, then its C-terminus Gly conjugates to Cys^{234} on Apg3 via a thioester bond (Fig. 19). Ubiquitination-like pathways occur sequentially via thioester bonds formation between a modifier and respective enzymes (E1 and E2) (Fig. 19). Thus, Apg8 behaves like a modifier in ubiquitination-like system (Fig. 19)

Sequential enzyme reaction in Apg8 system is essential for Apg8-PE

After this work, Kirisako et al. found that a portion of Apg8 is covalently linked to phosphatidylethanolamine (PE).

The C-terminal Arg of nascent Apg8 is removed by Apg4 protease, leaving a Gly at the C-terminus. This Apg8FG (cleavaged form of Apg8 by Apg4) is covalently linked via the C-terminal Gly to the primary amine of phosphatidylethanolamine (PE) (Fig. 20). The Apg8-PE is distinguishable from nascent Apg8 and Apg8FG by two points; 1) unlipidated Apg8 in 100 k *g* pellet is completely solubilized by 1 M NaCl treatment, although Apg8-PE still remains. 2) The electrophoretic mobility of Apg8-PE is faster than that of other forms of Apg8 on SDS-PAGE containing 6 M urea (urea-SDS-PAGE).

I examined that ubiquitination-like Apg8 system is related to Apg8-PE. First, I performed NaCl solubilization test with pelletable Apg8. Each $Apg7^{C507A}$, $Apg7^{G333A}$,

or $Apg3^{C234A}$ expressed cells were converted to spheroplasts, and lysed osmotically. The total lysate was centrifuged at 100 k *g* to separate pellet and supernatant. The pellet was suspended into 1 M NaCl lysis buffer using sonication, and then incubated on ice for 1 h. The suspension was separated to soluble and insoluble fractions by recentrifugation at 100 k *g*. Resulting pellet and supernatant were subjected to SDS-PAGE and immunoblotted using anti-Apg8 antibody. In cells impeded the reaction of Apg8 system, the unlipidated Apg8 was completely solubilized by NaCl treatment (Fig. 21). Kirisako reported that *Δapg4* cells show a similar result (Kirisako et al., 2000). I also asked the Apg8-PE using urea-SDS-PAGE. Mutant cells had a defect in any one of enzymatic step of Apg8 system with expressing $Apg7^{C507S}$ or $Apg3^{C234S}$ respectively, were disrupted in lysis buffer by vortexing with glass beads, resulting total lysates were analyzed by immunoblotting with anti-Apg8 antibody on urea-SDS-PAGE. In wild-type cells, Apg8-PE was identified as the fastest migrating band among other forms of Apg8 (ex. Apg8FGR, Apg8FG) (Fig. 22). On the other hand, expressed either $Apg7^{C507S}$ or $Apg3^{C234S}$ cells lost the Apg8-PE band on urea-SDS-PAGE (Fig. 22). These results indicated that Apg8-PE is generated by sequential enzymatic reaction in Apg8 system like a ubiquitination pathway (Fig. 20).

Apg7 acts as a common E1 both Apg8 and Apg12

A modifier is usually activated by individual E1 in ubiquitination or ubiquitination-like pathway. Interestingly, Apg7 activates not only Apg12 but also Apg8 (Fig. 23). The amino acid sequences between Apg12 and Apg8 demonstrated significant homology in their C-termini, which might be important to association with Apg7 (Fig. 24).

Apg12 and Apg8 should be specifically recognized by Apg10 and Apg3 for the accurate modification. I investigated the specificity of conjugation reaction by Apg3 for Apg8 or by Apg10 for Apg12. pRS426Apg3 and/or pRS425Apg10-HA were introduced in wild-type cells. Cells expressing Apg3 and/or HA-Apg10 were disrupted in IP buffer by vortexing with glass beads. Total cell lysates were immunoprecipitated with using anti-Apg3 or anti-HA antibody, and then obtained co-precipitates were immunoblotted with anti-Apg3, anti-HA and anti-Apg8 antibodies. The immunoblotting showed that the signal of Apg8 appeared in the co-precipitated

sample of Apg3 by using anti-Apg3 antibody, but not in that of HA-Apg10 by using anti-HA antibody (Fig. 25). Hence, Apg8 seems to bind to Apg3 selectively. Next, cells harboring both pRS424Apg3 and pRS426Myc-Apg12 were analyzed by immunoprecipitation with anti-Apg3 or anti-Myc antibody. Obtained immunoprecipitates were analyzed by immunoblotting using anti-Apg3 and anti-Myc antibodies. This immunoblotting showed that Myc-Apg12 was co-precipitated by Apg3 in wild-type and in *Δapg10* cells, but was not in *Δapg7* cells. Conversely, Apg3 was co-precipitated by Myc-Apg12 in wild-type and *Δapg10* cells, but was not in *Δapg7* cells. Thus, Apg12 associates to Apg3 in an Apg7 dependent manner (Fig. 26). Whereas I can not conclude that Apg3 bind to Apg12 via thioester bond, I did not see any candidates of Apg12-Apg3 thioester conjugate in the previous displayed conjugation band by non-reduced SDS-PAGE sample (Fig. 18). Furthermore, Apg3 is not essential for the Apg12-Apg5 conjugation (data not shown). I also analyzed the interaction of Apg7-Apg3. Apg7-Myc and/or HA-Apg8 were introduced to *Δapg8Δapg7* cells via multi copy plasmids, pRS424Apg7-Myc and pRS426HA-Apg8, respectively. The lysates from resulted transformant were subjected to immunoprecipitation using anti-Myc or anti-HA antibody. Each sample was subjected to SDS-PAGE and immunoblotted by anti-Myc, anti-Apg3, and anti-HA antibodies. The immnunoblotting by anti-Apg3 antibody showed that all immunoprecipitates contained Apg3 even in the absence of Apg8 (Fig. 27). These results indicated that Apg3 directly associates with Apg7 (Fig. 28). Komatsu et al. recently reported the interaction between Apg7 and Apg3, and the homodimer of Apg7 as an active form (Komatsu et al., 2001). It is consistent with my results. The physical interaction between Apg12 and Apg3 probably occurs at an activation step of Apg12 by the Apg7, associates to Apg3 (Fig. 28).

Apg8-PE conjugation system is essential for autophagy

While Apg7 acts for both conjugates Apg12-Apg5 and Apg8-PE, Apg3 acts only for the formation of Apg8-PE. It has been reported previously that Apg12-Apg5 and Apg8-PE are essential for autophagy and the Cvt-pathway. I confirmed the autophagic activity and API transport in cells expressing $Apg3^{C234A}$, which should be blocked at the specific step before PE conjugate to Apg8FG. Tn125 wild-type,

Tn125 Δ*apg3* and Tn125 Δ*apg3* harboring pRS315Apg3^{C234A} cells were grown in YEPD to OD_{600} = 1.0, and then shifted to SD (-N) for 4.5 h. These cells were harvested by centrifugation, and disrupted in ALP assay buffer by vortexing with glass beads. A part of the resulting lysates was taken for the immunoblot analysis of API. Remaining lysates were analyzed by ALP assay according to described in Materials and Methods. The ALP assay indicated the loss of autophagic activity in cells expressing Apg3^{C234A} (Fig. 29), additionally the API transport via the Cvt-pathway was completely blocked in that mutant (Fig. 29). These results suggested that Apg8-PE conjugation system is essential for autophagy and the Cvt-pathway.

Apg8-Apg3 conjugates increase during starvation conditions

Ubiquitination-like system results in a covalent conjugation of modifier to its target molecule. It is generally believed that the target molecule is a protein. However, the target of Apg8 is a PE. It is still possible that Apg8 form conjugate with certain protein. Total lysates were prepared by disruption with glass beads from late-log phase cells and subjected to SDS-PAGE. The separated proteins in SDS-PAGE were immunoblotted by anti-Apg8 antibody. When I sought the possible signals of Apg8 conjugates on immunoblot with anti-Apg8 antibody by comparison between wild-type and mutant forms of Apg8 system, there were no extra bands specific to Apg8 system (data not shown). On the other hand, when total lysates were extracted by alkaline treatment, their immunoblotting with anti-Apg8 antibody displayed an approximate 58 kDa band that depended on enzymes of Apg8 system such as Apg4, Apg7, and Apg3 (Fig. 30 and 31). The Apg8 specific 58 kDa band was detectable in alkali extracts from late-log phase cells, but not in other extracts using mechanical or osmotical lysis. As mentioned early, both Apg8 and Apg3 increase during starvation conditions (Fig. 5 and 6). I examined the change of 58 kDa band during starvation conditions. Wild-type cells were grown in YEPD until early-log phase, and then shifted to SD (-N). Cells were lysed by alkaline lysis, and subjected to immunoblot with anti-Apg8 antibody. The signal of 58 kDa band was intensified upon shift to the starvation conditions (Fig. 32). Late-log phase cells in YEPD also resulted in the increase of 58 kDa product (Fig. 32). Apg8FG is linked to Apg3 via thioester bond and which is sensitive to reducing reagents (Fig. 18). As previous shown, Apg8-Apg3

conjugates disappeared under presence of 100 mM DTT (Fig. 18). However, the observed size of Apg8-Apg3 was very closely to the 58 kDa band on SDS-PAGE. I asked that the 58 kDa band is an Apg8-Apg3 thioester conjugate. Immunoblotting with anti-Apg3 antibody clearly displayed the same size signal of 58 kDa (Fig. 32). Hence, I concluded that the 58 kDa band is an intact Apg8-Apg3 thioester conjugate. In the cell extracts of alkaline treatment, the Apg8-Apg3 conjugation still remained in the presence of 200 mM DTT (data not shown). As a result, the immunoblotting of total lysate using anti-Apg8 antibody did not show any specific bands corresponding to Apg8-protein conjugation other than Apg8-Apg3 (Fig. 30). Thus, the target molecule of Apg8FG must be only a PE. During these experiments, I noticed that Apg8-Apg3 conjugates increase under starvation conditions, in accordance with induction both of Apg8 and Apg3 (Fig. 32).

Distribution of Apg3

Apg8 is conjugated with PE after Apg8-Apg3 conjugation. However, I don't have any lines of evidence for the direct transition from Apg8-Apg3 to Apg8-PE. To get insight on the Apg8-PE conjugate reaction after Apg8-Apg3, I assess the intracellular distribution of Apg3 by subcellular fractionation. Wild-type and *Δapg7* cells were grown in vegetative or starvation conditions, and converted to spheroplasts. The subcellular fractionation was carried out according to the previous method (Fig. 3), and each fraction was subjected to SDS-PAGE. Immunoblot analysis by using organelles marker antibodies against Kex2 (Golgi), ALP (Vacuole), and ADH (Cytosol) displayed proper distribution of each protein. Then, immunoblot analysis of anti-Apg3 antibody showed that most of Apg3 distributed to the HSS fraction (Fig. 33). Cells expressing $Apg3^{C234S}$ formed an ester bond between Apg8 C-terminus Gly and Ser^{234} residue in $Apg3^{C234S}$ instead of thioester bond. *Δapg7* and *Δapg3* both cells expressing $Apg3^{C234S}$ were grown in nitrogen starvation conditions for 6 h, and subjected to subcellular fractionation. To determine the distribution of Apg8-$Apg3^{C234S}$ ester conjugate, immunoblot analysis with anti-Apg8 or anti-Apg3 antibody was performed. The immunoblotting indicated that the activation of Apg8 by Apg7 is certainly required for the formation of ester conjugate in Apg8-$Apg3^{C234S}$ as well as thioester bond of Apg8-Apg3, and the resulted Apg8-$Apg3^{C234S}$ ester conjugates mainly existed in HSS

fraction (Fig. 34).

To find the detailed population of Apg3, I next carried out sucrose density gradient fractionation of Apg3. Wild-type cells were grown in YEPD to mid-log phase, then the cells were converted to spheroplasts, and osmoticaly lysed in lysis buffer. Resulting total lysate was loaded on top of a 5-20% linear sucrose density gradient (w/w), and centrifuged at 100 k *g* for 16 h. Proteins in the sucrose density gradient were fractionated in 20 fractions from top to bottom. Each fraction was subjected to SDS-PAGE and immunoblotted with anti-Apg3 or anti-Apg8 antibody (Fig. 35). The immunoblot showed that Apg3 distributed in two peaks, and Apg8 dispersed in every fraction (Fig. 35). The first peak of Apg3 was observed in very low-density fraction (Fig. 35). It implied that a portion of Apg3 associates with lipid-like molecule.

Reconstitution of Apg8 system in *Escherichia coli*

The details of Apg8 lipidation step after Apg8-Apg3 conjugation remains unclear. Many ubiquitination systems require E3 molecules to bind their targets. It is thought that the E3 plays a critical role for recognition of its specific target. Next question is whether any other molecule, like E3 is required for the Apg8-PE conjugation. I attempted to reconstitute the Apg8-PE conjugation system in *Escherichia coli*. I constructed Apg8FG, Apg7-Myc and Apg3 expression plasmids, by insertion to pBAD plasmids (pBAD18 encodes P_{BAD} promoter, *araC*, *bla* (ampicillin resistance), and pBR origin, pBAD33 encodes P_{BAD} promoter, *araC*, *cat* (chloramphenicol resistance), and pACYC origin). These plasmids contain the P_{BAD} promoter of arabinose operon and its regulatory gene, *araC*. The AraC protein binds to arabinose and positively regulates the expression from P_{BAD} promoter. When cells are grown in the presence of glucose, the expression from P_{BAD} promoter turns off by the low level of intracellular 3', 5'-cyclic AMP. Thus, this *araC*-P_{BAD} promoter system is tightly regulated by addition of arabinose and glucose.

For expression of each component of Apg8 system in *E. coli*, I used two constructed plasmids, one is based on pBAD18 for the expression of Apg7-Myc (pBAD-Apg7-Myc) and another is based on pBAD33 for the expression of Apg3 and/or Apg8FG (pBADC-Apg8FG and pBADC-Apg3Apg8FG) (Fig. 36). Co-transformed *E. coli* cells, XL1blue by pBAD-Apg7-Myc and either pBADC-Apg8FG or pBADC-

Apg3Apg8FG were selected on LB plates supplemented with ampicillin (Amp) (50 μg/ml), chloramphenicol (Cm) (25 μg/ml). Resulting transformants were grown in LB liquid culture containing Amp, Cm at 37℃ for overnight. The fresh overnight cultures were diluted 1 : 100 and grown to OD_{600} =0.5 in LB supplemented with Amp, Cm at 37℃. After addition of 0.2% arabinose, cells were incubated further at 37℃ during 3 h. At the indicated time, the cells were harvested and boiled with SDS-PAGE sample buffer (Fig. 36). Obtained samples were subjected to urea-SDS-PAGE and analyzed by immunoblotting with anti-Myc, anti-Apg3, and anti-Apg8 antibodies (Fig. 36). The immunoblot showed the expression of respective Apgs, which were induced efficiently by the addition of arabinose (Fig. 36). The cells expressing Apg7-Myc, Apg3, and Apg8FG demonstrated three Apg8 related bands on urea-SDS-PAGE gel (Fig. 36). The fast migrating band corresponded to Apg8-PE in yeast (Fig. 38). Another middle migrating band corresponded to Apg8FG of yeast (Fig. 38). The upper band of Apg8FG was unknown, although it was found in the cells expressing Apg8FG alone (data not shown). In addition, the two different migrating bands of Apg8FG on urea-SDS-PAGE gel became a single band on normal SDS-PAGE gel, suggesting that the upper band of Apg8FG are possibly a kind of conformances (data not shown). As shown in Fig. 36, by immunoblot with anti-Apg8 antibody, two bands (upper and middle) were observed in both cells expressing Apg8FG, whereas the fast migrating band was detected in only the cells expressing all components of Apg8 system. When these cell lysates separated to supernatant and pellet fraction by centrifugation at 100 k *g* for 60 min, almost Apg8FG band (upper and middle) remained in S100 fraction, but most of fast migrating band was recovered to P100 fraction (Fig. 37). These results clearly indicated that Apg8FG was modified via Apg7 and Apg3. Next, I examined the modification of Apg8FG in *E. coli* using $Apg7^{C507S}$ and $Apg3^{C234S}$ mutant protein. Cells co-expressing either $Apg7^{C507S}$-Myc or $Apg3^{C234S}$ and other components of Apg8 system were grown in LB supplemented with 0.2% arabinose, Amp, and Cm for 3 h. Harvested cells were suspended in SDS-PAGE sample buffer and boiled for 5 min, and subjected to urea-SDS-PAGE. Immunoblot by using anti-Myc, anti-Apg3, and anti-Apg8 antibodies showed that the cells expressed any mutant form of Apg8 system, resulted in the loss of modified Apg8FG just like their non-expressing cells, ΔApg3 and ΔApg7 (Fig. 39). Furthermore, a conjugate band of Apg8FG-$Apg3^{C234S}$ was found in

cells expressing Apg3^{C234S}, depending on Apg7. The Apg8FG-Apg3^{C234S} conjugate was observed under reducing conditions, and corresponded to the ester bond of Apg8FG-Apg3^{C234S} in yeast (Fig. 34 and 39). These results suggested that enzymatic reactions on Apg8 system in *E. coli* succeed and resulted in a modified Apg8FG (Fig. 37, 38, and 39). The ester bond of Apg8FG-Apg7^{C507S}-Myc was not found in the cells expressing Apg7^{C507S}-Myc, but it was hardly detected even in yeast cells expressing Apg7^{C507S}, by unknown reason.

Characterization of modified Apg8FG by reconstituted Apg8 system in *E. coli*

To characterize the modified Apg8FG, cells expressing components of Apg8 system were disrupted in lysis buffer (10 OD_{600} unit/ml) by sonication as described in Materials and Methods, resulting lysates were separated to supernatant and pellet fraction by centrifugation at 200 k *g* for 17 h. Immunoblot analysis with anti-Apg8 antibody showed that most of modified Apg8FG was exclusively recovered into the pellet (P200), while Apg8FG and a portion of the modified Apg8FG distributed to the supernatant fraction (S200) (Fig. 40). These results agree with the fractionation by 100 k *g* for 60 min (Fig. 37). In previous analysis of Apg8-PE conjugate, Apg8-PE with mild alkaline treatment removed fatty acids from its PE and shifted to a band lower mobility as just Apg8FG. I tested this reaction to the modified Apg8FG in P200 fraction. The P200 fraction was treated with 0.06 M NaOH in 30% CH_3OH at 40℃ for 1 h, and subjected to urea-SDS-PAGE. Immunoblotting with anti-Apg8 antibody displayed a molecular size-shift of the modified Apg8FG by mild alkaline treatment (Fig. 40). Molecular size of the visualized band was very close to that of unmodified Apg8FG (Fig. 40). These results suggested that the Apg8FG might link to a glycerophospholipid, such as PE, via the reaction of Apg8 system components in *E. coli*.

Reconstituted Apg8 system in cell-free

Next, I reconstructed the biochemical reactions within Apg8 system by using cell-free system. For this purpose, I used wild-type and mutant form of Apg (Apg7^{C507S}-Myc or Apg3^{C234S}). These proteins were induced in *E. coli* by *araC*-P_{BAD} promoter for 6 h under the presence of 0.4% arabinose. The cells were harvested and suspended in lysis buffer (20 OD_{600} units/ml), and then the cells were disrupted by

sonication on ice. For the composition of Apg8 system, each lysate was mixed as follows (a ratio of volume); Apg7-Myc : Apg3, Apg8FG (1 : 2), Apg7^{C507S}-Myc : Apg3, Apg8FG (1 : 2), Apg7-Myc : Apg3^{C234S}, Apg8FG (1 : 2), and Apg7^{C507S}-Myc : Apg3^{C234S}, Apg8FG (1 : 2). Cell-free reaction of Apg8 system components was performed in the presence of ATP regeneration system (0.5 mM ATP, 10 mM $MgCl_2$, 10 mM phosphocreatine, and 5 μg creatine kinase) at 30℃ for 15 h. The reaction was terminated by the addition of SDS-PAGE sample buffer and boiling for 5 min. Obtained samples were subjected to urea-SDS-PAGE and immunoblotted with anti-Apg8 antibody. The immunoblotting showed that a portion of Apg8FG was converted to modified Apg8FG via reaction of Apg8 system in cell-free (Fig. 41).

Using mutant form of Apg (Apg7^{C507S}-Myc or Apg3^{C234S}) in the cell-free system, the modified Apg8FG never appeared. When there was Apg3^{C234S} in the cell-free reaction mixture, Apg8FG-Apg3^{C234S} conjugate via ester bond could be detected by immunoblotting with anti-Apg8 antibody, instead of the modified Apg8FG (Fig. 41). This conjugate of Apg8FG-Apg3^{C234S} depended on Apg7-Myc, because it was not found in the reaction mixture containing Apg7^{C507S}-Myc (Fig. 41).

The modified Apg8FG via cell-free reconstituted Apg8 system also disappeared by the presence of ATP depletion system (20 mM 2-deoxyglucose, 0.2 mg hexokinase) or 5 mM EDTA, and incubation at 4℃ (Fig. 42 and data not shown). These results indicated that the enzymatic reaction of Apg8 system is reconstituted in the cell-free system.

E. coli cytosolic factor is not required for *in vitro* Apg8 system reconstitution

Subcellular fractionation by *E. coli* cells, which carrying the three components of Apg8 system, revealed that modified Apg8FG distributes mainly in P100 (or P200) fraction. It also shows a little amount of modified Apg8FG in S100 (or S200) fraction. To investigate this population, I used purified Apgs. For the purification of each Apg involving in Apg8 system, I constructed GST-fusion Apgs (GST-Apg7-Myc, GST-Apg3, and GST-Apg8FG) based on pGEX vector. Resulting plasmids were introduced into *E. coli* (XL1blue), and then expression of GST-fusion proteins was induced by IPTG. GST-fusion Apgs were separated with gluthathione sepharose 4B and digested by thrombin. Purified Apgs were quantified by BCA assay, and confirmed with SDS-

PAGE gel by CBB staining. *In vitro* reconstitution of Apg8 system was carried out with following reaction mixture; *E. coli* total lysate (0.24 OD_{600} unit), Apg7-Myc (0.06 mg/ml) (2.0 μl: calculated 1.5 pmoles), Apg3 (0.3 mg/ml) (0.5 μl: calculated 4.0 pmoles), and Apg8FG (0.5 mg/ml) (0.2 μl: calculated 7.0 pmoles), under the presence of ATP regeneration system. After incubation at 30℃ for 15 h, the sample was subjected to urea-SDS-PAGE and immunoblotted with anti-Apg8 antibody. The immunoblotting showed the modified Apg8FG via *in vitro* reaction of Apg8 system components (Fig. 43). Thus, all purified Apgs was found to be functional. When S100 or P100 fraction was subjected to the *in vitro* reconstitution of Apg8 system, almost Apg8FG changed to modified form by the reaction with P100. On the other hand, S100 fraction partially generated the modified Apg8FG (Fig. 43). These results indicated that *in vitro* reaction of Apg8 system components leads the modification of Apg8FG and which efficiently occurs in the presence of *E. coli* P100 fraction. Accordingly, at least S100 factor of *E. coli* is not required for the modification of Apg8FG. A part of modified Apg8FG appeared in S100 fraction mixture either subcellular fractionation or *in vitro* reaction system, probably they are caused by contamination of small membrane fragments.

Modification of Apg8FG in cell-free Apg8 system depends on PE in *E.coli* membrane

Glycerophospholipids in *E. coli* cells consist of PE, phosphatidylglycerol (PG), and cardiolipin (CL). PE is a major glycerophospholipid (~75% of total) in the *E. coli*. Biosynthesis of PE requires phosphatidylserine (PS) and PS decarboxylase. PS synthase of *E. coli* is encoded by *pssA*. *E. coli*, GN10 is a *pssA* null mutant of W3110 (wild-type), thus indicating PE-defective phenotype, which is viable in the presence of high Mg^{2+} (Kikuchi et al., 2000). It has been previously observed that GN10 is devoid of PE. To confirm it in this study, I checked the total phospholipids in the GN10 and W3110. These cells were grown in LB (for W3110) or LB supplemented with 50 mM $MgCl_2$ (for GN10) at 37℃ to stationary phase, and harvested by centrifugation (10 g wet-weight cells). Total phospholipids of the cells were extracted by chloroform/methanol/water (1/2/0.8), then recovered in the chloroform fraction. Resulting total phospholipids were separated by two-dimensional TLC. After iodine

staining, each spot of phospholipids was identified and quantified. Iodine stained PE can be observed abundantly in W3011, but not in GN10. Further, phospholipid compositions are PE/PG/CL/phosphatidic acid (PA) (75.4/16.6/8.59/3.57) in W3110, whereas PE/PG/CL/PA (<0.01/52.6/33.6/11.4) in GN10. These results corresponded to the published results (Kikuchi et al., 2000). By using GN10 cell lysate, modification of Apg8FG was investigated in the cell-free reaction of Apg8 system components. GN10 and W3011 were grown in LB supplemented with 50 mM $MgCl_2$ to OD_{600} =1.5 at 37℃. Total cell lysates were prepared by previous methods (20 OD_{600} units/ml lysis buffer), then *in vitro* reconstitution of Apg8 system was carried out by the following reaction mixture; *E. coli* total lysate (0.2 OD_{600} unit), Apg7-Myc (1 μl: calculated 0.64 pmoles), Apg3 (0.5 μl: calculated 1.0 pmol), and Apg8FG (0.07 μl: calculated 0.9 pmoles), under the presence of ATP regeneration system. The reaction sample was incubated at 30℃ for 15 h, then subjected to urea-SDS-PAGE, and analyzed by immunoblotting with anti-Apg8 antibody. The immunoblotting showed the modified Apg8FG via the cell-free reaction of Apg8 system components with W3110 total lysate (Fig. 44). However, using GN10 total lysate in this experiment, modified form of Apg8FG was not detected (Fig. 44). These results clearly indicated that PE is a requisite for the modification of Apg8FG.

***In vitro* reaction of Apg8 system components results in Apg8-PE**

To identify the modified form of Apg8FG via *in vitro* reaction of Apg8 system components, I used liposome in the *in vitro* study. Total phospholipids in W3110 and GN10 were extracted as described above. The resulting *E. coli* total phospholipids (1 μmol) were transferred to glass tube, and chloroform was removed by rotary evaporater. Generated lipid film was further dried in desiccator under vacuum for 20 min. The lipid film was suspended in 1 ml TBS (10 mM Tris-HCl, pH 7.4, 150 mM NaCl) by vortexing to form multilamellar liposome (1 mM total lipids). Unilamellar liposome was prepared from the multilamellar liposome by sonic treatment on ice. I tested a complete *in vitro* reconstituted Apg8 system using liposome by the following reaction mixture; liposome (total lipid: 5 nmoles), Apg7-Myc (1 μl: calculated 0.64 pmoles), Apg3 (0.5 μl: calculated 1.0 pmol), and Apg8FG (0.07 μl: calculated 0.9 pmoles) under the presence of ATP regeneration system. After incubation at 30℃ for 15 h, reaction

was terminated by addition of SDS-PAGE sample buffer. The sample was subjected to urea-SDS-PAGE, and analyzed by immunoblotting with anti-Apg8 antibody. In this *in vitro* reaction of Apg8 system components, by using a total lipid liposome derived from W3011, the modified form of Apg8FG was shown (Fig. 45). When used total lipid liposome derived from GN10, the modified Apg8FG was not detectable (Fig. 45). However, using PE-liposome, in which contains GN10 total lipids and *E. coli* PE, the *in vitro* Apg8 system reaction resulted in modified form of Apg8FG (Fig. 45). Also, the modification of Apg8FG was observed with PE dose dependency within 65-85% PE content of total lipids, suggesting that there is an appropriate PE content of liposome (as described below) (Fig. 45). Surprisingly, *in vitro* reaction of Apg8 system components by using 100% *E. coli* PE-liposome demonstrated the modified Apg8FG (Fig. 46). Hence, I concluded that the modified Apg8FG, by reconstituted reaction in Apg8 system, is Apg8-PE. Apg8-PE formation is accomplished completely by only its conjugation system (Apg7, Apg3, and Apg8FG) and its target (PE) in the presence of ATP but not other molecule as such E3-like protein.

Apg8-PE conjugation depends on PE content of liposome

Apg8FG conjugates with PE via its reconstituted reaction by *in vitro* and in *E. coli*. Using yeast total lipid liposome, a small amount of Apg8FG was converted to Apg8-PE by *in vitro* reaction of Apg8 system components (Fig. 45). In contrast, *E. coli* total lipid liposome accumulates a significant amount of Apg8-PE by the same experiments (Fig. 45). Total phospholipid of yeast (SEY6210) was quantified, and then their composition was calculated. The phospholipid of *E. coli* includes approximate 75% PE, as previous described, whereas that of yeast showed a lower concentration of PE as follows, PE/PC/PS/phosphatidylinositol (PI) (16.6/51.7/13.7/18.0). It is implying that the PE content of liposome affects the Apg8-PE conjugation. To investigate the PE dose effect, I made *E. coli* PE-liposome based on GN10 total lipids, whose PE content increases as indicating ratio (0~100%) (Fig. 46). *In vitro* reconstituted conjugation system of Apg8-PE was carried out by the following reaction mixture; liposome (total lipid: 5 nmol), Apg7-Myc (1 μl: calculated 0.64 pmoles), Apg3 (0.5 μl: calculated 1.0 pmol), Apg8FG (0.07 μl: calculated 0.9 pmoles), and ATP regeneration system, then *in vitro* reaction and immunoblot analysis with anti-

Apg8 antibody were performed as described previously. Apg8-PE appeared in the reaction mixture containing 20% PE-liposome (Fig. 46). The conjugate of Apg8-PE gradually increased in the reaction from 20% PE to 50% PE-liposome, and it seems to be saturated within 50-80% PE-liposome (Fig. 46). Interestingly, the amount of Apg8-PE decreased in the reaction from 80% PE to 100% PE-liposome (Fig. 46). From these results, I conclude that 50-80% PE content per liposome efficiently drives the conjugation reaction of Apg8-PE. This composition (50-80%) of PE-liposome resembles that of *E. coli* membrane.

E. coli total lipid liposome whose abundant PE influences their membrane structure, it is known to be a non-bilayer. To assess the lipid structural effect on Apg8-PE conjugation, I used two different lipid liposomes, which contained dioleoylphosphatidylethanolamine (DOPE) and 1-palmitoyl-2-oleoylphoshatidylcholine (POPC). Lipid bilayer structures are stabilized depending upon the concentration of POPC. *In vitro* reconstituted reaction in Apg8 system was designed by the following mixture; Apg7-Myc (1 μl: calculated 0.64 pmoles), Apg3 (0.5 μl: calculated 1.0 pmol), Apg8FG (0.07 μl: calculated 0.9 pmoles), and each indicated 5.0 nmoles total lipids liposome (DOPE/GN10 liposome (PE content 70%), or DOPE/POPC liposome (PE content 0, 10, 20, 50, 75, or 100%)), and ATP regeneration system. *In vitro* reaction and immunoblot analysis were performed as previous described. Immunoblotting with anti-Apg8 antibody showed that using DOPE/GN10 liposome (70% DOPE), the *in vitro* reaction yielded a sufficient Apg8-PE (Fig. 47). The resulting Apg8-PE by 70% DOPE and *E. coli* PE indicated a comparable activity (Fig. 46 and 47). Using DOPE/POPC liposome in this test, Apg8-PE was observed under the presence from 50% to 100% DOPE per DOPE/POPC liposome (Fig. 47). Importantly, 20% DOPE per DOPE/POPC liposome did not link to the Apg8FG. Further, the Apg8-PE conjugate is strongly accumulated at 75% PE content per DOPE/POPC liposome than 50% PE content (Fig. 47). The attachment of Apg8FG to DOPE significantly reduces by the shift from 75% to 100% DOPE per DOPE/POPC liposome (Fig. 47). These results suggested that high amount of POPC, forming a lipid bilayer, do not enhance the activity on Apg8-PE conjugate reaction.

I next analyzed the inhibitory effect on Apg8-PE conjugation under the PE rich conditions. *In vitro* reconstitution of Apg8-PE conjugation system was carried out by

the following reaction mixture; Apg7-Myc (1 μl: calculated 0.64 pmoles), Apg3 (0.5 μl: calculated 1.0 pmol), Apg8FG (0.07 μl: calculated 0.9 pmoles), ATP regeneration system, and either *E. coli* total lipid liposome or 100% PE-liposome (*E. coli* total lipid liposome containing 0.095-5.278 nmoles PE, and PE liposome containing 0.005-5.0 nmoles PE) (Fig. 48 and 49). *In vitro* reaction and immunoblot analysis with anti-Apg8 antibody were performed as described previously. The conjugation of Apg8FG to PE in liposomes of *E. coli* total lipid was observed weakly at as low as 0.189 nmoles PE per reaction mixture, then the Apg8-PE conjugation increased at 0.754 nmoles PE per reaction mixture (Fig. 48). The signal of Apg8-PE was not changed from 0.754 to 5.278 nmoles PE per reaction mixture (Fig. 48). On the other hand, Apg8-PE conjugation with PE liposome was not recovered by the low PE in a reaction mixture, even when PE content was reduced from 5.0 to 0.5 nmoles (Fig. 49). Thus, high concentration of PE in a reaction mixture does not prevent the conjugation of Apg8-PE, although high PE contents liposome shows a defect in the conjugation of Apg8-PE (Fig. 49). These results and previous shown results suggested that appropriate PE content of liposome accumulates the Apg8-PE conjugate, and its optimal PE contents in liposome is approximate 70%.

High amounts of Apg7 and Apg3 stimulate the Apg8-PE conjugation *in vitro*

As previous shown, *in vitro* reconstitution experiments of Apg8-PE conjugate showed that a significant amount of free Apg8FG remained in the reaction mixture despite whose high PE content (Fig. 49). I searched the optimal conditions for Apg8-PE conjugation reaction by varying molecular ratio of Apg7-Myc : Apg3 : Apg8FG. Reconstitution of Apg8FG conjugate with PE *in vitro* was carried out by using 5.0 nmoles *E. coli* total lipid liposome, purified Apgs, and ATP regeneration system. Purified Apgs, Apg7-Myc, Apg3, and Apg8FG respectively were added to the reaction mixture at the indicated varying molecular ratio (Fig. 50). Reaction mixtures were incubated at 30℃ for 15 h, and subjected to urea-SDS-PAGE. Immunoblotting with anti-Apg8 antibody showed that Apg8-PE conjugate activity was affected by the molecular ratio of Apg8 system components (Fig. 50). Standard molecular ratio of the Apg8 system components was adjusted by a volume ratio of 1 : 1 : 1 (μl) (Apg7-Myc : Apg3 : Apg8FG), of which calculated molar value indicated 0.64 : 1.0 : 0.9 (pmol), and

this molecular ratio was the same condition on the previous *in vitro* studies. By using 3- or 6-fold Apg7-Myc (Apg7-Myc : Apg3 : Apg8FG = 3 : 1 : 1 or 6 : 1 : 1(μl)), the product of Apg8-PE increased slightly (Fig. 50). Similar effects were observed, when the reaction contained 3- or 6-fold Apg3 (Apg7-Myc : Apg3 : Apg8FG = 1 : 3 : 1 or 1 : 6 : 1(μl)). When the reaction mixtures were composed by 3- or 6-fold both Apg7-Myc and Apg3 (Apg7-Myc : Apg3 : Apg8FG = 3 : 3 : 1, 6 : 3 : 1, 3 : 6 : 1, or 6 : 6 : 1(μl)), Apg8-PE conjugation significantly stimulated, therefore most of free Apg8FG changed to Apg8-PE (Fig. 50). High concentration of Apg8FG (3- or 6-fold) did not enhance the yield of Apg8-PE conjugate, but which increased for the more addition of Apg7-Myc and Apg3 (Fig. 50). These results suggested that Apg7 and Apg3 play a role of the E1 and the E2, respectively, although their action is not catalytic reaction through the *in vitro* reaction of Apg8 system. Accordingly, high amounts Apg7 and Apg3 might stimulate the Apg8FG conjugation to PE.

In vitro Apg8 system reaction shows loss of Apg8-PE by high amount of Apg8FG

In vitro reconstituted Apg8 system demonstrated the optimal molecular ratio of its Apg components that is Apg7 : Apg3 : Apg8FG = approximation 2 : 3 : 1 (mol). This molecular ratio implies that a large amount of Apg8FG fails the Apg8-PE conjugation system. I next tested the Apg8-PE conjugation system, under the presence of high concentrated Apg8FG, by using cell-free system. Cell extract was prepared from *E. coli* cells co-expressing Apg7-Myc and Apg3, both of which were induced by *araC*-P_{BAD} promoter for 6 h supplemented with 0.2% arabinose. Resulted total lysate contained Apg7-Myc and Apg3, and showed a sufficient activity for Apg8-PE conjugation in the cell-free system (data not shown). Each concentration of purified Apg8FG (0.1, 0.5, and 5.0 μg) was added in the above total lysates (0.56 OD_{600} unit) containing Apg7-Myc and Apg3, and incubated with ATP regeneration system at 30℃ for 15 min, 1 h, and 3 h. Reaction samples were suspended in SDS-PAGE sample buffer, and then equivalent volume of Apg8 was subjected to urea-SDS-PAGE. The immunoblot analysis with anti-Apg8 antibody showed that the product of Apg8-PE increased in a time-dependent manner (Fig. 51). The reaction samples containing low amounts of Apg8FG (0.1 or 0.5 μg) efficiently accumulated the Apg8-PE, but high Apg8FG amount (5.0 μg) did not (Fig. 51). 0.1 μg and 0.5 μg Apg8FG samples

demonstrated the time dependent production of Apg8-PE. Moreover, 0.1 μg Apg8FG promoted Apg8-PE conjugate reaction at the early time (15 min), than 0.5 μg Apg8FG (Fig. 51). These results suggested that high concentration of Apg8FG is inhibitory in Apg8-PE conjugation system.

The rate of conjugate reaction of Apg8-PE

To elucidate the conjugation mechanism of Apg8-PE, I observed the conjugate of Apg8FG to PE *in vitro* reconstituted Apg8 system in a time-dependent manner. For this experiment, I reconstituted Apg8 cell-free system by using Apg7-Myc, Apg3 lysate (0.56 OD_{600} unit) and purified Apg8FG (0.02μg), as previous described. The cell-free reaction mixture was incubated at 30℃ for 60 min in the presence of ATP regeneration system. A portion of reaction mixture was taken every 10 minutes, and then its reaction terminated by the addition of SDS-PAGE sample buffer. Resulted samples were subjected to urea-SDS-PAGE, and immunoblot analysis was carried out by anti-Apg8 antibody. The immunoblting revealed the appearance of Apg8-PE at 20 min, then the amounts of Apg8-PE increase to 60 min. The resulting signal intensity of Apg8-PE demonstrates a non-linear increase of Apg8-PE to the time course (Fig. 52). I measured and estimated the quantity of Apg8-PE by using NIH image. The accumulation of Apg8-PE from 20 min to 30 min was apparently different from that of over 30 min. This result indicated that there is a lag phase in the Apg8-PE conjugation reaction (Fig. 52).

Intracellular distribution of expressed Apg7, Apg3 and Apg8 by P_{BAD} promoter in *E. coli*

Next, I examined the cellular distribution of expressed Apg8 system components in *E. coli*. Cells were transformed with Apg8 system component encoded plasmids, which expressing Apg7-Myc, Apg7C507S-Myc, Apg3, Apg3C234S, and Apg8FG via P_{BAD} promoter, respectively. Resulted transformants were grown in LB supplemented with Amp and/or Cm. Respective Apgs were induced by addition of 0.2% arabinose for 3 h, then cells were harvested and suspended into lysis buffer (10 OD_{600} unit/ml) as described in Material and Methods. These cells were disrupted by sonication on ice, and cell debris was removed by centrifuge at 5 k rpm for 5 min.

Resulted total lysate (total) was separated to supernatant (S100) and pellet (P100) fraction by centrifugation at 100 k *g* for 1 h. Each fraction was subjected to SDS-PAGE and analyzed by immunoblot using anti-Myc, anti-Apg3 and anti-Apg8 antibody. The immunoblotting showed that Apg7-Myc distributes equally both S100 and P100 fraction. Apg8-PE mainly located in P100 fraction, whereas a part of Apg8-PE was shown into S100 fraction as previous observation (Fig. 53). Apg3 and Apg8FG were detected predominantly in S100 fraction (Fig. 53). Interestingly, whereas Apg3 exclusively fractionated to S100 fraction, a small amount of Apg3 distributed to P100 fraction in the presence of Apg7-Myc (Fig. 53). I have found a complex of Apg7-Apg3 in yeast as previously described. These results suggested that Apg7 and Apg3 cooperates to promote the Apg8-PE conjugate reaction.

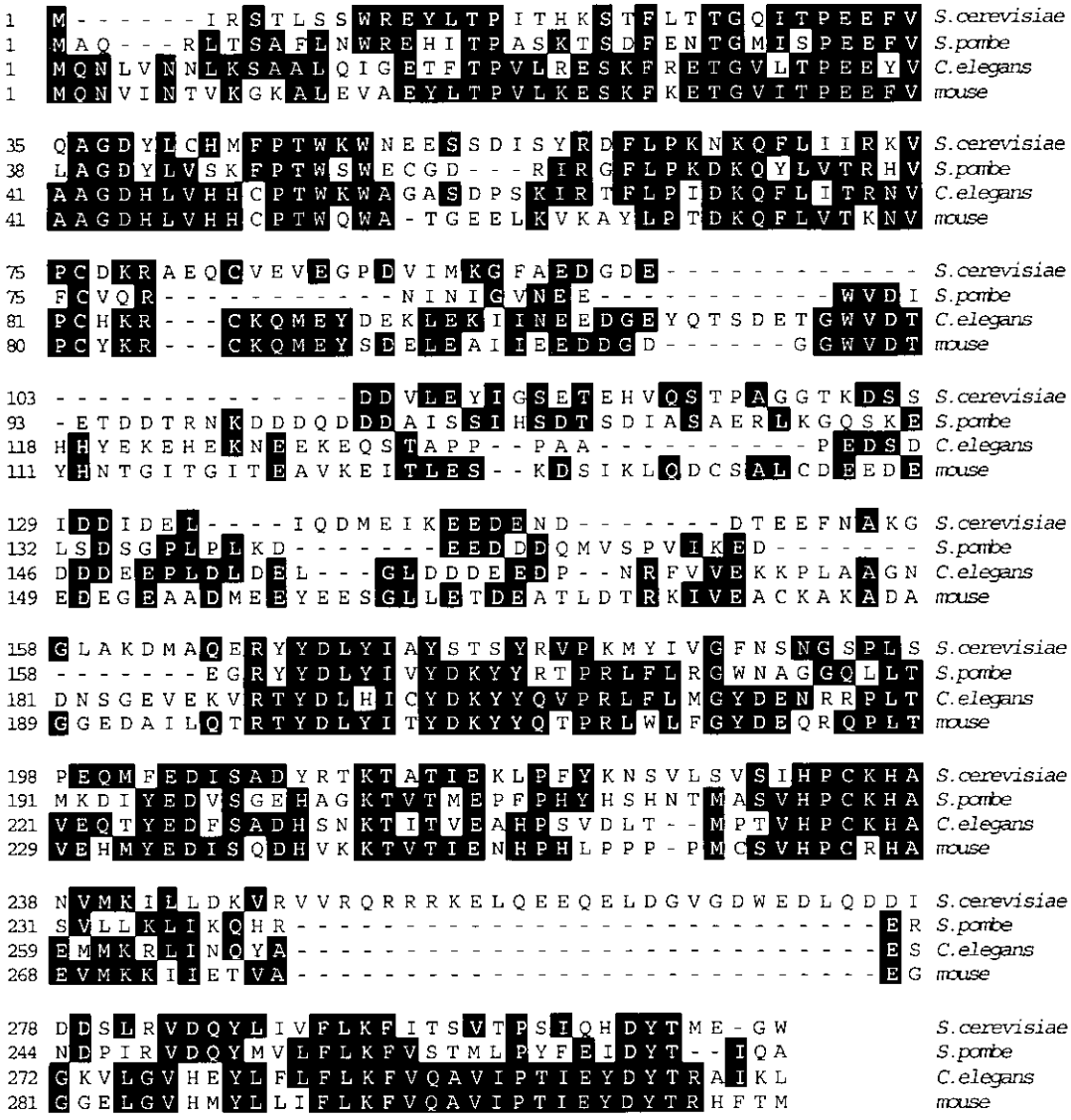

Figure 2. Amino acid sequence of Apg3 in yeast and its homologues in other species.

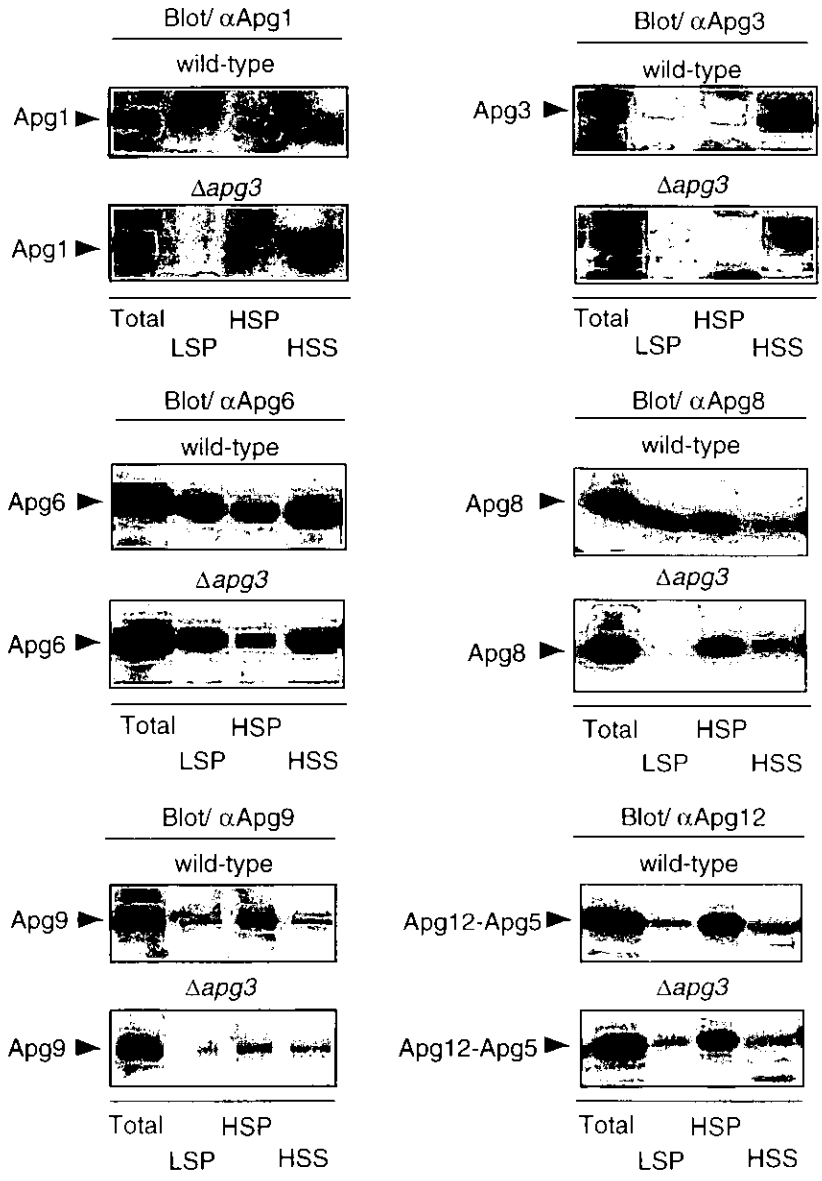

Figure 3. Subcellular distribution of Apg proteins in *Δapg3*.

Wild-type and *Δapg3* cells were grown in YEPD at 30℃ to OD_{600} =1.0, and converted to spheroplasts as described in Material and Methods. Spheroplasts were suspended in lysis buffer (0.2 M sorbitol, 20 mM PIPES-KOH, pH 6.8, 1 mM PMSF, and protease inhibitor cocktail) and osmotically lysed on ice for 5min. The lysate was centrifuged at 2,000 rpm for 5 min at 4℃ to remove debris. Resulted lysate (Total) was centrifuged at 13 k *g* for 15 min to separate the supernatant (LSS) and the pellet (LSP). The supernatant (LSS) was recentrifuged at 100 k *g* for 1 h at 4℃ to generate the pellet (HSP) and supernatant (HSS). Each fraction was subjected to SDS-PAGE and analyzed by immunoblotting with anti-Apg1, anti-Apg3, anti-Apg6, anti-Apg8, anti-Apg9, and anti-Apg12 antibodies.

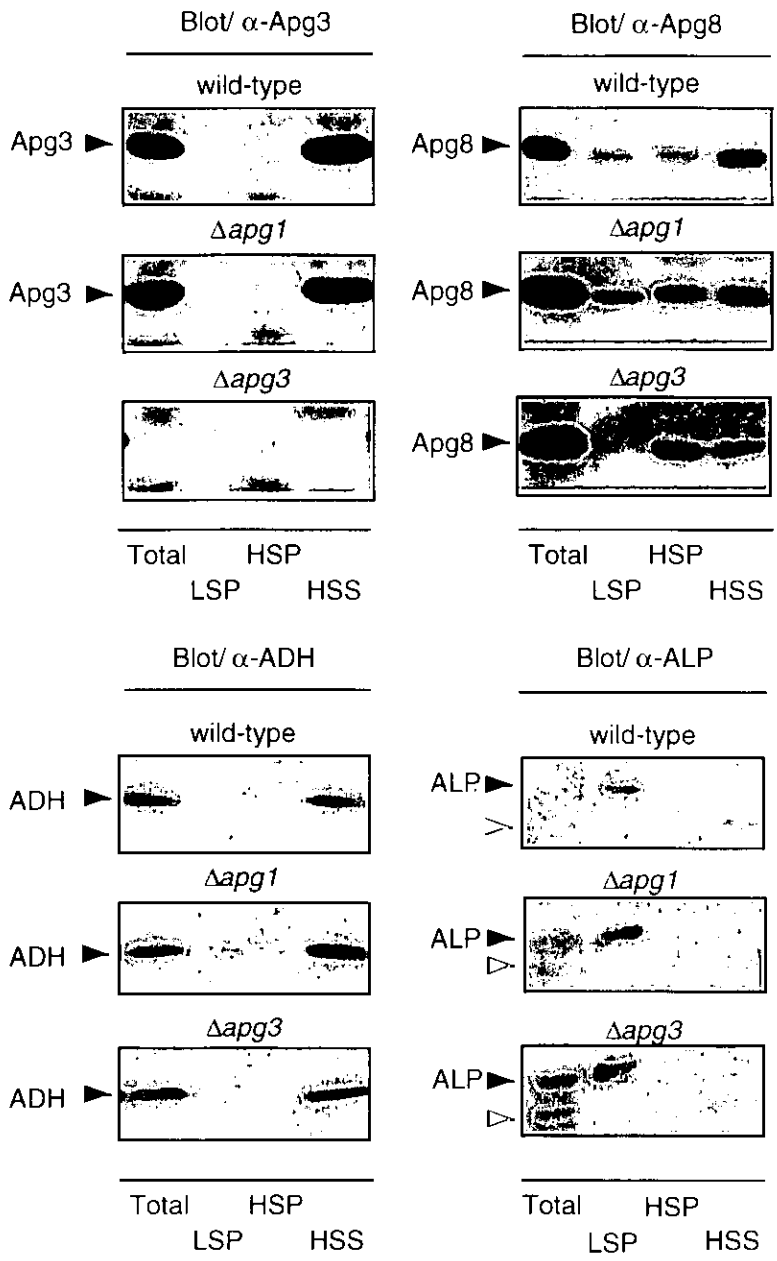

Figure 4. Subcellular distribution of Apg8 in *Δapg1* and *Δapg3*.

Wild-type, *Δapg1*, *Δapg3*cells were grown in YEPD at 30℃ to OD_{600}=1.0, and converted to spheroplasts as described in Material and Methods. Subcellular fractionation was performed as Fig. 2 and each fraction was subjected to SDS-PAGE and analyzed by immunoblotting with anti-Apg3, anti-Apg8, anti-ADH, and anti-ALP antibodies. ADH indicates a cytosolic marker. ALP is a vacuolar marker (arrow head; mature form, open arrow head; proteolytic product).

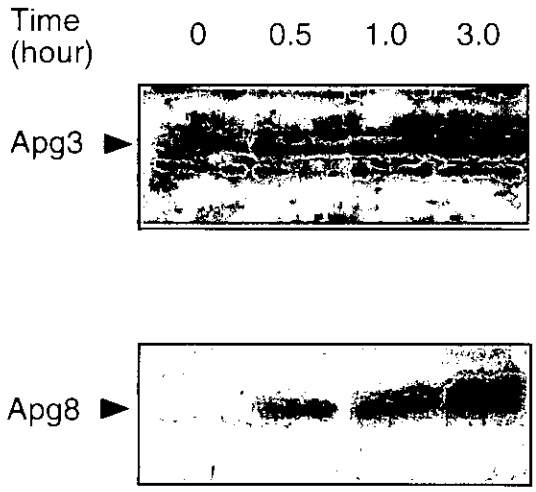

Figure 5. The amount of Apg3 increased under starvation conditions.

Wild-type cells were grown in YEPD at 30℃ to OD_{600} =0.8, and the cells were resuspended in SD(-N) and incubated at 30℃ (0 h). At the indicated time, the cells were harvested and disrupted by vortexing with glass beads. After removing cell debris by centrifugation at 5,000 rpm, the resulting total lysate (20 μg protein) was subjected to immunoblot analysis using anti-Apg3 or anti-Apg8 antibodies.

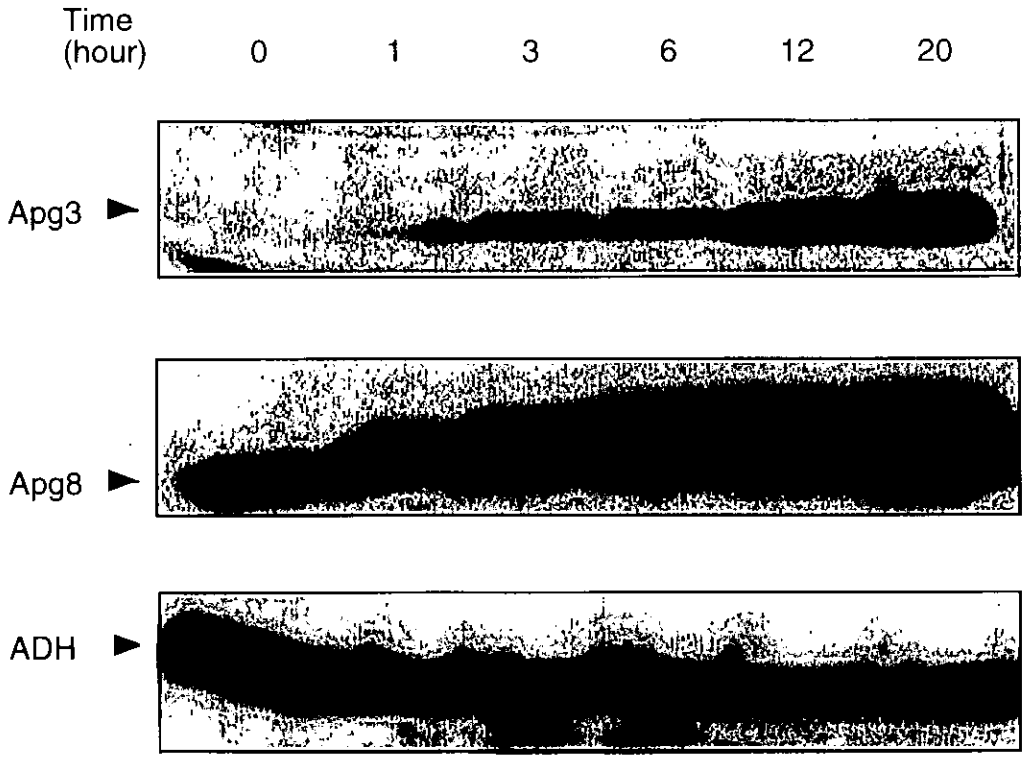

Figure 6. The amount of Apg3 increased in late-log phase cells.

Wild-type cells were pre-cultured in YEPD at 30℃ to logarithmic phase. The cells were diluted to OD_{600} =0.5 in YEPD, then the incubation started at 30℃ (0 h). At the indicated time, the cells were harvested and lysed in NaOH/2-mercaptoethanol. Total protein was recovered with cold-aceton precipitation and suspended in SDS-PAGE sample buffer. The resulted sample (50 OD_{600} unit/ml) of which equivalent amounts were subjected to immunoblot analysis using anti-Apg3, anti-Apg8, or anti-ADH antibodies.

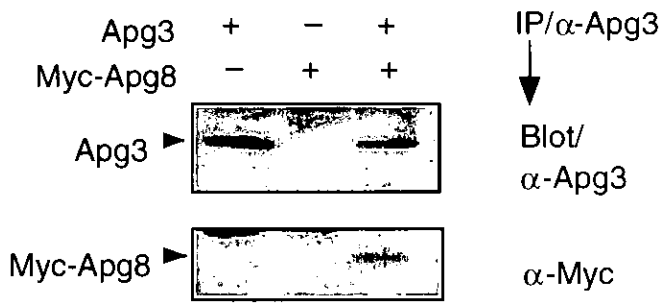

Figure 7. Apg8 interacts physically with Apg3.

Δapg8 cells harboring pRS426-Myc-Apg8 (2μ: multicopy plasmid) were grown in YEPD at 30℃ to OD_{600} =1.0. Cell lysate was prepared by vortexing with glass beads. Resulted lysate was immunoprecipitated with anti-Apg3 antibody. Co-immunoprecipitated proteins were suspended in SDS-PAGE sample buffer and subjected to SDS-PAGE. The immunoblot analysis was performed with anti-Apg3 or anti-Myc antibody.

Figure 8. The interaction between Apg8 and Apg3 requires Apg4 processing.

Wild-type (wt), *Δapg1*, *Δapg3*, and *Δapg4* cells were transformed with pRS426-HA-Apg8 (2μ; multicopy plasmid). The transformants were grown in YEPD at 30℃ to OD_{600} =1.0, and each cell lysate was obtained by vortexing with glass beads. The lysate was subjected to immunoprecipitation with anti-HA antibody and analyzed by immunoblotting with anti-Apg3 or anti-HA antibody.

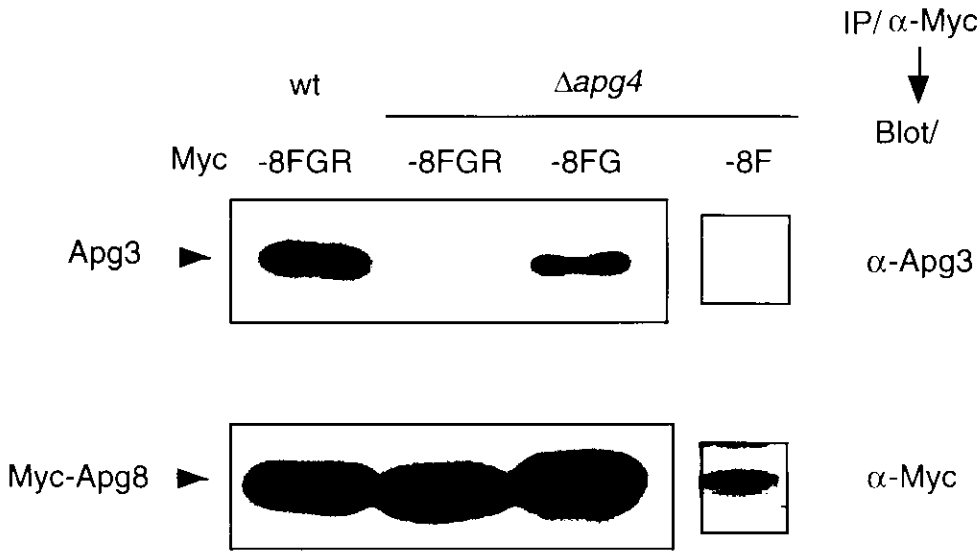

Figure 9. Apg8 C-terminus Gly is essential for the physical interaction to Apg3.

Wild-type (wt) cells were co-transformed with pRS425-Apg3 (2μ) and pRS426-Myc-Apg8FGR (2μ). Δ*apg4* cells were co-transformed with pRS425-Apg3 and either pRS426-HA-Apg8FGR, -HA-Apg8FG, or -HA-Apg8F. The transformed cells were grown in YEPD at 30℃ to OD_{600} =1.0. Each cell lysate was obtained by vortexing with glass beads, then subjected to immunoprecipitation with anti-HA antibody. The resulting immunocomplexes were analyzed by immunoblotting with anti-HA or anti-Apg3 antibody.

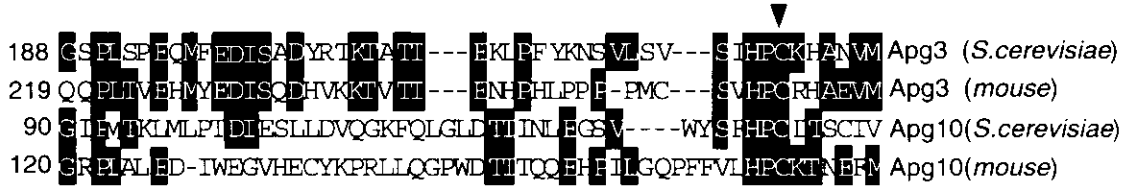

Figure 10. Homology between Apg3 and Apg10 at the active site regions.

Arrowhead indicates active site at cycteine-133 of Apg10 and its corresponding cysteine-234 of Apg3.

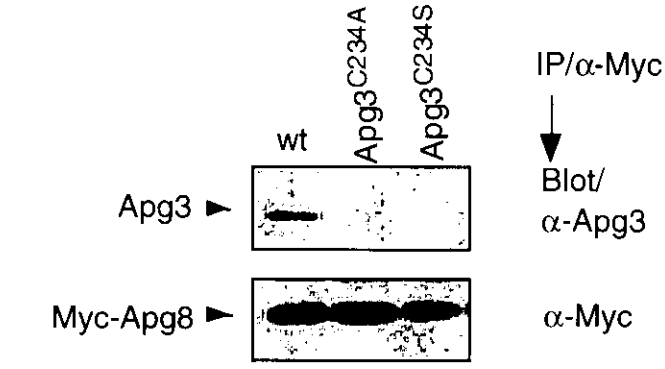

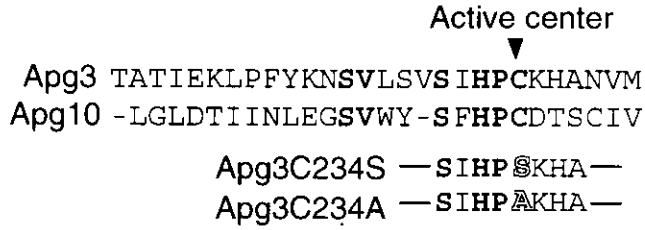

Figure 11. The interaction of Apg8 and Apg3 requires Cys234 residue of Apg3.

Wild-type cells were transformed with pRS426-Myc-Apg8 (2μ). Δ*apg3* cells were co-transformed with pRS426-Myc-Apg8 and either pRS425-Apg3C234A (2μ) (Cys234 in Apg3 replaced by arginine) or pRS425-Apg3C234S (2μ) (Cys234 in Apg3 replaced by serine). The transformed cells were grown in YEPD at 30℃ to OD_{600} =1.0. Each cell lysate was obtained by vortex disruption with glass beads, then subjected to immunoprecipitation with anti-Myc antibody. The immunocomplexes were analyzed by immunoblotting with anti-Apg3 or anti-Myc antibody.

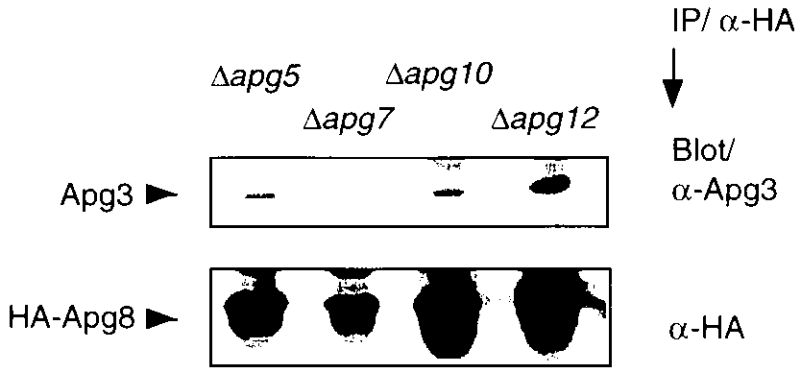

Figure 12. The interaction of Apg8 and Apg3 requires Apg7.

Δapg5, *Δapg7*, *Δapg10*, and *Δapg12* cells expressing HA-Apg8 (2μ) were grown in YEPD at 30℃ to OD_{600} =1.0. Each cell lysate was obtained by vortexing with glass beads, then subjected to immunoprecipitation with anti-Myc antibody. The immunocomplexes were analyzed by immunoblotting with anti-Apg3 or anti-HA antibody.

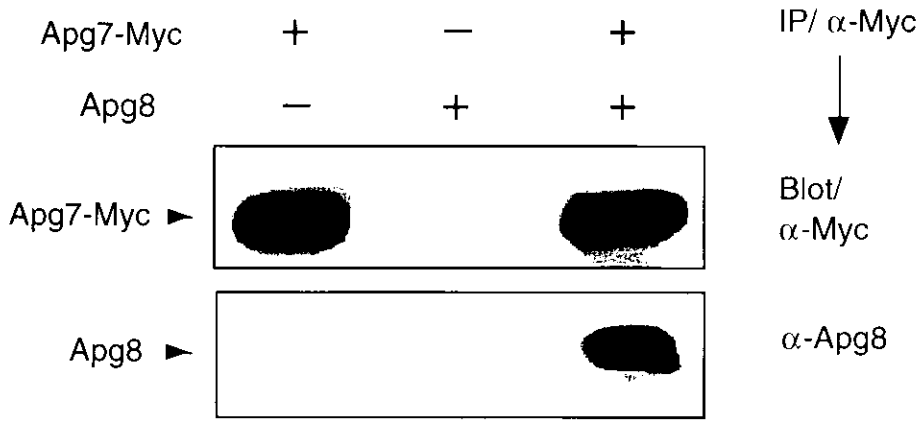

Figure 13. Apg8 interacts physically with Apg7.

The *Δapg7Δapg8* cells were transformed with pRS424-Apg7-Myc (2μ) and/or pRS426-Apg8 (2μ), and grown in YEPD at 30℃ to OD_{600} =1.0. Each cell lysate was obtained by vortexing with glass beads, then subjected to immunoprecipitation with anti-Myc antibody. The immunocomplexes were analyzed by immunoblotting with anti-Myc or anti-Apg8 antibody.

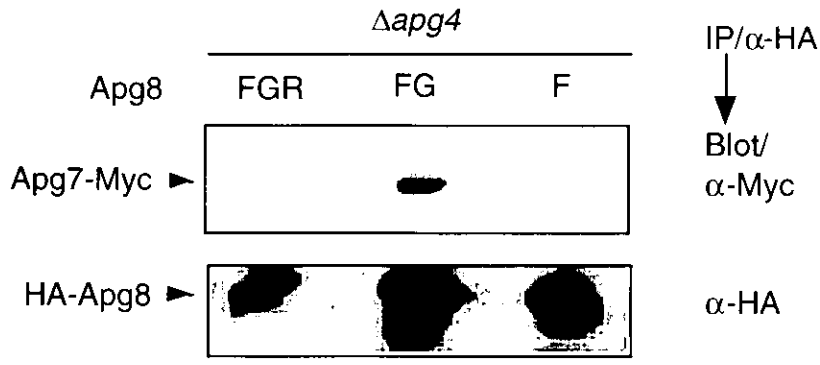

Figure 14. Apg8 C-terminus Gly is essential for the physical interaction to Apg7.

The *Δapg4* cells were co-transformed with pRS424-Apg7-Myc (2μ) and either pRS426-HA-Apg8FGR, -HA-Apg8FG, or -HA-Apg8F (2μ). The transformed cells were grown in YEPD at 30℃ to OD_{600} =1.0. Each cell lysate was obtained by vortex disruption with glass beads, then subjected to immunoprecipitation with anti-HA antibody. The immunocomplexes were analyzed by immunoblotting with anti-Myc or anti- HA antibody.

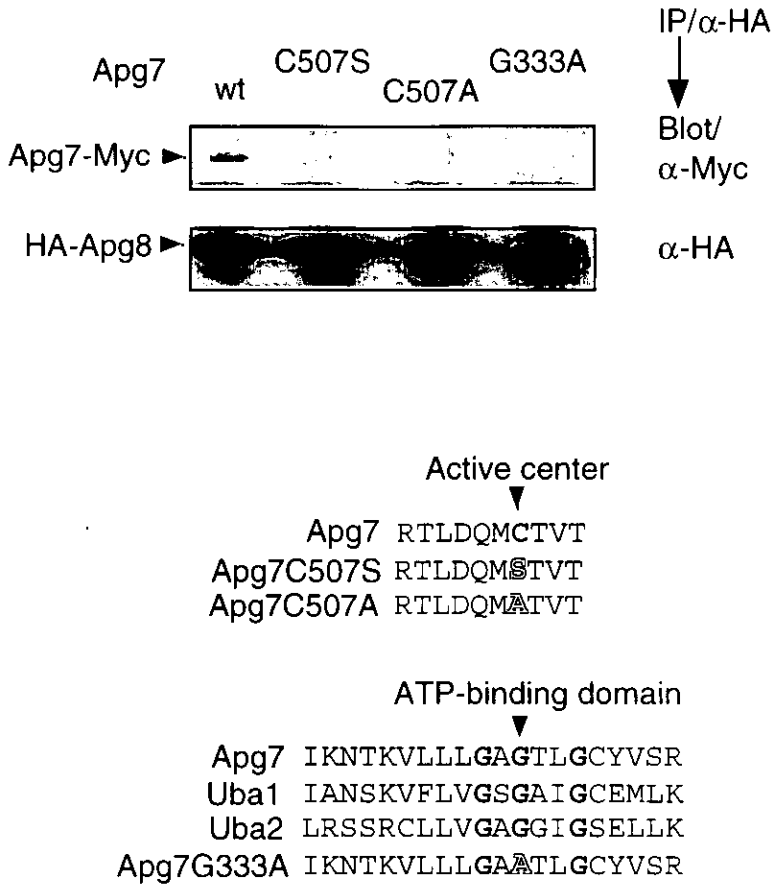

Figure 15. Mutant forms of Apg7 is defective in the association to Apg8.

The *Δapg7Δapg8* co-expressing HA-Apg8 (2μ) and either Apg7-Myc (wt), Apg7C507S-Myc (Cys507 of Apg7 replaced by serine), Apg7C507A-Myc (Cys507 replaced by alanine), or Apg7G333A-Myc (Gly333 replaced by alanine) (*CEN*) cells were grown in YEPD at 30℃ to OD_{600} =1.0. Each cell lysate was obtained by vortex disruption with glass beads, then subjected to immunoprecipitation with anti-HA antibody. The resulting immunocomplexes were analyzed by immunoblotting with anti-Myc or anti-HA antibody.

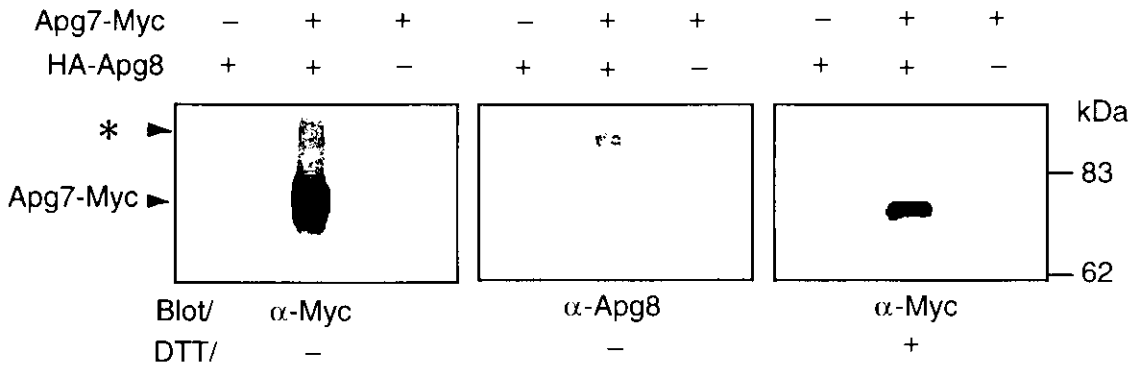

Figure 16. Apg8 conjugated with Apg7 via thioester bond.

The *Δapg7Δapg8* co-expressing HA-Apg8 (2μ) and/or Apg7-Myc (2μ) cells were grown in YEPD at 30℃ to OD_{600} =3.0. Each cell lysate was obtained by vortexing with glass beads, then subjected to immunoprecipitation with anti-HA antibody. The resulting immunocomplexes were subjected to SDS-PAGE with or without 100 mM DTT and analyzed by immunoblotting with anti-Myc or anti-Apg8 antibody. * indicates Apg8-Apg7 conjugate.

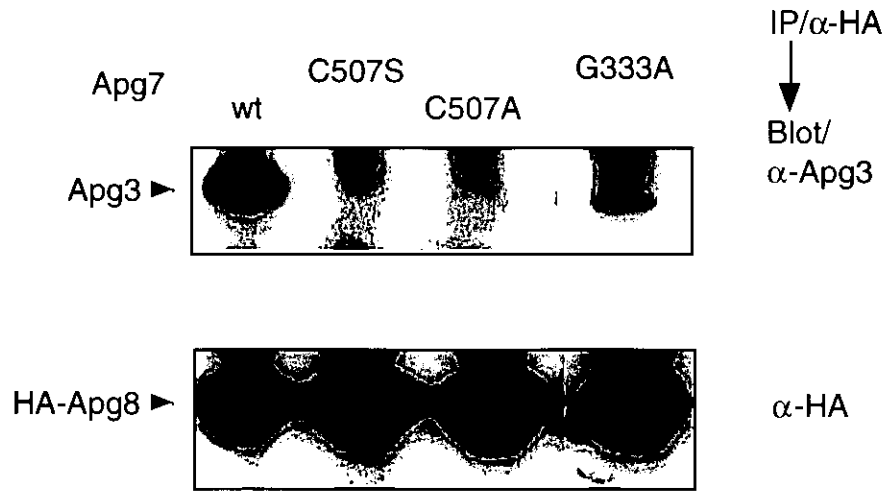

Figure 17. Mutant forms of Apg7 are defective in the interaction of Apg3-Apg8.

The *Δapg7Δapg8* cells co-expressing HA-Apg8 (2μ) and either Apg7-Myc (wt), Apg7C507S-Myc (C507S), Apg7C507A-Myc (C507A), or Apg7G333A-Myc (G333A) (CEN) were grown in YEPD at 30℃ to OD_{600} =1.0. Each cell lysate was obtained by vortexing with glass beads, then subjected to immunoprecipitation with anti-HA antibody. The resulting immunocomplexes were analyzed by immunoblotting with anti-Apg3 or anti- HA antibody.

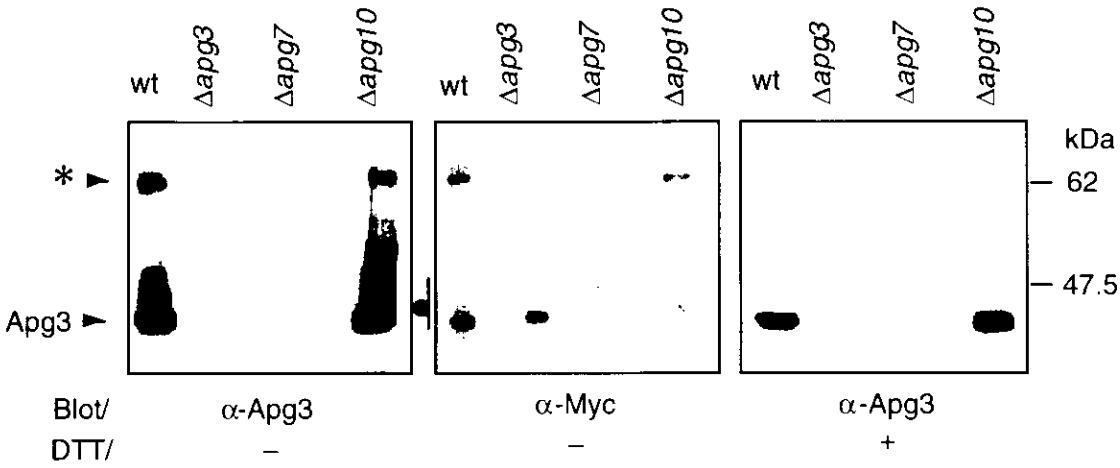

Figure 18. Apg8 conjugated with Apg3 via thioester bond.

The *Δapg3Δapg8* cells expressing Apg3 (2μ) and/or Myc-Apg8 (2μ) were grown in YEPD at 30℃ to OD_{600} =3.0. Each cell lysate was obtained by vortexing with glass beads, then subjected to immunoprecipitation with anti-Myc antibody. The resulting immunocomplexes were subjected to SDS-PAGE with or without 100 mM DTT and analyzed by immunoblotting with anti-Apg3 or anti-Myc antibody. * indicates Apg8-Apg3 conjugate. ● indicates non-specific signal.

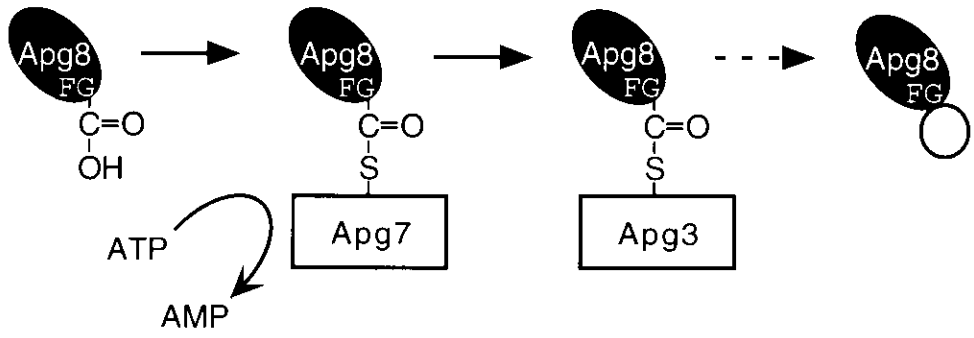

Figure 19. Ubiquitination-like pathway of Apg8.
Apg7 activates Apg8 depending on ATP, then transferred to Apg3.

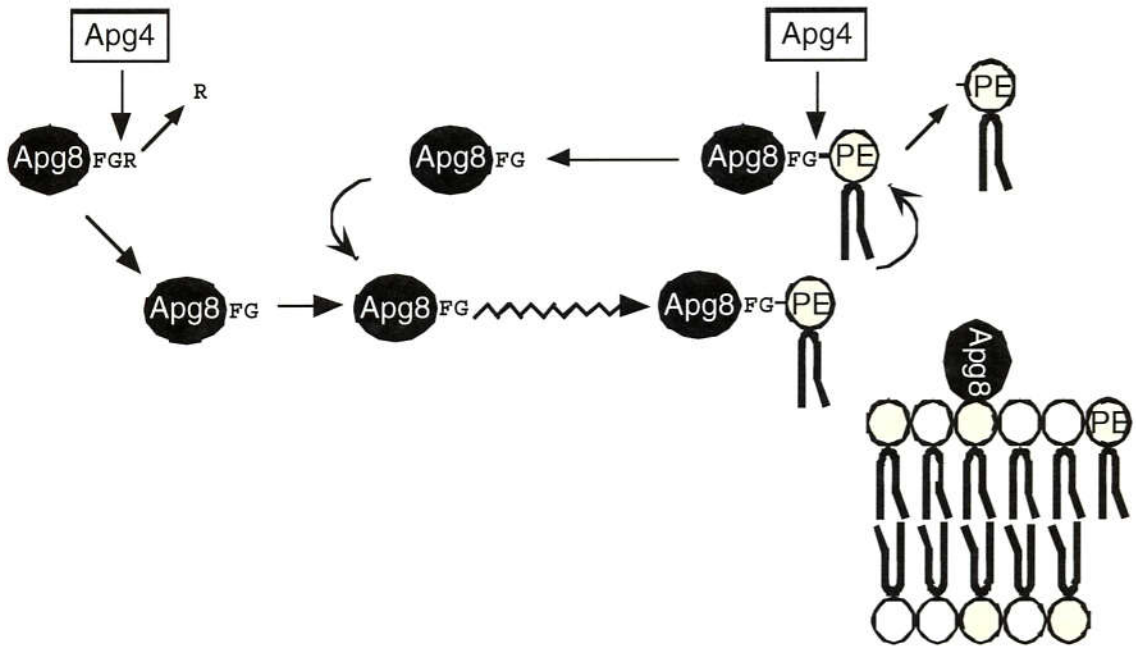

Figure 20. Apg8 links to PE, and becomes to tightly membrane-bound form.

Newly synthesized Apg8 (Apg8FGR) is processed by Apg4 protease, then resulted Apg8FG attached to some membrane. The membrane bound Apg8 is cleaved by Apg4. (This pathway has been found by Kirisako et. al. (Kirisako, 2000)).

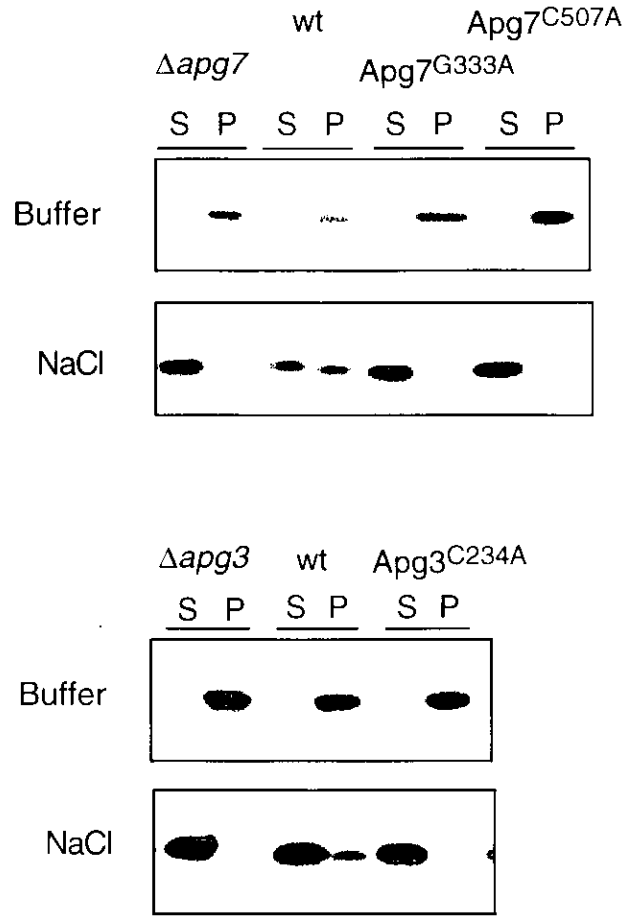

Figure 21. Membrane protein-like Apg8 was formed by Apg7 and Apg3.

The cells [wild-type (wt), Δ*apg7*, Δ*apg7* (Apg7G333A), Δ*apg7* (Apg7C507A), Δ*apg3*, and Δ*apg3* (Apg3C234A)] were grown in YPD to mid-log phase. They were converted to spheroplasts, and lysed osmotically in lysis buffer. The lysate was precleared by centrifugation at 2,500 rpm for 5 min at 4℃. The supernatant was centrifuged at 100 k *g* for 30 min. The pellet fraction was suspended into lysis buffer with or without 1 M NaCl. After incubation on ice for 30 min, they were recentrifuged at 100 k *g* for 1 h to generate supernatant (S) and pellet (P). Proteins in each fraction was precipitated with 10% TCA and resuspended with equal volume of SDS-PAGE sample buffer. Each sample was subjected to SDS-PAGE and analyzed by immunoblotting with anti-Apg8 antibody.

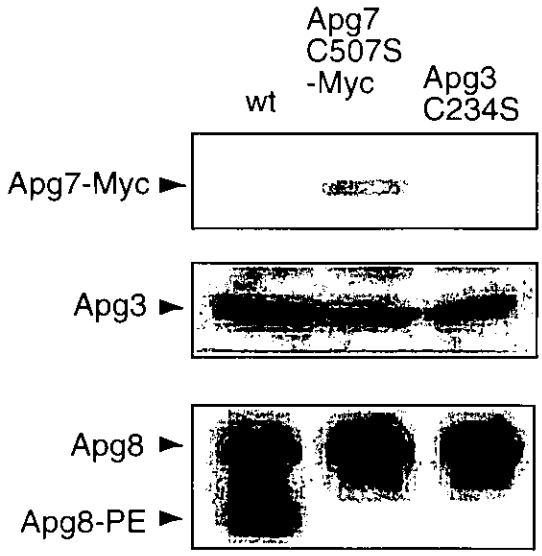

Figure 22. Cells expressing mutant form of either Apg7 or Apg3 do not form the Apg8-PE.

The wild-type (wt), Δ*apg7* expressing Apg7C507S-Myc, and Δ*apg3* expressing Apg3C234S cells were grown in YEPD to mid-log phase. Harvested cells were disrupted in lysis buffer by vortex with glass beads. After removing the cell debris by centrifugation at 10,000 rpm for 1 min, the resulting total lysate was suspended in SDS-PAGE sample buffer and subjected to SDS-PAGE containing 6 M urea gel. Immunoblotting was performed with anti-myc, anti-Apg3 and anti-Apg8 antibodies.

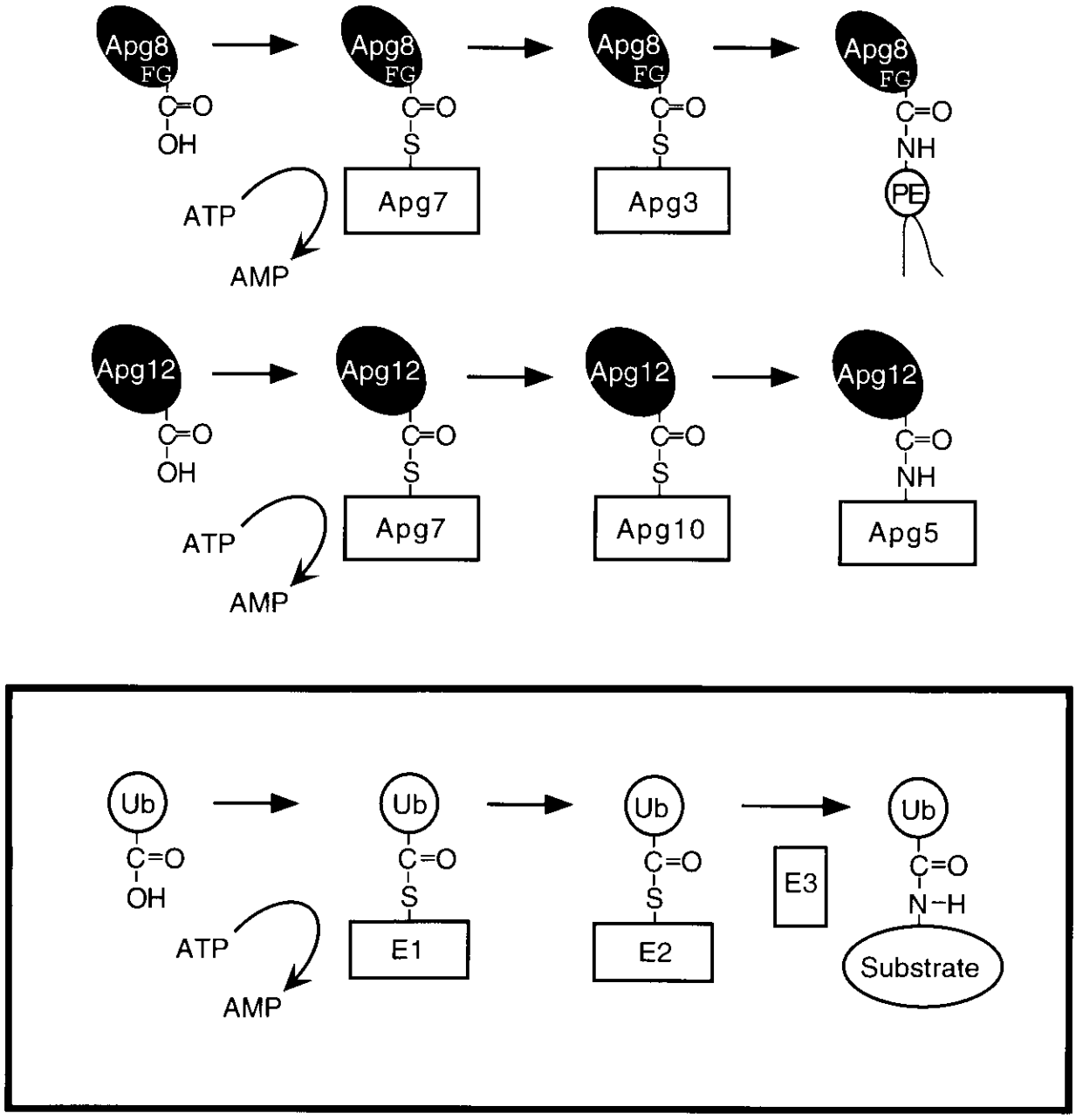

Figure 22. Apg8-PE is mediated by ubiquitination-like system.
Apg8FG is activated by Apg7, transferred to Apg3, and linked to PE. Another ubiquitination-like system involved in autophagy, Apg12-Apg5 conjugation system has been reported previously. Apg12 is also activated by Apg7, then transferred to Apg10, and finally Apg12 covalently links to Apg5. Thus, Apg7 activates not only Apg12 but also Apg8FG.
Ubiquitin pathway is explained by three steps; activation of ubiquitin by the E1, transfer of the activated Ub to the E2 conjugating enzyme, and transfer of the Ub to its substrate through the E3 ligase.

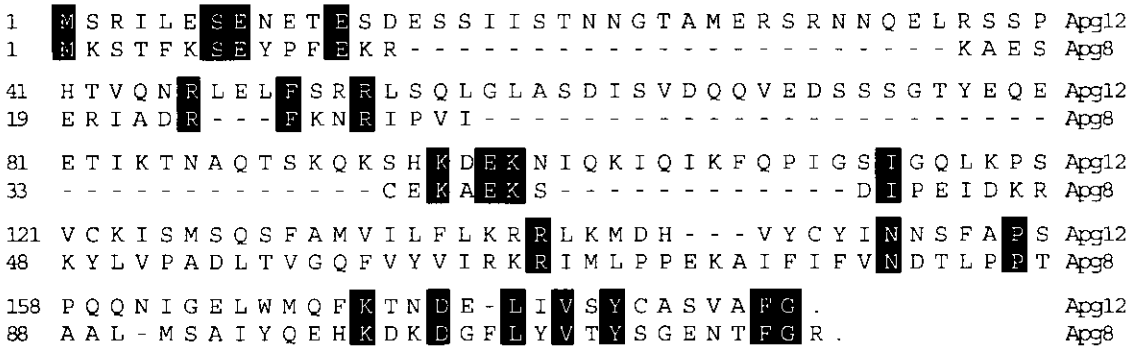

Figure 24. Comparison of amino acid sequences between Apg12 and Apg8.

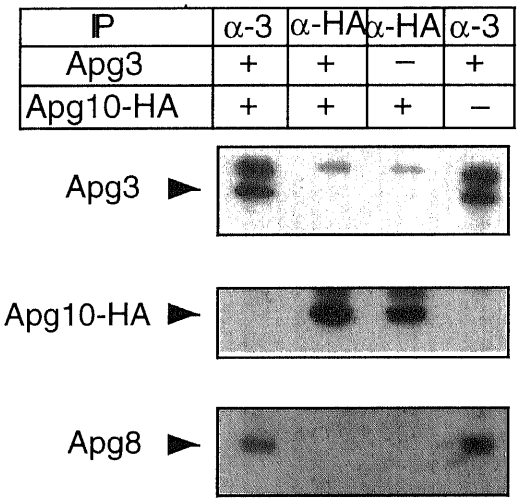

Figure 25. Binding specificity of the E2 in autophagy related ubiquitination reactions.

Wild-type cells were transformed with pRS426Apg3 and/or pRS425Apg10-HA. They were disrupted by vortexing with glass beads, and each lysate was obtained by centrifugation to remove cell debris, then subjected to immunoprecipitation by using anti-Apg3 or ant-HA antibody. Resulted immunocomplexes were analyzed by immunoblotting with anti-Apg3, anti-HA, and anti-Apg8 antibodies.

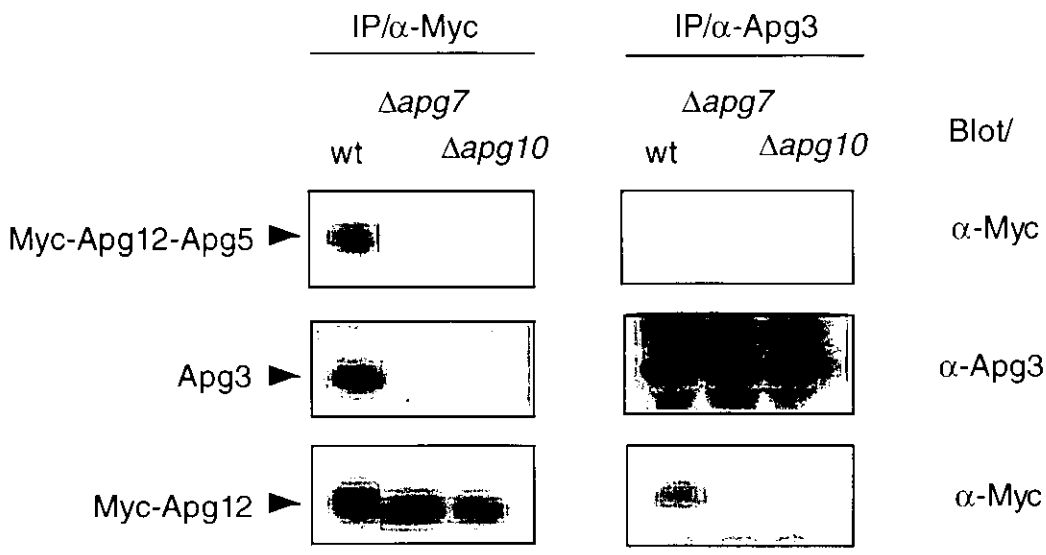

Figure 26. Apg7 interacts physically with both Apg3 and Apg12.

Wild-type (wt), Δ*apg7*, and Δ*apg10* cells were co-transformed with pRS424-Apg3 (2μ) and pRS426-Myc-Apg12 (2μ). The transformants were grown in YEPD to mid-log phase. They were disrupted by vortexing with glass beads, and each lysate was obtained by centrifugation to remove cell debris, then subjected to immunoprecipitation by using ant-Myc or anti-Apg3 antibody. Resulted immunocomplexes were analyzed by immunoblotting with anti-Apg3, anti-Myc antibodies.

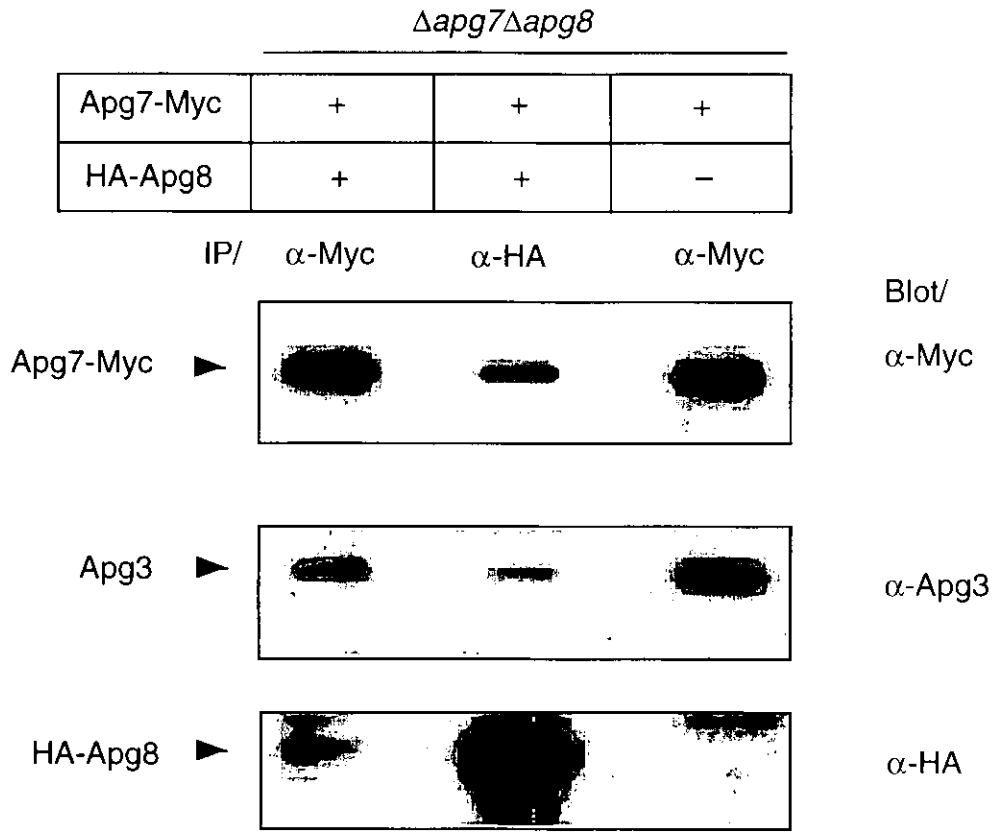

Figure 27. Apg7 and Apg3 form a heterocomplex.

Δapg7Δapg8 cells were transformed with either Apg7-Myc only or Apg7-Myc and HA-Apg8. The transformants were grown in YEPD to mid-log phase. They were disrupted by vortexing with glass beads, and each lysate was obtained by centrifugation to remove cell debris, then subjected to immunoprecipitation by using ant-Myc or anti-HA antibody. The immunocomplexes were subjected to immunoblot analysis using anti-Myc, anti-Apg3, or anti-HA antibody.

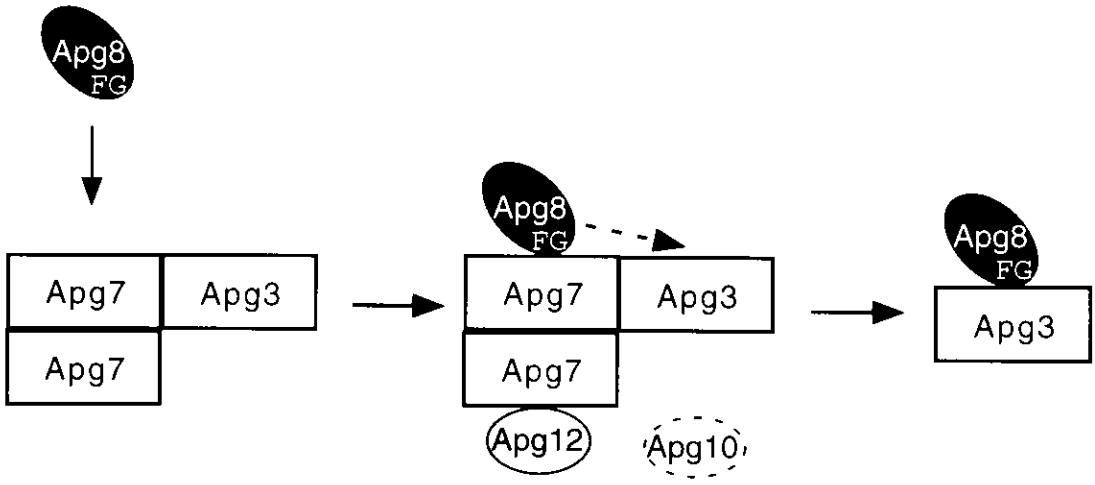

Figure 27. Apg8 is activated and conjugated by the heterocomplex of Apg7 and Apg3.
As shown in Fig. 26, Apg3 has a direct association with Apg7. The interaction between Apg12 and Apg3 is mediated by Apg7 in this model.

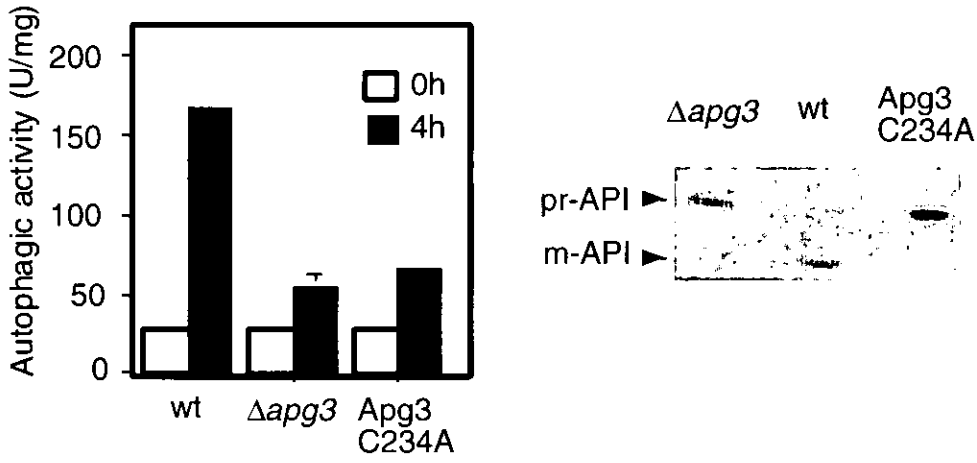

Figure 29. *Δapg3* and *Δapg3* expressing Apg3C234A cells were defective in autophagy and the Cvt-pathway.

Left panel; Wild-type (wt), *Δapg3* and *Δapg3* expressing Apg3C234A cells were grown in YEPD (open bar), and then they were shifted to SD(-N) for 4 h (filled bar). Autophagic activity was measured as described in Material and Methods. Right panel; Total lysates of growing cells were subjected to SDS-PAGE and analyzed by immunoblotting with anti-API antibody to show the Cvt-pathway. Pr-API; proform of API, m-API; mature form of API.

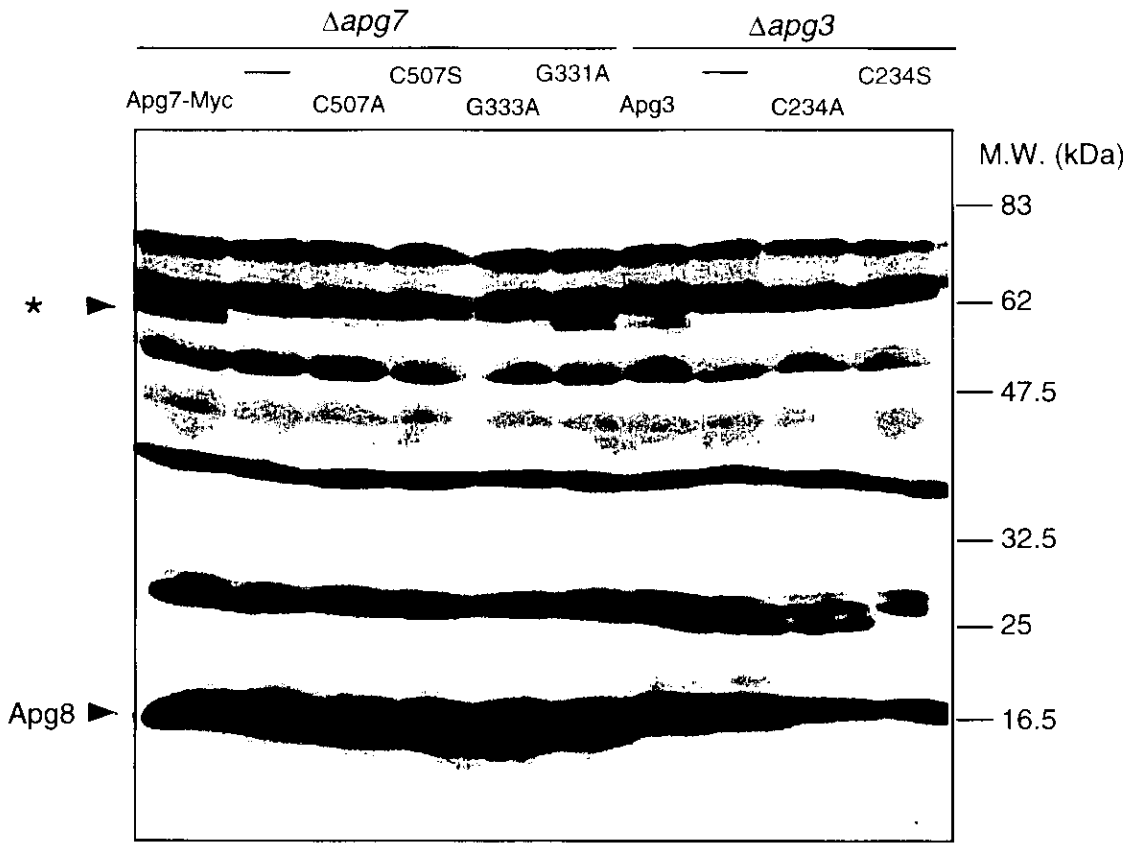

Figure 30. Apg8-protein conjugates in Apg8 system.

The cells [Δ*apg7* and Δ*apg7* cells harboring pRS314-Apg7-Myc, Apg7C507A-Myc, -C507S-, -G333A-, -G331A- (*CEN*), Δ*apg3* and Δ*apg3* cells harboring pRS315-Apg3, Apg3C234A, -C234S (*CEN*)] were grown in YEPD to late-log phase. These cells were lysed in NaOH/2-mercaptoethanol (see Material and Methods), and the resulting total lysate was subjected to immunoblot analysis using anti-Apg8 antibody. * indicates Apg8-protein conjugate band.

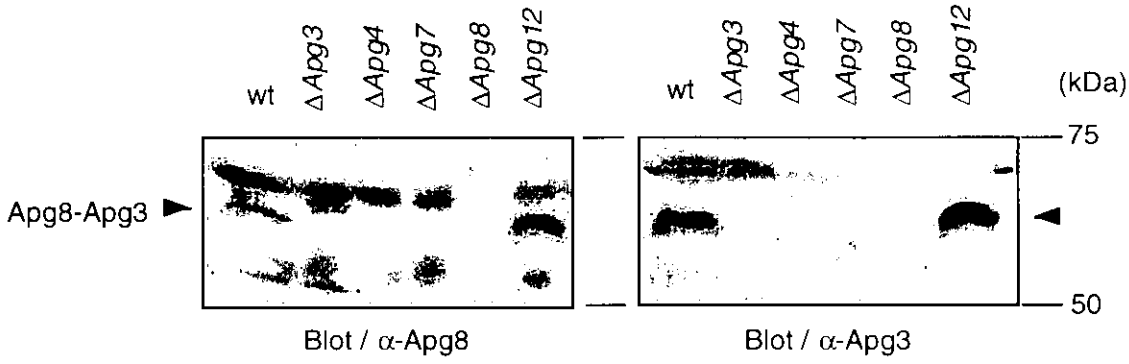

Figure 31. Detection of Apg8-Apg3 conjugate.

The wild-type, Δ*apg3*, Δ*apg4*, Δ*apg7*, Δ*apg8*, and Δ*apg12* cells were grown in YEPD to late-log phase (OD_{600} =8.0) and lysed by NaOH/2-mercaptoethanol (see Material and Methods). Total lysate was suspended in SDS-PAGE sample buffer and subjected to standard SDS-PAGE. Immunoblot analysis was performed by using anti-Apg8 or anti-Apg3 antibody. Arrow head denotes Apg8-Apg3 conjugation.

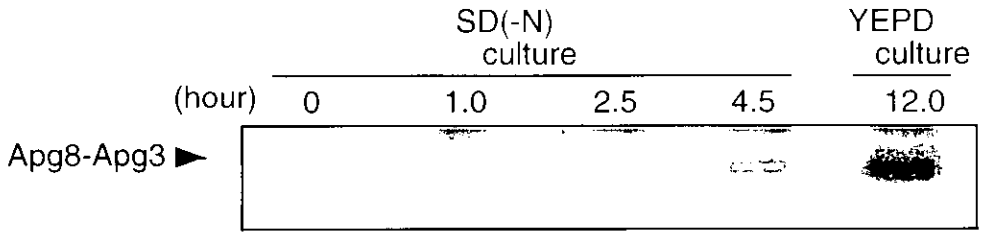

Figure 32. The conjugate of Apg8-Apg3 increases during starvation condition.

Wild-type cells were grown in YEPD to OD_{600} =1.0, then one aliquot was shifted to SD(-N) and the other aliquot was further grown in YEPD for 12 h (OD_{600} =~8.0). The cells were collected at the indicated time point, and they were lysed by NaOH/2-mercaptoethanol (see Material and Methods). Resulted total lysate was suspended in SDS-PAGE sample buffer (50 OD_{600} unit/ml), in which equivalent amounts of which were subjected to immunoblot analysis using anti-Apg8.

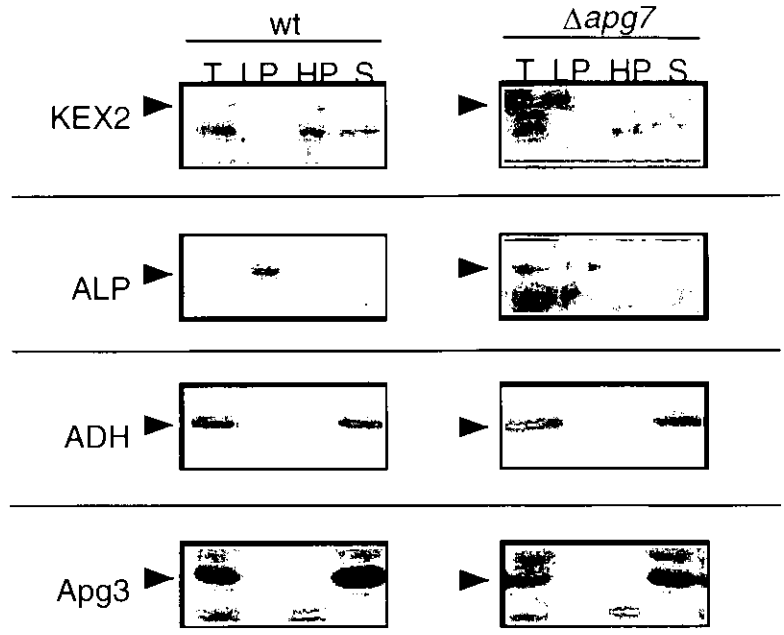

Figure 33. Subcellular fractionation of Apg3.

Wild-type (wt) and Δ*apg7* cells were grown in YEPD to OD_{600} =1.0 and converted to spheroplasts and osmotically lysed in lysis buffer as described in Material and Methods. After preclearing step to remove cell debris, the total lysate (T) was centrifuged at 13 k *g* for 15 min to generate supernatant (S13) and pellet (P13). S13 fraction was recentrifuged at 100 k *g* for 1 h to generate supernatant (S100) and pellet (P100). Resulting pellet and supernatant fractions denote LP (P13), HP (P100), and S (S100). Each fraction was suspended to SDS-PAGE sample buffer and subjected to SDS-PAGE. Fractions were analyzed by immunoblotting with anti-Kex2, anti-ALP, anti-ADH, and anti-Apg3 antibodies (Kex2; Golgi marker, ALP; Vacuolar marker, ADH; Cytosolic marker).

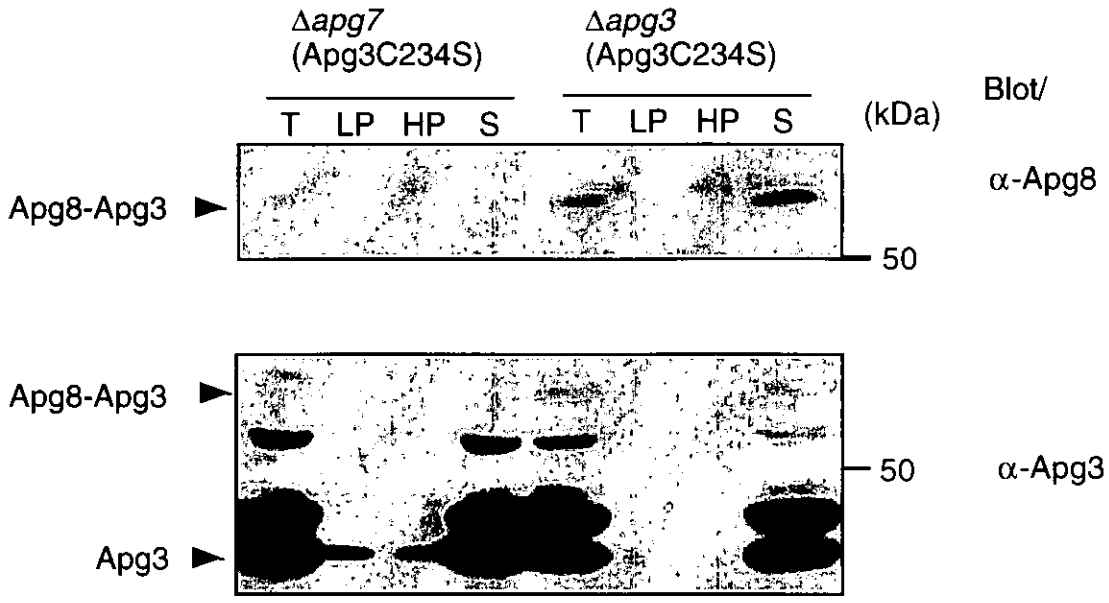

Figure 34. Subcellular distribution of Apg8-Apg3^{C234S} conjugates.

Δapg7 and *Δapg3* cells were transformed with pRS425Apg3^{C234S} and grown in SD (-N) for 6 h. Harvested cells were converted to spheroplasts and osmotically lysed in lysis buffer as described in Material and Methods. After pleclearing step to remove cell debris, the total lysate (T) was centrifuged at 13 k *g* for 15 min to generate supernatant (S13) and pellet (P13). S13 fraction was recentrifuged at 100 k *g* for 1 h to generate supernatant (S100) and pellet (P100). Resulting pellets and supernatant fraction denote LP (P13), HP (P100), and S (S100). Each fraction was suspended to SDS-PAGE sample buffer and subjected to SDS-PAGE. Fractions were analyzed by immunoblotting with anti anti-Apg8 or anti-Apg3 antibody.

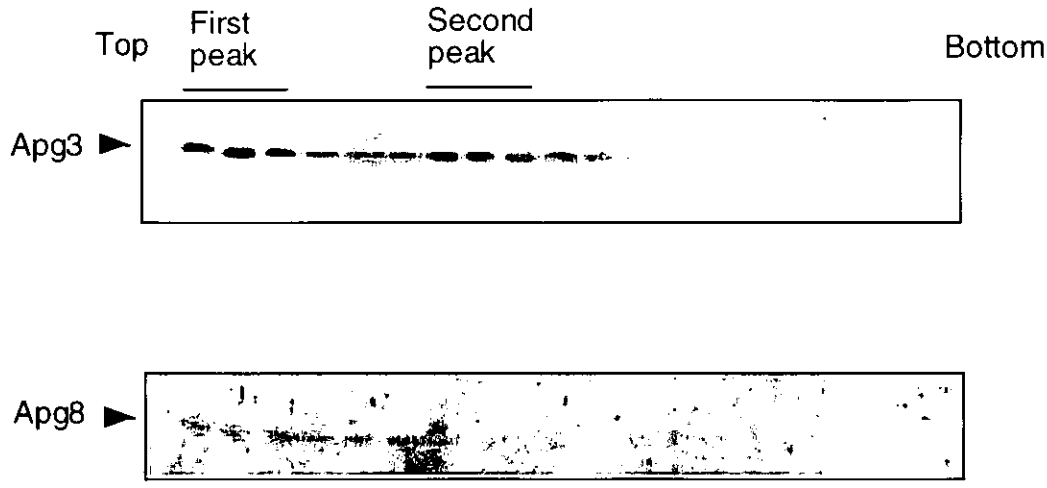

Figure 35. Apg3 showed two populations in sucrose density gradient separation.

Wild-type cells were grown in YEPD to mid-log phase. The cells were converted to spheroplasts and osmotically lysed as described in Material and Methods. The resulting lysate was precleared by centrifuge at 2,500 rpm for 5 min, and then total lysate was layered on top of the sucrose gradient buffer (5-20%). Fractionation was performed after centrifugation at 100 k *g* for 16 h at 4℃ and recovered in 20 fractions. Each fractions was subjected to SDS-PAGE and immunoblotted by using anti-Apg3 or anti-Apg8 antibody. The distribution of Apg3 shows two peaks, which indicates to first and second peak.

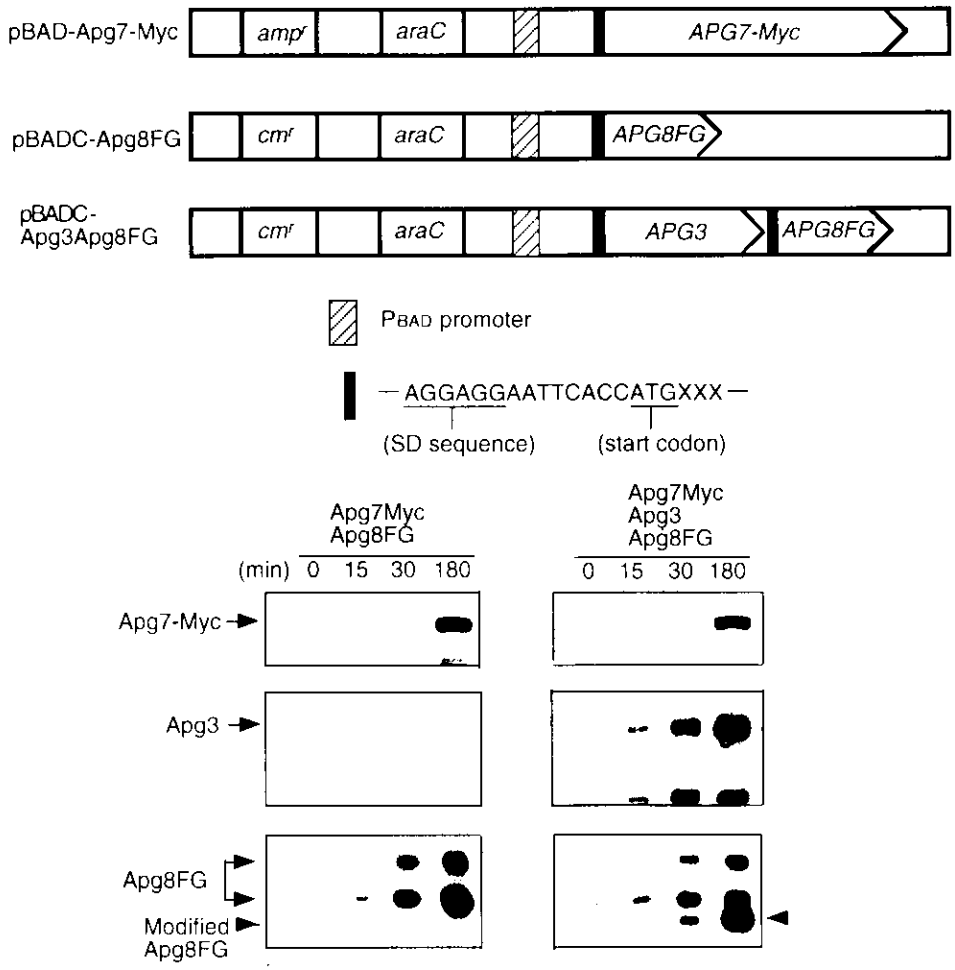

Figure 36. Reconstitution of Apg8 system in *E.coli*.

E. coli (XL1Blue) cells were transformed with pBAD-Apg7-Myc and either pBADC-Apg8FG or pBADC-Apg3Apg8FG (pBAD encodes P_{BAD} promoter, AraC, Amp^r (ampicillin resistance), and pBR origin, pBADC encodes P_{BAD} promoter, AraC, Cm^r (chloramphenicol resistance), and pACYC origin) and grown in LB supplemented with ampicillin (Amp) (50 μg /ml), chloramphenicol (Cm) (25 μg /ml). The construction of expressing vector of Apg7-Myc, Apg3, and Apg8FG was described in Materials and Methods. SD box indicates Shine-Dalgarno sequence. The transformed cells were grown in LB supplemented with Amp and Cm at 37℃ to OD600 =0.5 After addition of 0.2% arabinose, cells were cultured at 37℃ for 3 h to induction of each Apg. The cells were harvested at the indicated time point and suspended into SDS-PAGE sample buffer. The samples were boiled for 5 min and subjected to SDS-PAGE containing 6 M urea. Immunoblot was carried out by anti-Myc, anti-Apg3, and anti-Apg8 antibody. Arrow head indicated modified Apg8FG. * arrow indicates unidentified signal related to Apg8.

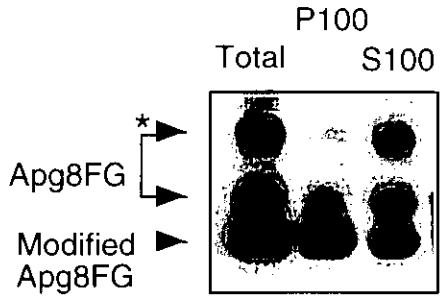

Figure 37. Cellular distribution of modified Apg8 in *E.coli*.

E. coli (XL1Blue) cells harboring pBAD-Apg7-Myc and pBADC-Apg3Apg8FG were grown in LB supplemented with Amp, Cm, and 0.2% arabinose at 37°C for 3 h. Harvested cells were suspended in lysis buffer and disrupted by sonication as described in Material and Methods. The resulting lysate (Total) was separated to supernatant (S100) and pellet (P100) by centrifugation at 100 k *g* for 60 min. Each fraction was subjected to SDS-PACE containing 6 M urea and analyzed by immunoblotting with anti-Apg8 antibody. * indicates an unidentified signal related to Apg8.

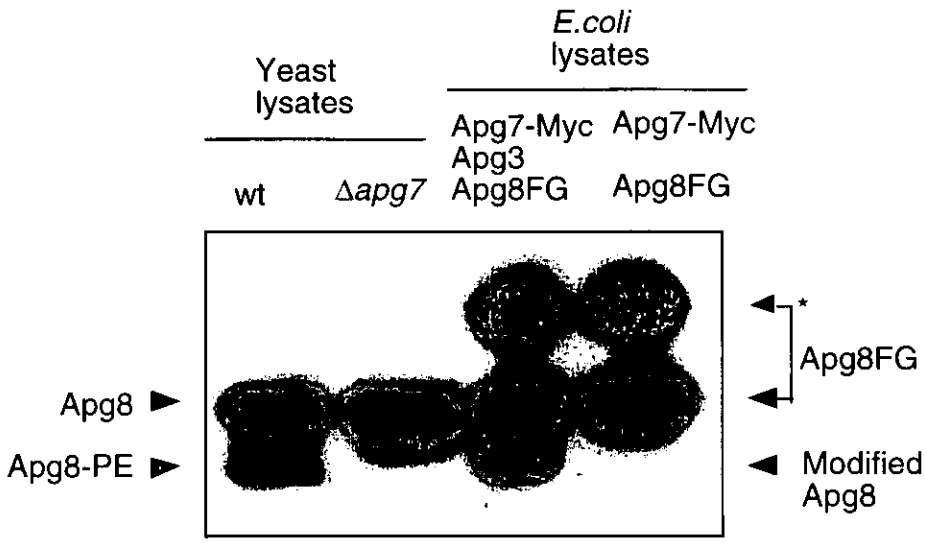

Figure 38. Mobility of modified Apg8FG in *E. coli*

E. coli (XL1Blue) cells harboring pBAD-Apg7-Myc and either pBADC-Apg3Apg8FG or pBADC-Apg8FG were grown in LB supplemented with Amp, Cm, and 0.2% arabinose at 37℃ for 3 h. The cells were suspended into SDS-PAGE sample buffer, and boiled for 5 min, then the samples were subjected to SDS-PAGE containing 6 M urea. Yeast cells, wild-type (wt) and Δ*apg7* were grown in YEPD to mid-log phase and disrupted by vortexing with glass beads. After remove cell debris by centrifugation, the resulting total lysate was subjected to SDS-PAGE containing 6 M urea. Immunoblot analysis was performed with anti-Apg8 antibody. * indicates an unidentified signal related to Apg8.

Apg7	+	+	-	CS	CS	+	-
Apg3	+	-	+	-	+	CS	CS
Apg8FG	+	+	+	+	+	+	+

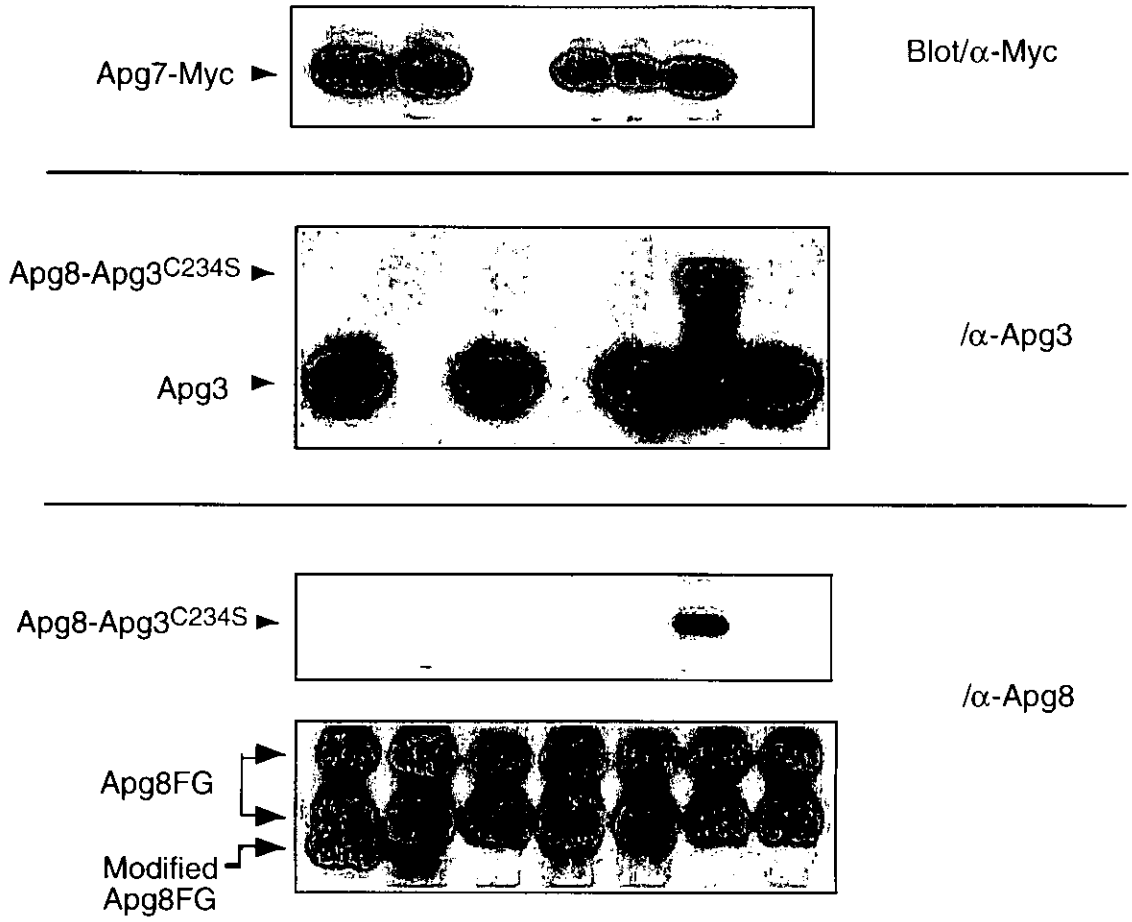

Figure 39. Enzymatic reaction in *E. coli* reconstituted Apg8 system.

E. coli (XL1Blue) cells were transformed with plasmids, pBAD-Apg7-Myc, pBADC-Apg3Apg8FG, pBADC-Apg8FG, pBADC-Apg3, pBAD-Apg7C507S-Myc (Substitutant of Ser507 in Apg7), and pBADC-Apg3C234SApg8FG (Substitutant of Ser234 in Apg3). The transformed cells were grown in LB supplemented with amp, cm, and 0.2% arabinose at 37℃ for 3 h. Cells were collected and suspended into SDS-PAGE sample buffer, then the samples were boiled for 5 min. Each sample was subjected to SDS-PAGE containing 6 M urea and analyzed by immunoblotting with anti-Myc, anti-Apg3, and anti-Apg8 antibody. * indicates an unidentified signal related to Apg8.

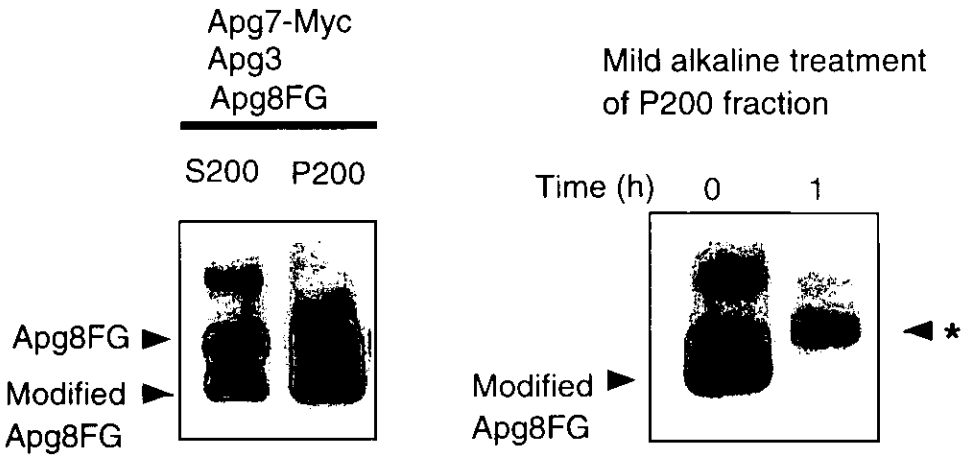

Figure 40. Characterization of the modified Apg8 by reconstituted Apg8 system in *E.coli*.

E. coli (XL1Blue) cells harboring pBAD-Apg7-Myc and/or pBADC-Apg3Apg8FG were grown in LB supplemented with Amp, Cm, and 0.2% arabinose at 37℃ for 3 h. Harvested cells were suspended in lysis buffer and disrupted by sonication as described in Material and Methods. The resulting lysate (Total) was separated to supernatant (S200) and pellet (P200) by centrifugation at 200 k *g* for 17 h, and then each fraction was subjected to immunoblot analysis with anti-Apg8 antibody (left panel). A part of P200 fraction was resuspended to lysis buffer, and it was treated with 0.06 M NaOH in 30% methanol at 40℃ for 1 h. Alkali treated sample was added 0.06 N HCl and suspended in SDS-PAGE sample buffer. The sample was subjected to SDS-PAGE containing 6 M urea and analyzed by immunoblotting with anti-Apg8 antibody (right panel). * indicates a band of modified Apg8FG shifted after mild alkaline treatment.

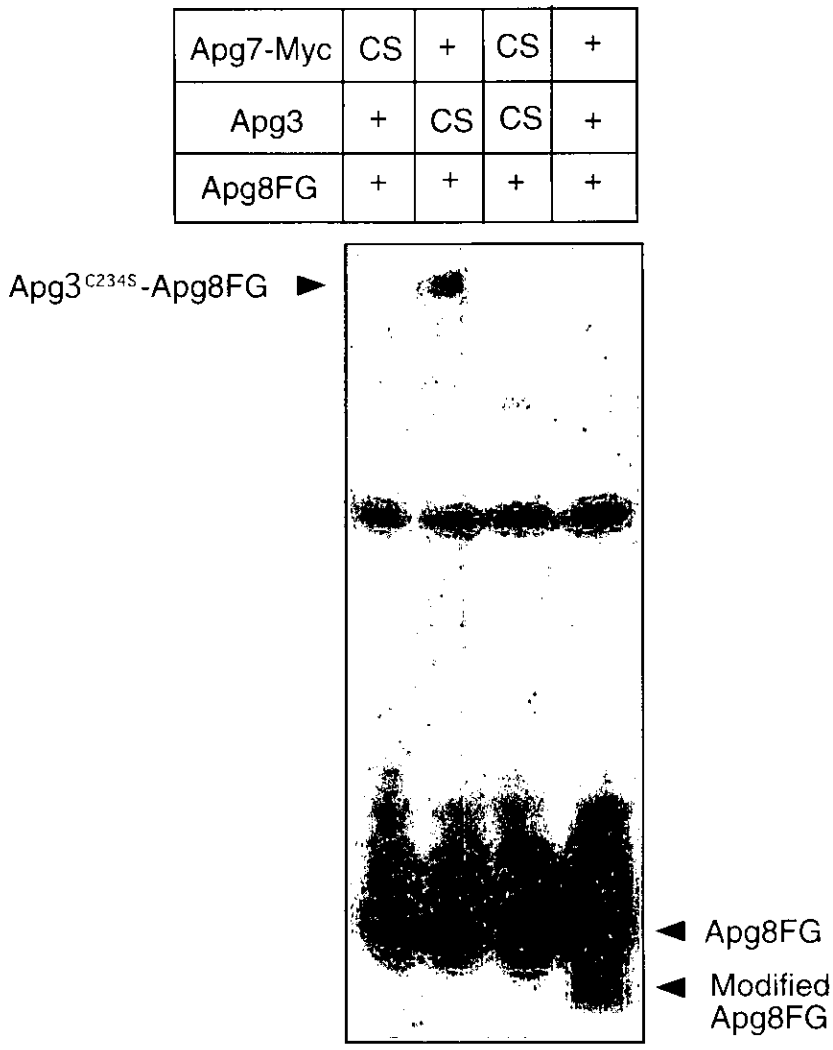

Figure 41. Reconstitution of Apg8 system in cell-free experiment.

E. coli (XL1Blue) cells were transformed with pBAD-Apg7-Myc, pBAD-Apg7C507S-Myc, pBADC-Apg3Apg8FG, and pBADC-Apg3C234SApg8FG, respectively. They were grown in LB supplemented with Amp, Cm, and 0.4% arabinose for 6 h. Harvested cells were suspended in lysis buffer, and then the cells were disrupted by sonic on ice as described in Material and Methods. Resulted cell lysates were mixed as following ratios (volume : volume), Apg7-Myc : Apg3 Apg8FG (1 : 2), Apg7C507S-Myc : Apg3 Apg8FG (1 : 2), Apg7-Myc : Apg3C234S Apg8FG (1 : 2), and Apg7C507S-Myc : Apg3C234S Apg8FG (1 : 2). Cell-free reaction was performed in the presence of an ATP regeneration system (0.5 mM ATP, 10 mM phosphocreatine, and 5 μg creatine kinase) at 30℃ for 15 h in a reaction volume 25 μl. The reaction was terminated by the addition of SDS-PAGE sample buffer. After boiling for 5 min, obtained samples were subjected to SDS-PAGE containing 6 M urea. Immunoblot analysis was performed with anti-Apg8 antibody.

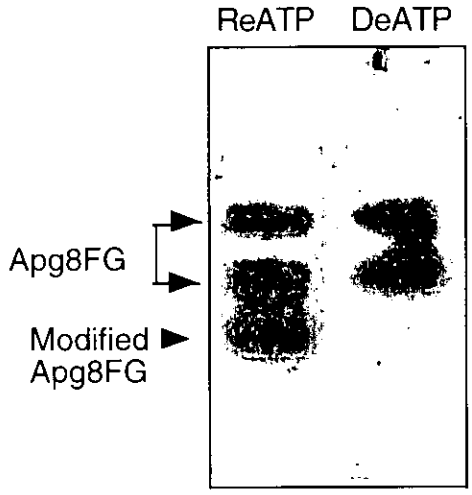

Figure 42. Apg8FG is modified by cell-free Apg8 system in an ATP dependent manner.

E. coli (XL1Blue) cells were grown in LB at 37℃ to OD600 =2.0, then cells were harvested and disrupted in a lysis buffer by sonication on ice (10 OD600 unit/ml). After removal of cell debris by centrifugation at 8 k rpm for 5 min, resulted total lysate was recentrfuged at 100 k *g* for 1 h to generate S100 and P100. The P100 fraction was resuspended with lysis buffer (10 OD600 unit/ml). The purification of Apg7-Myc, Apg3, and Apg8FG was done as described in Material and Methods, subsequently each purified Apg was used for cell-free reaction (Apg7-Myc: 0.27 mg/ml, Apg3: 0.08 mg/ml, Apg8FG: 0.19 mg/ml). Cell-free Apg8 system was designated as follows, P100 fraction (10 µl), Apg7-Myc (1 µl: ca. 0.64 pmoles), Apg3 (0.5 µl: ca. 1.0 pmol), Apg8FG (0.07 µl: ca. 0.9 pmoles), and ATP regeneration or depletion system. ATP regeneration system contained 0.5 mM ATP, 10 mM $MgCl_2$, 10 mM phosphocreatine, and 5 µg creatine kinase (ReATP). ATP depletion system contained 20 mM 2-deoxyglucose, 0.2 mg hexokinase (DeATP). Cell-free reaction was performed at 30℃ for 3 h in a reaction volume 20 µl. The reaction was terminated by the addition of SDS-PAGE sample buffer. After boiling for 5 min, one tenth volume of each sample was subjected to SDS-PAGE containing 6 M urea. Immunoblot analysis was performed with anti-Apg8 antibody.

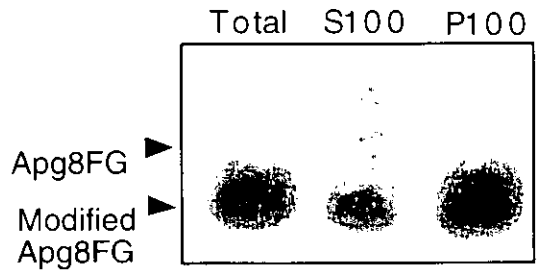

Figure 43. Apg8FG is modified efficiently by cell-free Apg8 system in the presence of membrane fraction.

E. coli (XL1Blue) cells were grown in LB at 37℃ to OD600 =2.0, then cells were harvested and disrupted in lysis buffer by sonication on ice (10 OD600 unit/ml). After removing the cell debris by centrifugation at 8 k rpm for 5 min, resulted total lysate was recentrifuged at 100 k *g* for 1 h to generate S100 and P100. The P100 fraction was resuspended with lysis buffer (10 OD600 unit/ml). Cell-free Apg8 system was designated as follows. Apg7-Myc (1 µl: ca. 0.64 pmoles), Apg3 (0.5 µl: ca. 1.0 pmol), Apg8FG (0.07 µl: ca. 0.9 pmoles), ATP regeneration system (0.5 mM ATP, 10 mM $MgCl_2$, 10 mM phosphocreatine, and 5 µg creatine kinase), and either total lysate (10 µl), S100 (10 µl), or P100 (10 µl). Cell-free reaction was performed at 30℃ for 15 h in a reaction volume 20 µl. The reaction was terminated by the addition of SDS-PAGE sample buffer. After boiling for 5 min, one tenth volume sample was subjected to SDS-PAGE containing 6 M urea. Immunoblot analysis was performed with anti-Apg8 antibody.

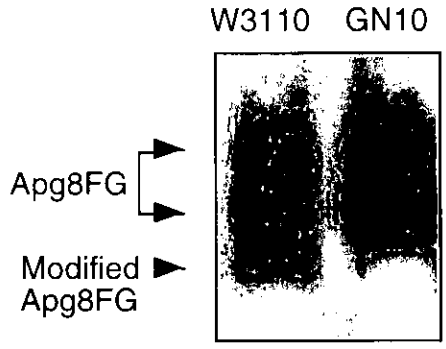

Figure 44. Phosphatidylethanolamine is essential for the modification of Apg8FG by cell-free Apg8 system

E. coli, W3110 (wild-type) and GN10 (PE deficient strain) were grown in LB supplemented with 50 mM $MgCl_2$ at 37℃ to OD600 =1.5. The cells were harvested by centrifugation and suspended in lysis buffer (20 OD600 unit /ml). Then cells were disrupted by sonic on ice. Each total lysate was generated by centrifugation at 8 k rpm for 5 min to remove cell debris. Cell-free reaction was designated as follows mixture, total lysate (W3110 or GN10) (10 μl), Apg7-Myc (1 μl: ca 0.64 pmoles), Apg3 (0.5 μl: ca 1.0 pmol), Apg8FG (0.07 μl: ca 0.9 pmoles), and ATP regeneration system (0.5 mM ATP, 10 mM $MgCl_2$, 10 mM phosphocreatine, and 5 μg creatine kinase). Reaction mixture (20 μl) was incubated at 30℃ for 15 h in a reaction volume 20 μl and suspended in SDS-PAGE sample buffer. Each sample (1/10 amount) was subjected to SDS-PAGE containing 6 M urea and detected by immunoblotting with anti-Apg8 antibody.

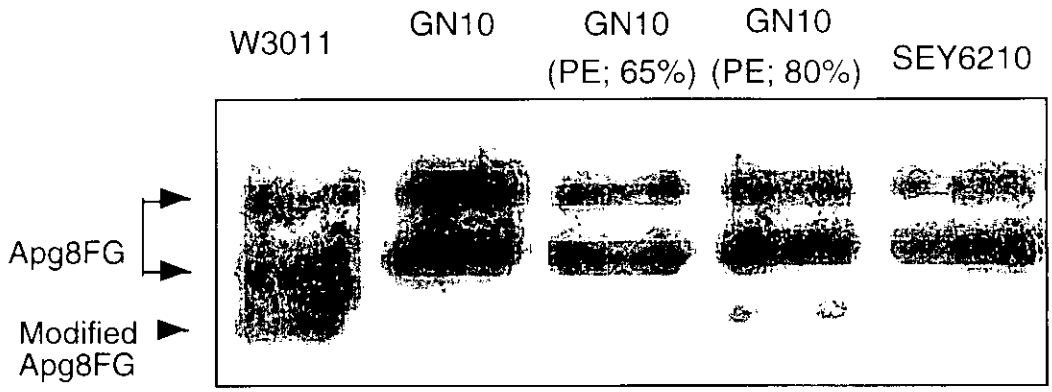

Figure 45. *In vitro* reconstitution of Apg8 system with liposome.

Total lipid extraction from *E. coli* (W3110, GN10) and from Yeast (SEY6210) was performed as described in Materials and Methods. Preparation of unilamellar liposome was described in Materials and Methods. Total lipid liposome (1 mM phospholipids) was prepared from each cellular total lipid (W3011, GN10, SEY6210). *E. coli* PE was added to total lipid of GN10 (molecular ratio of PE (*E.coli*) : total lipid (GN10) = 2 : 1 (65% PE), 4 : 1 (80% PE)). *In vitro* reaction mixture consists of liposome (5 µl (5 nmoles total lipid)), Apg7-Myc (1 µl: ca 0.64 pmoles), Apg3 (0.5 µl: ca 1.0 pmol), Apg8FG (0.07 µl: ca 0.9 pmoles), and ATP regeneration system (0.5 mM ATP, 10 mM $MgCl_2$, 10 mM phosphocreatine, and 5 µg creatine kinase). Reaction mixture (20 µl) was incubated at 30℃ for 15 h and suspended in SDS-PAGE sample buffer. Each sample (1/10 amount) was subjected to SDS-PAGE containing 6 M urea and analyzed by immunoblotting with anti-Apg8 antibody.

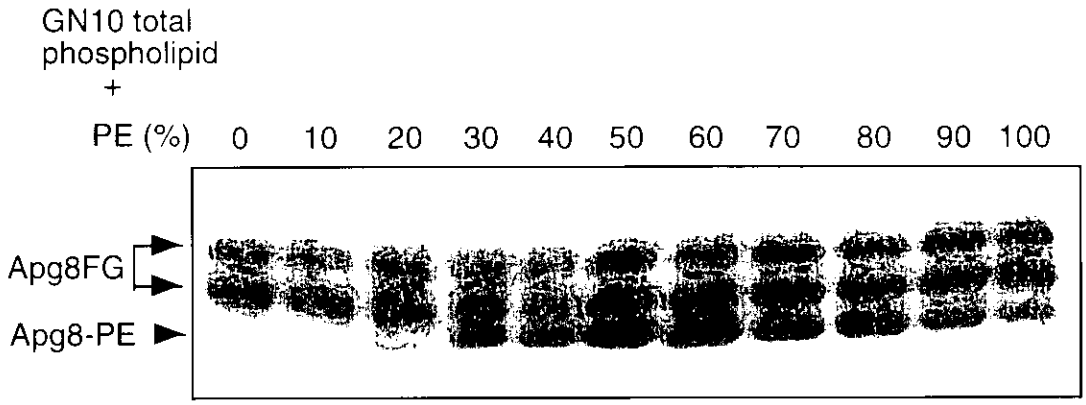

Figure 46. PE content of liposome affects Apg8-PE conjugation.

Liposome (1 mM total phospholipids) was prepared from both GN10 total lipid and *E. coli* PE as described in Materials and Methods. The resulting liposome contains indicated amount of *E. coli* PE (0-90% (mol/mol)) in GN10 total lipid. 100% PE-liposome consists of *E. coli* PE only. *In vitro* reaction was designated as follows, liposome (5 µl (5 nmoles total lipid)), Apg7-Myc (1 µl: ca. 0.64 pmoles), Apg3 (0.5 µl: ca. 1.0 pmol), Apg8FG (0.07 µl: ca. 0.9 pmoles), and ATP regeneration system (0.5 mM ATP, 10 mM $MgCl_2$, 10 mM phosphocreatine, and 5 µg creatine kinase). The reaction mixture (20 µl) was incubated at 30℃ for 15 h and suspended in SDS-PAGE sample buffer. Each sample (1/10 amount) was subjected to SDS-PAGE containing 6 M urea and analyzed by immunoblotting with anti-Apg8 antibody.

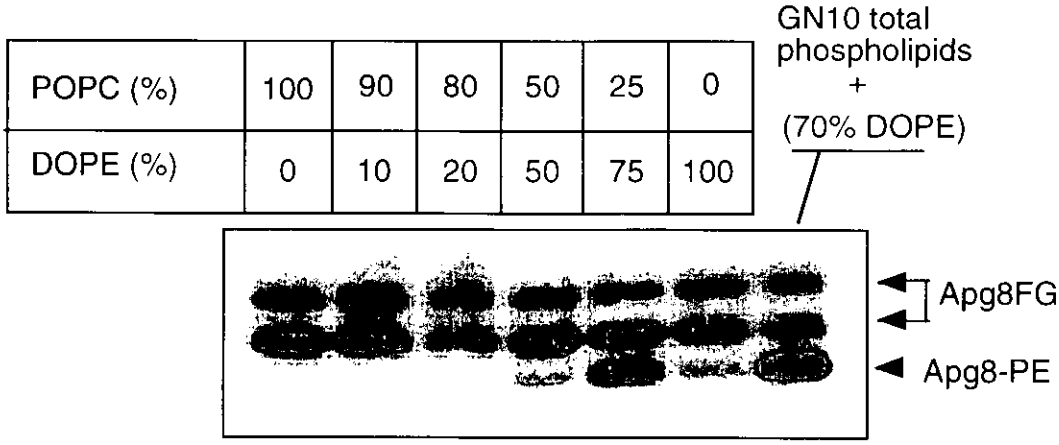

Figure 47. The influence of lipid composition in liposome on Apg8-PE conjugation.

Liposome (1 mM total phospholipids) was prepared from both 1-palmitoyl-2-oleoylphoshatidylcholine (POPC) and dioleoylphosphatidylethanolamine (DOPE) as described in Materials and Methods. The composition of POPC/DOPE was designated as indicated ratio (mol/mol (%)). *In vitro* reaction was designated as follows, liposome (5 µl (5 nmoles total lipid)), Apg7-Myc (1 µl: ca. 0.64 pmoles), Apg3 (0.5 µl: ca. 1.0 pmol), Apg8FG (0.07 µl: ca. 0.9 pmoles), and ATP regeneration system (0.5 mM ATP, 10 mM $MgCl_2$, 10 mM phosphocreatine, and 5 µg creatine kinase). The reaction mixture (20 µl) was incubated at 30℃ for 15 h and suspended in SDS-PAGE sample buffer. Each sample (1/10 amount) was subjected to SDS-PAGE containing 6 M urea and analyzed by immunoblotting with anti-Apg8 antibody.

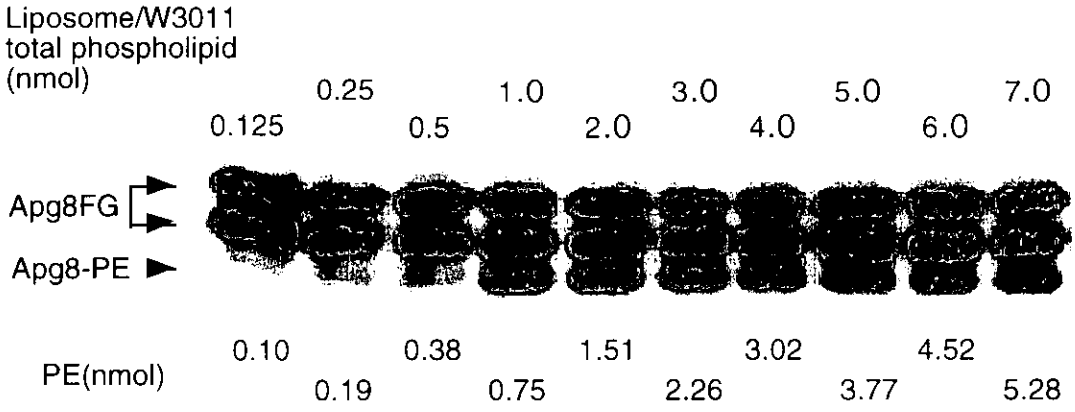

Figure 48. Apg8-PE conjugation *in vitro* by using the *E. coli* total lipid liposome (75% PE liposome). Liposome was prepared from total lipid of W3110 as described in Materials and Methods. *In vitro* reaction mixture contains described amount of liposome (0.125 µl - 5 µl (0.125 - 5 nmoles total lipid)), Apg7-Myc (1 µl: ca. 0.64 pmoles), Apg3 (0.5 µl: ca. 1.0 pmol), Apg8FG (0.07 µl: ca. 0.9 pmoles), and ATP regeneration system (0.5 mM ATP, 10 mM $MgCl_2$, 10 mM phosphocreatine, and 5 µg creatine kinase). The indicated amount of PE (0.095 - 5.278 nmoles PE) was calculated from the PE content of total lipid in W3110 (PE: 75.4% in total lipid). Reaction (total volume 20 µl) was carried out at 30°C for 15 h and suspended in SDS-PAGE sample buffer. Each sample (1/10 amount) was subjected to SDS-PAGE containing 6 M urea and analyzed by immunoblotting with anti-Apg8 antibody.

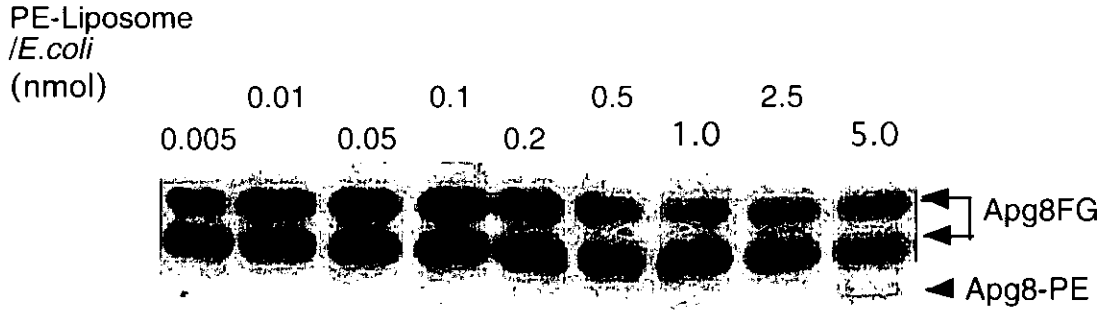

Figure 49. Apg8-PE conjugation *in vitro* by using the 100% PE liposome.

Liposome was prepared from *E. coli* PE only as described in Materials and Methods. *In vitro* reaction mixture contains described amount of liposome (0.005 µl–5.0 µl (PE content 0.005-5.0 nmoles)), Apg7-Myc (1 µl: ca. 0.64 pmoles), Apg3 (0.5 µl: ca. 1.0 pmol), Apg8FG (0.07 µl: ca. 0.9 pmoles), and ATP regeneration system (0.5 mM ATP, 10 mM $MgCl_2$, 10 mM phosphocreatine, and 5 µg creatine kinase). Reaction (total volume 20 µl) was carried out at 30℃ for 15 h and suspended in SDS-PAGE sample buffer. Each sample (1/10 amount) was subjected to SDS-PAGE containing 6 M urea and analyzed by immunoblotting with anti-Apg8 antibody.

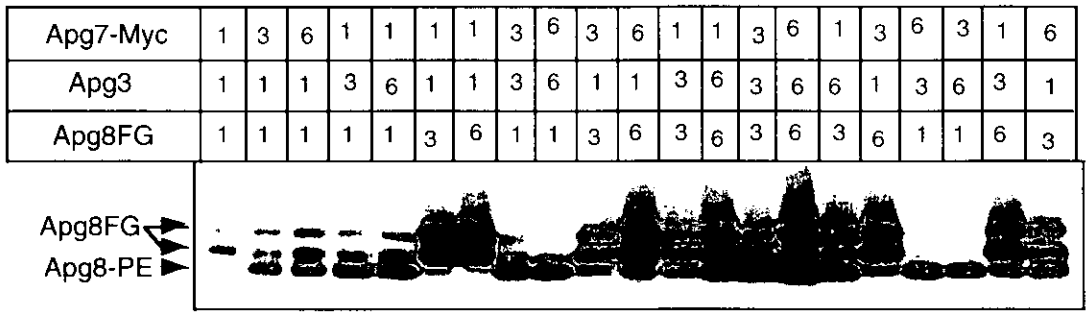

Figure 50. High amounts of Apg7 and Apg3 stimulate Apg8-PE conjugation.

Liposome was prepared from total lipid of W3110 as described in Materials and Methods. *In vitro* reaction mixture contains 5 µl liposome (5.0 nmoles total lipid includes 3.77 nmoles PE), various amounts of Apg7-Myc/Apg3/Apg8FG, and ATP regeneration system (0.5 mM ATP, 10 mM $MgCl_2$, 10 mM phosphocreatine, and 5 µg creatine kinase). Apg7-Myc, Apg3, and Apg8FG were mixed by indicated volume (µl) (1-6 : 1-6 : 1-6 (µl); ca. 0.64-3.84 : 1.0-6.0 : 0.9-5.4 (pmol)). Reaction (total volume 20 µl) was carried out at 30℃ for 15 h and suspended in SDS-PAGE sample buffer. Each sample (1/10 amount) was subjected to SDS-PAGE containing 6 M urea and analyzed by immunoblotting with anti-Apg8 antibody.

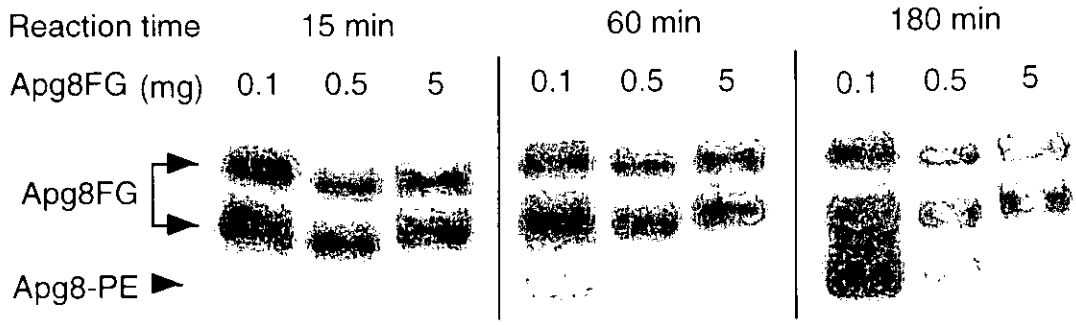

Figure 51. High amount of Apg8FG blocks the Apg8-PE conjugation.

E. coli (XL1Blue) cells were co-transformed with pBAD-Apg7-Myc and pBADC-Apg3. The transformants were grown in LB supplemented with Amp and Cm, and Apg7-Myc and Apg3 were expressed by addition of 0.2% arabinose for 6 h. They were harvested and lysed in lysis buffer by sonication on ice. After centrifugation to preclear, resulted total lysate was used for the cell-free Apg8 system. The total lysate (0.56 OD_{600} unit) was mixed with purified Apg8FG (0.1, 0.5, and 5.0 μg), and the reaction mixture was incubated at 30℃ for 15 min, 1 h, and 3 h in the presence of ATP regeneration system. Reaction sample (total volume 20 μl) was suspended in SDS-PAGE sample buffer, and then equivalent amount of Apg8 was subjected to SDS-PAGE containing 6 M urea. The immunoblot analysis was performed with anti-Apg8 antibody.

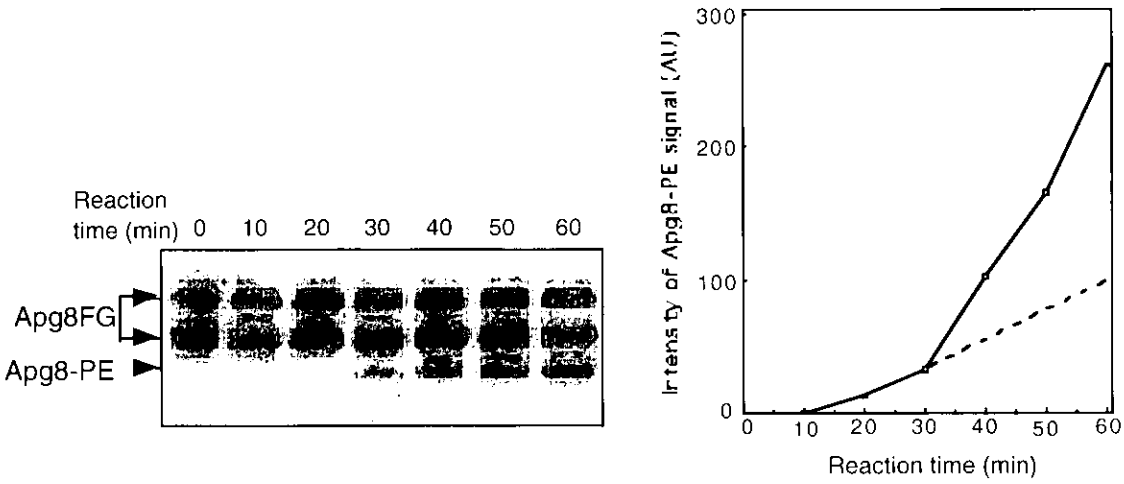

Figure 52. Time course of Apg8-PE conjugate reaction

E. coli (XL1Blue) cells were co-transformed with pBAD-Apg7-Myc and pBADC-Apg3. The transformants were grown in LB supplemented with Amp and Cm, and both Apg7-Myc and Apg3 were expressed by addition of 0.2% arabinose for 6 h. They were harvested and lysed in lysis buffer by sonication on ice. After centrifugation to preclear, resulted total lysate was used for the cell-free Apg8 system. The total lysate (0.56 OD_{600} unit) was mixed with purified Apg8FG (0.2 μg), then the reaction was started at 30℃. Samples at each time point were collected and subjected to SDS-PAGE containing 6 M urea. The immunoblot analysis was performed with anti-Apg8 antibody (left panel). The intensity of Apg8-PE signal was measured by NIH image (AU; arbitrary unit) (right panel).

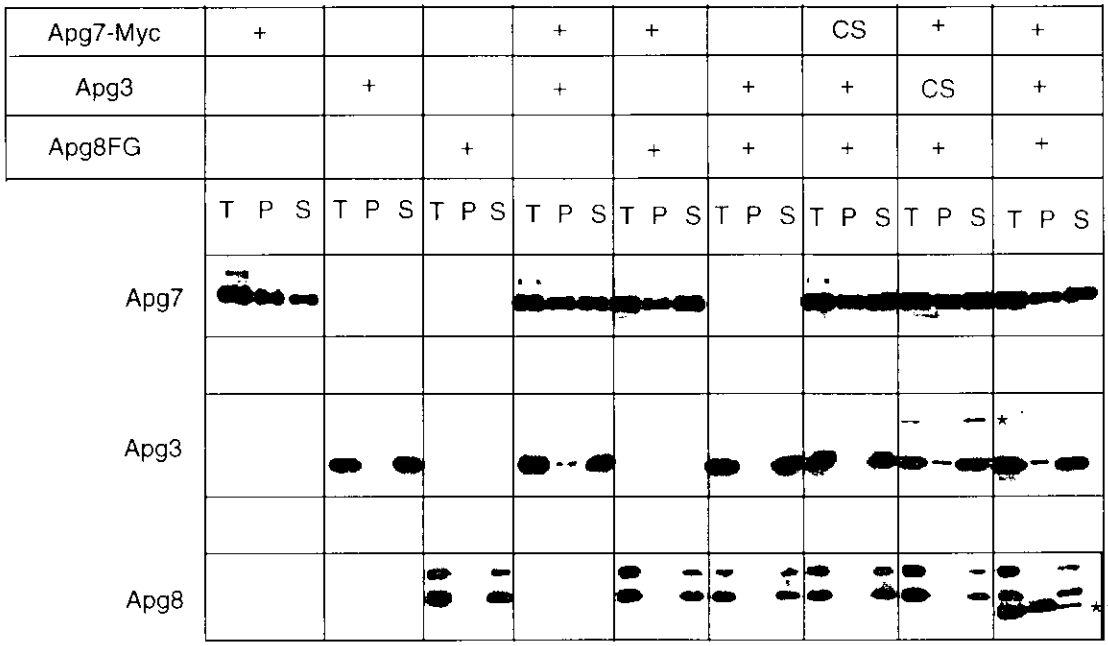

Figure 53. Distribution of Apg7, Apg3 and Apg8 by P_{BAD} promoter in *E. coli*

E. coli cells were transformed with described plasmids containing PBAD promoter. Resulted transformants were grown in LB supplemented with Amp and/or Cm. Respective Apgs were induced by addition of 0.2% arabinose for 3 h, then cells were harvested and disrupted by sonication on ice, then the cell debris was removed by centrifugation. Resulted total lysate (total) was separated to supernatant (S100) and pellet (P100) by centrifugation at 100 k *g* for 1 h. Each fraction was subjected to SDS-PAGE and analyzed by immunoblot with anti-Myc, anti-Apg3 and anti-Apg8 antibody. *indicates a Apg8-Apg3^{C234S} conjugate. **indicates Apg8-PE conjugate.

Discussion

Novel Ubl system mediates protein lipidation

In the previous study on yeast autophagy, Mizushima et al. reported a unique covalent conjugation of Apg12-Apg5 by a similar manner to ubiquitination (Mizushima et al., 1998). The Apg12 conjugates to Apg5 via activation of Apg7 (E1) and conjugation to Apg10 (E2) (Mizushima et al., 1998) (Shintani et al., 1999). Here I discovered the second ubiquitination-like system related to molecular mechanism in autophagy. The processed form of Apg8 by Apg4 protease, Apg8FG exposes a glycine residue at its carboxy terminus. Apg7 (E1) adenylates the Apg8FG with ATP hydrolysis, and sequentially the C-terminal Gly of Apg8FG attaches to a cysteine residue of Apg7 by a thioester bond. The Apg8FG is then transferred to a cysteine residue of Apg3 (E2). Finally, the C-terminal Gly of Apg8FG conjugates with a primary amine of phosphatidylethanolamine (PE) (Fig. 23). The Apg8-PE conjugation system constitutes a novel type of protein lipidation, and its system is required for autophagy. Surprisingly, about a half number of known Apg proteins participate in these ubiquitination-like systems.

Both ubiquitin-proteasome and autophagy play important role for intracellular protein degradation, but their proteolytic mechanisms are absolutely different. They however show a similar post-translational modification at the molecular level in both pathways. The ubiquitination-like systems are transfer reactions from sequential high-energy thioester bond to final amide bond and utilize a set of specific enzymes in the individual pathways. These serial transfers might provide the strict regulation of cellular events such as protein degradation.

Apg8 plays a crucial role for autophagosome formation by PE conjugation

The three-dimensional structure of GATE-16 (Golgi-associated ATPase enhancer of 16 kDa), a mammalian homologue of Apg8 was reported in a recent study by Paz et al (Paz et al., 2000). The structure of GATE-16 was found to have a ubiquitin domain superfold, featuring the ββαβαβ fold. This structural similarity between GATE-16 and ubiquitin supports my results. The crystal structure of ubiquitin shows a part of flexible C-terminus, the Gly residue at which is involved in

the thioester bond formation with their enzymes and amide bond formation with their targets. The GATE-16 structure also revealed the extended C-terminal tail, which located in similar position as in ubiquitin relative to the overall protein fold. This structural similarity was also found in SUMO1 (small ubiquitin-related modifier) (Bayer et al., 1998). Other cognate Ubls may share a similar ubiquitin-fold. Overall structure of GATE-16 contains a ubiquitin-fold and two additional N-terminal α helices that are absent in ubiquitin or other ubiquitin-like proteins. The N-terminal region might be important for the unique feature of Apg8 homologues.

Most intriguingly, Apg8 is conjugated to PE, not a protein. Generally, ubiquitination-like system is known as post-translationally modification to forming a covalent bond between two proteins, modifier and substrate. It is ppossible that Apg8 attaches to PE via ubiquitination-like system, because the primary amine of PE resembles the side chain of lysine, usual target site for ubiquitin and Ubls.

In other report showed that ubiquitin is modified with phospholipid in baculo viral membrane, but it may not be relevant to my findings, since the lipid is not attached to the carboxy terminal glycine (Guarino et al., 1995). I failed to show any protein conjugate with Apg8 in covalently via Apg8 modification system (Fig. 30). The target of Apg8 is presumably only a PE.

The previous morphological analysis indicated that Apg8 plays an important role for autophagosome formation (Kirisako et al., 1999). Apg8-PE probably supplies the PE to the membrane of autophagosome, and it will be required for the expansion of autophagosome. Many lines of evidence, support this idea, 1) Apg8 is localized on autophagosome intermediate structures (Kirisako et al., 1999). 2) The recruitment of Apg8 to autophagosome intermediate structure requires Apg4 and Apg7, and Apg3 (Kim et al., 2001). 3) In mammalian study, Apg5-Apg12 locates on isolation membrane and co-works with LC3 (Apg8 mammalian homologue) in the membrane elongation process (Mizushima et al., 2001). 4) The dissociation of Apg8 from Apg8-PE is essential for autophagosome formation (Kirisako et al., 2000). 5) Abnormally small autophagomes are generated by the induction block of Apg8 (Abeliovich et al., 2000).

The shape of membrane lipids depends on the relative size of its polar head group and apolar tails. PE has a small head group and forms cone-shape. The cone-

shaped PE is assumed to be essential for curvature of membrane. Immunoelectron microscopic analysis shows the localization of Apg8 on small membrane sac and semicircular isolation membrane during autophagosome formation. The membrane topological change in autophagosome formation process may be coordinated by the PE buried in the isolation membrane.

The delivered PE from Apg8-PE to autophagosome membrane would be required for the expansion step and the physical properties of autophagosome membrane.

In higher eukaryotes, Apg8 comprises a protein family including rat microtuble-associated protein 1 light chain 3 (LC3), GATE-16 and γ-aminobutyric acid A receptor-associated protein (GABARAP) (Kabeya et al., 2000) (Sagiv et al., 2000) (Wang et al., 1999). Recent report indicated that LC3 localizes on autophagosome membrane after post-translational modification, and plays an important role for autophagosome formation (Kabeya et al., 2000). GATE-16 distributes in Golgi and is likely to stimulate the intra-Golgi transport by interacting with NSF and GOS-28 (v-SNARE in Golgi) (Sagiv et al., 2000). GABARAP binds $GABA_A$-receptor and promotes clustering of the receptor and binding to microtubles (Wang et al., 1999). The Apg8 family in mammal seems to have different functions at different place. However, all homologues of Apg8 show the conserved glycine residue at their carboxy terminal regions. Also, they bind to mammalian homologue of Apg7 by a thioester linkage, suggesting that these Apg8 homologues be conjugated to proteins or lipids (Tanida et al., 2001). Miller et al reported the physical interaction of Apg8 with Nyv1 (vacuolar v-SNARE), although Nyv1 is dispensable for autophagy (Legesse-Miller et al., 2000) (Ishihara et al., 2001). Cell-free intra-Golgi transport assay revealed that Apg8 can partially replace GATE-16 activity (Legesse-Miller et al., 2000). Apg8-PE may possibly participate in some membrane fusion machinery. To understand the physiological role of Apg8-PE, further analysis is needed.

Apg7 is an activating enzyme for not only Apg12 but also Apg8.

In recent years, several E1-like enzymes have been discovered in the ubiquitination-like systems (Uba2, Uba3, and Uba4) (Hochstrasser, 2000). Apg7 shows slight homology to the ubiquitin E1 enzyme (Uba1) and other E1-like enzymes

(Tanida et al., 1999). Among of the homologous region, the ATP-binding domain in Apg7 shows a significant similarity with that of E1 and E1-like enzymes, and their ATP-binding domain called as boxI; GxGxxG (Fig. 15) (McGrath et al., 1991). The E1 activity of proteins must be characterized by the boxI domain. Notably, Apg7 activates not only Apg12 but also Apg8 by utilizing same ATP-binding domain and cysteine residue (Tanida et al., 1999). It is the first case in ubiquitination-like system that a common E1 enzyme activates two distinct proteins.

The human homologue Apg7 has been previously reported and also found to play a role for E1 function in the human Apg12-Apg5 conjugation system (Tanida et al., 2001). Furthermore, Apg7 seems to activate the mammalian Apg8 homologues, LC3, GATE-16, and GABARAP (Tanida et al., 2001). The activation manner of Apg7 must be well conserved among eukaryotes.

In this study, I also showed the physical interaction between Apg7 and Apg3 in the immunoprecipitation experiments (Fig. 27). Recently, a comprehensive analysis of protein-protein interaction in yeast, *S. cerevisiae* by two-hybrid screening revealed that Apg7 interacts not only with Apg12 and Apg8 but also with Apg3 (Ito et al., 2000). Furthermore, Komatsu et al. reported that the Apg7 forms a homodimer via their carboxy terminal region, and Apg3 associates to the carboxyl terminal region of homodimerized Apg7 (Komatsu et al., 2001). These results are well consistent with my conclusion; Apg7-Apg3 forms an E1-E2 complex. This complex seems to work for the efficient Apg8-PE conjugate (discussed in below). It is still remained that the E1-E2 complex is a heteromultimer with stoichiometry of two each of the Apg7 and Apg3.

The homodimerization of Apg7 is known to be required for the activation of Apg12 and Apg8 (Komatsu et al., 2001). In the early purification experiments by Ciechanover et al, mammalian Uba1 has been found to consist of two subunit (Ciechanover et al., 1982). The carboxy terminal region of Apg7 indicates a slight similarity with that of Uba1. These findings suggest that Uba1 also forms a homodimer. Moreover, genetical interaction analyzes indicate the homodimer of Uba4 (Furukawa et al., 2000). The dimer structure may be required for the function of Uba1 and Uba4.

More recently, the crystal structure of MoeB-MoaD complex revealed as

heterotetramer (Lake et al., 2001). The MoeB and MoaD are involved in molybdenum cofactor (Moco) biosynthesis in *Escherichia coli*, and the MoeB activates the MoaD in an ATP-dependent manner. The MoeB activates the carboxy terminus MoaD, in which C-terminus presents Gly-Gly motif like ubiquitin, and adenylated MoaD converts to thiocarboxylated MoaD to be a sulphur donor during Moco biosynthesis. This process is mechanistically similar to ubiquitin activating reaction. The crystal structure of MoeB-MoaD-ATP ternary complex demonstrated that the C-terminus of MoaD is inserted to the interface of dimerized MoeB and very closed to the ATP binding domains of MoeB, subsequently the dimeric structure has a critical role for ATP binding and hydrolysis. This MoeB-like structure may be arranged into the E1 or E1-like homodimer, to facilitate the adenylation of C-terminus glycine in their modifiers.

Apg3 acts for conjugating enzyme in Apg8-PE conjugation system

Ubiquitin-like protein is conjugated and transferred by E2 enzyme, to their targets, or sometimes through E3 (Fig. 23). In eukaryotes, the E2 family is characterized by a highly conserved E2 motif contains an active site cysteine and tripeptide region, His-Pro-Asn at upstream the active Cys (Haas and Siepmann, 1997). The amino acid sequence of Apg10 and Apg3 is distinct from that of E2 family. However, their catalytic domains are conserved between both homologues, and it indicates another tripeptide region, His-Pro-Cys containing an active site cysteine (Fig. 10). The unique active center suggests a novel E2 family. The conjugation step of Apg12 to Apg10 or Apg8 to Apg3 must be a critical reaction of dual functions of Apg7. However, the detailed mechanism is unclear (discussed in below).

I found the increase of Apg3 during starvation conditions (Fig. 5 and 6). In the previous study, it is known that the amount of Apg8 increases by transcriptional upregulation during starvation conditions (Kirisako et al., 1999). STRE sequence is known in various stress induced promoter, such as CTT1 (cytosolic catalase T) (Schuller et al., 1994). The STRE-like sequence was found at the upstream region of Apg8 promoter, although it was observed as a negative regulator in vegetative conditions (Kirisako et al., 1999). The STRE-like sequence was also found at the upstream region of Apg3 promoter. The transcription of Apg3 may be enhanced in the same regulation manner of Apg8 by shifting to the starvation conditions. Recently,

micro-array analysis demonstrates the increase of mRNA of Apg3 under starvation conditions (Chu et al., 1998). These findings support my results. I also found the increment of Apg8-Apg3 conjugates, is correlated with the increase both Apg8 and Apg3 under the starvation conditions (Fig. 32). The increase of Apg8-Apg3 might be required for a large amount of Apg8-PE during starvation conditions.

The homology search of Apg3 by BLAST scan presents a potential sequence among several species (Fig. 2). These candidates of which function is unknown, but sequences around the cysteine 234 residue are well conserved. It suggests that the conjugating enzyme reaction of Apg3 be highly conserved in these homologues.

Targeting mechanism of Apg8 to PE

Where is Apg8FG conjugated with PE in yeast? The origin of autophagosome membrane is not identified at present, and it is a most interesting issue for us.

Apg8-PE conjugation was reconstituted by simply Apg7, Apg3, Apg8FG, and PE *in vitro* system, suggesting that the Apg8-PE conjugation directly occurs following the thioester bond of Apg8-Apg3 (Fig. 46). Interestingly, the distribution pattern of Apg3 by sucrose density gradient centrifuge demonstrates the two peaks (Fig. 35). The first peak seemed to be a very low density fraction, where Apg3 is likely to associate some lipid-like molecule (Fig. 35). It is suggested that Apg3 may be a critical molecule that is implicated in the recognition of PE. *E. coli* cells expressing Apg8 system components showed a half amount of Apg7 in P100 fraction (Fig. 53). Then, a portion of Apg3 distributed to P100 fraction of the cells co-expressing Apg7 (Fig. 53). These results indicate the heterocomplex of Apg7-Apg3 exists closely to membrane. On the other hand, most Apg3 in yeast presented in S100 fraction (Fig. 33, 34, and 53). Kim et al. has previously proposed that a part of Apg7 weakly associates with membrane fraction (P13) under starvation condition (Kim et al., 1999). From these results, it is probable that Apg7-Apg3 heterocomplex associates with some membrane in yeast by weak membrane affinity of Apg7 or Apg3, and Apg3 could be directly interacted to PE in order to transfer of Apg8FG.

Further, in yeast, subcellular fractionation analysis exhibited the localization of Apg8 in both LSP and HSP of wild-type, but there was no signal of Apg8 in the LSP of Δ*apg3* cells (Fig. 4). These results indicated that Apg8-PE was recovered exclusively

in LSP fraction, and the significant amount of unlipidated Apg8 distributed in HSP fraction as a peripheral membrane protein (Fig. 4 and 21). The conjugate of Apg8FG with PE may occur at the some membrane in HSP fraction. The Apg8-PE conjugation system begins thioester bond formation of Apg8-Apg7. There is a possibility that the peripheral membrane Apg8 is required for the membrane association or approach of Apg7-Apg3 complex.

It is still remained whether there is a direct interaction between Apg3 and PE. Moreover, since PE is included in every biological membranes, the detailed analysis about Apg8 associated membrane is necessary. I constructed *in vitro* assay technique for Apg8-PE reconstitution in this study, taking advantage of which the donor membrane of the PE should be clarified in the near feature.

Miller et al. has reported the physical interaction of Apg8 with Bet1 (v-SNARE in ER-Golgi transport), and the localization of Apg8 (peripheral membrane form) at Golgi compartment (Legesse-Miller et al., 2000). They proposed that the Apg8 participate in membrane trafficking at early secretory pathway. As previous described, three different mammalian Apg8 homologues indicate the distinct intracellular roles. Apg8 may function on other vesicle, like on autophagosome. It is however unknown in yeast whether the Apg8-PE form is required for other functions (or localization), other than autophagy and the Cvt-pathway.

The reaction mechanism in Apg8-PE conjugation system

Notably, Apg7 activates not only Apg12 but also Apg8. The ATP-binding region site (Gly333) and active site (Cys507) of Apg7 are essential for the activation both Apg12 and Apg8 (Fig. 15). Apg7 apparently activates Apg12 and Apg8 in the same catalytic manner. Is there any confusion when Apg7 activate Apg12 and Apg8 at the same time? As described previously, Apg3 has a physical interaction with Apg7 (Fig. 27). Then, Apg3 also associates to Apg12 in an Apg7 dependent manner, but it is not conjugation via thioester bond (Fig. 18 and 26). The physical interaction between Apg3 and Apg12 might be mediated by Apg7-Apg3 complex (Fig. 26 and 28). Furthermore, the Apg3 is not essential for Apg12-Apg7 and for Apg8-Apg7 conjugation step (data not shown). These observations indicate that activation of Apg8 and Apg12 by Apg7 does not need the Apg7-Apg3 complex. On the other hand, significant

amount of Apg3 interacts physically with Apg7, the complex probably facilitate the transfer of Apg8 from Apg7 to Apg3. The conjugate reaction of Apg10 with Apg12 must occur on Apg7, following associate with Apg7. Apg3 does not physically interact with Apg10 in the presence of Apg7, suggesting that the Apg7 is no longer the complex with Apg3 in the association of Apg10 (Fig. 26). Probably, Apg10 recognizes specifically the conjugate of Apg12-Apg7, and it will abolish the interaction between Apg7 and Apg3, to conjugating of the Apg10 to Apg12. This interaction model is able to explain the divergence of E2 conjugates, Apg12-Apg10 and Apg8-Apg3, from their common E1, Apg7. Consequently, Apg3 and Apg10 serve the recognition of their targets directly, PE for Apg8 and Apg5 for Apg12 (Fig. 23).

By the reconstituted Apg8-PE conjugation system, the *E:coli* cells accumulated a significant amount of Apg8-PE (Fig. 36). Phospholipids are the only lipid constituent in the bacterial inner-membrane. The phospholipid content of the *E. coli* envelope comprises ~75% PE against ~20% PE in yeast. Further, each component of Apg8 system is overproduced in *E.coli.* by *araC*-P_{BAD} promoter (Fig. 36). Accordingly, a large amount of Apg8-PE would be formed in *E. coli* harboring Apg8-PE conjugation system. In spite of the highly accumulated Apg8-PE, cells expressing the components of Apg8 system demonstrated a normal growth in LB medium containing arabinose, in similar to wild-type (data not shown). PE-deficient *E. coli* shows a morphological change as fiber shape (Rietveld et al., 1993). Such morphological change was not identified by light-microscopic observation in cells carrying Apg8-PE, compared with wild-type. In this study, the expression of respective Apgs involving in Apg8 system was regulated with *araC*-P_{BAD} promoter. This promoter is inducible efficiently by arabinose addition, but its expression level is not strong, thereby minimizies the alterations in cell physiology (Guzman et al., 1995).

Optimal condition for Apg8-PE conjugate reaction

Apg8FG was conjugated with PE in *E. coli* total lipid liposome by purified Apg8 system *in vitro* consisting of Apg7, Apg3, and Apg8FG (Fig. 48). Among these experiments, 0.9 pmoles Apg8FG was significantly converted to Apg8-PE by 1.0 nmol total lipid liposome, which contained 0.754 nmoles PE, thus the calculated molecular ratio indicated approximate 1 : 838 (Apg8FG : PE) (Fig. 48). Resulted Apg8-PE

appears to be saturated at 0.754 nmoles PE above (Fig. 48). These results suggest that Apg8-PE conjugation reaction is not stimulated beyond the proportion of an 1 : 838 (Apg8FG: PE) molecular ratio under these reaction conditions.

By a cell-free system, unchanged Apg8FG was observed in the Apg8 system components reaction mixture containing PE-deficient cell liposome, but the Apg8-PE was restored by the mixing of *E. coli* PE from 20% to 90% per 5.0 nmoles total lipid liposome (PE content 1.0-4.5 nmoles) (Fig. 46). The Apg8-PE conjugate was markedly accumulated by 50-80%-PE liposome (PE content 2.5-4.0 nmoles) and reduced by 90%-100%-PE liposome (PE content 4.5-5.0 nmoles) (Fig. 46). 100% PE liposome showed a lower level of Apg8-PE even the presence of below 4.0 nmoles PE in the reaction mixture (Fig. 49). The lipid composition in wild-type cell is usual tightly regulated. The lack of a PE in GN10 is compensated by a large amounts of phosohatidylglycerol (PG) and cardioripin (CL), of which liposome form the bilayer structures in the physiological condition (Dowhan, 1997). Thus, obtained GN10 liposome prefers bilayer to non-bilayer. To mimic the native phospholipids composition of *E. coli* in this analysis, the GN10 total lipid gradually replaced to *E. coli* PE, therefore resulted liposome assumable the phase-transition from bilayer to non-bilayer phase depending on their PE contents (Fig. 46). The transition from bilayer to non-bilayer would not be requisite for Apg8-PE conjugation, because the Apg8-PE could be detected at the point of 20% *E. coli* PE (Fig. 46) (Dowhan, 1997). Alternatively, the reduced Apg8-PE by 90%-100% PE liposome suggested that the excess PE forms a hexagonal phase, subsequent lost the accessibility to Apg8FG (Fig. 46) (Dowhan, 1997). These results indicate that the reconstitution of Apg8-PE is affected by the PE content of liposome rather than absolute amount of PE in the reaction mixture. This conclusion is coincident with below results using other lipids liposome. 1-palmitoyl-2-oleoylphoshatidylcholine (POPC) and dioleoyl phosphatidylethanolamine (DOPE) were mixed, and various lipid compositions in liposome were made. The resulted liposome showed that the 75% DOPE liposome significant accumulates the Apg8-PE conjugation than 50% and 100% DOPE liposome (Fig. 47). In addition, the yeast total lipid liposome contains ~20% PE, is slightly bound to Apg8FG (Fig. 45). Apg8-PE conjugation must be strongly affected by PE level of liposome and membrane, and in which optimal PE content seems to be 50~80%, resemble in *E. coli* membrane

composition.

Using various concentrations of the Apg components on Apg8 system *in vitro* assay, the increase of Apg8FG did not enhance the Apg8-PE, although high amounts of Apg7 and Apg3 dramatically promoted the Apg8-PE conjugation (Fig. 50). Further, the reconstitution experiments of Apg8-PE by cell-free system indicated a certain lag time at the early step in the Apg8-PE conjugation system (Fig. 52). These observations imply that the high amounts of Apg7 and Apg3 generate the sufficient E1-E2 complexes to facilitate the Apg8-PE conjugation. Moreover, Apg7 and Apg3 might lose their catalytic function in the *in vitro* system.

Interestingly, high concentration of Apg8FG showed an inhibitory effect on Apg8-PE conjugation in the cell-free system (Fig. 51). I previously discussed the ternary complex of Apg7-Apg3-Apg8 in yeast (Fig. 27). Apg8FG is likely to interact with the Apg7-Apg3 complex, and then the Apg7-Apg3 complex (or Apg3) probably acts for the transfer of Apg8FG to a target, PE. The excessive Apg8FG therefore may disorder the molecular interaction of Apg7-Apg3 or Apg7-Apg3-Apg8FG. This question will be resolved by the analysis of physical interaction between Apg7, Apg3, and Apg8FG *in vitro*.

Feature studies

Intriguingly, the amount of Apg8-PE in yeast is significantly reduced in the absence of Apg12-Apg5 conjugation. Recently, an E3-like factor involved in SUMO conjugation has been discovered (Johnson et al., 1997). The reconstituted SUMO conjugation system *in vitro* containing Uba2/Aos1 (E1) and Ubc9 (E2) demonstrates a weakly sumoylation of septins. When there is Siz1 (E3) in the *in vitro* reaction, the sumoylation of septins is highly stimulated. This character of E3 is defined as transfer activating factor of modifier from modifier-E2 complex to the target. In my study, Apg8FG was successfully conjugated to PE by *in vitro* reaction, where contained Apg7 (E1) and Apg3 (E2). Further, I found the accelerated reaction of Apg8-PE conjugation system *in vitro* by increment of Apg7 and Apg3. These results suggested that Apg8-PE conjugation arise from enzyme reactions both E1 and E2, but these enzymes *in vitro* do not have the catalytic function within the ubiquitination-like system cascade. Apg12-Apg5 conjugation possibly may help the recycle system of Apg7 and Apg3, by distinct

manner from E3 of sumoylation.

The detailed molecular mechanism in the both conjugation systems related to autophagosome formation still remains unclear. By taking advantage of *in vitro* reconstitution study of Apg8-PE, further insight can be gained to elucidate the molecular function in these two conjugation systems.

References

Abeliovich, H., W.A. Dunn, Jr., J. Kim, and D.J. Klionsky. 2000. Dissection of autophagosome biogenesis into distinct nucleation and expansion steps. *J Cell Biol.* 151:1025-1034.

Agarraberes, F.A., S.R. Terlecky, and J.F. Dice. 1997. An intralysosomal hsp70 is required for a selective pathway of lysosomal protein degradation. *J Cell Biol.* 137:825-834.

Baba, M., M. Osumi, S.V. Scott, D.J. Klionsky, and Y. Ohsumi. 1997. Two distinct pathways for targeting proteins from the cytoplasm to the vacuole/lysosome. *J Cell Biol.* 139:1687-1695.

Baba, M., K. Takeshige, N. Baba, and Y. Ohsumi. 1994. Ultrastructural analysis of the autophagic process in yeast: detection of autophagosomes and their characterization. *J. Cell Biol.* 124:903-913.

Bachmair, A., D. Finley, and A. Varshavsky. 1986. In vivo half-life of a protein is a function of its amino-terminal residue. *Science.* 234:179-186.

Bartel, B., I. Wunning, and A. Varshavsky. 1990. The recognition component of the N-end rule pathway. *Embo J.* 9:3179-3189.

Bartlett, G.R. 1958: Phosphorus assay in column chromatography. *J Biol Chem.* 234:466-468.

Baumeister, W., J. Walz, F. Zuhl, and E. Seemuller. 1998. The proteasome: paradigm of a self-compartmentalizing protease. *Cell.* 92:367-380.

Bayer, P., A. Arndt, S. Metzger, R. Mahajan, F. Melchior, R. Jaenicke, and J. Becker. 1998. Structure determination of the small ubiquitin-related modifier SUMO-1. *J Mol Biol.* 280:275-286.

Chu, S., J. DeRisi, M. Eisen, J. Mulholland, D. Botstein, P.O. Brown, and I. Herskowitz. 1998. The transcriptional program of sporulation in budding yeast. *Science.* 282:699-705.

Ciechanover, A. 1998. The ubiquitin-proteasome pathway: on protein death and cell life. *EMBO J.* 17:7151-7160.

Ciechanover, A., S. Elias, H. Heller, S. Ferber, and A. Hershko. 1980. Characterization of the heat-stable polypeptide of the ATP-dependent proteolytic system from reticulocytes. *J Biol Chem.* 255:7525-7528.

Ciechanover, A., S. Elias, H. Heller, and A. Hershko. 1982. "Covalent affinity" purification of ubiquitin-activating enzyme. *J Biol Chem.* 257:2537-2542.

Cuervo, A.M., and J.F. Dice. 1996. A receptor for the selective uptake and degradation of proteins by lysosomes. *Science.* 273:501-503.

Darsow, T., S.E. Rieder, and S.D. Emr. 1997. A multispecificity syntaxin homologue, Vam3p, essential for autophagic and biosynthetic protein transport to the vacuole. *J Cell Biol.* 138:517-529.

Dowhan, W. 1997. Molecular basis for membrane phospholipid diversity: why are there so many lipids?

Annu Rev Biochem. 66:199-232.

Dunn, W.A., Jr. 1990a. Studies on the mechanisms of autophagy: formation of the autophagic vacuole. *J Cell Biol.* 110:1923-1933.

Dunn, W.A., Jr. 1990b. Studies on the mechanisms of autophagy: maturation of the autophagic vacuole. *J Cell Biol.* 110:1935-1945.

Egner, R., M. Thumm, M. Straub, A. Simeon, H.J. Schuller, and D.H. Wolf. 1993. Tracing intracellular proteolytic pathways. Proteolysis of fatty acid synthase and other cytoplasmic proteins in the yeast Saccharomyces cerevisiae. *J Biol Chem.* 268:27269-27276.

Feldman, R.M., C.C. Correll, K.B. Kaplan, and R.J. Deshaies. 1997. A complex of Cdc4p, Skp1p, and Cdc53p/cullin catalyzes ubiquitination of the phosphorylated CDK inhibitor Sic1p. *Cell.* 91:221-230.

Funakoshi, T., A. Matsuura, T. Noda, and Y. Ohsumi. 1997. Analyses of APG13 gene involved in autophagy in yeast, Saccharomyces cerevisiae. *Gene.* 192:207-213.

Furukawa, K., N. Mizushima, T. Noda, and Y. Ohsumi. 2000. A protein conjugation system in yeast with homology to biosynthetic enzyme reaction of prokaryotes. *J. Biol. Chem.* 275:7462-7465.

Goldberg, A.L. 1992. The mechanism and functions of ATP-dependent proteases in bacterial and animal cells. *Eur J Biochem.* 203:9-23.

Gong, L., and E.T. Yeh. 1999. Identification of the activating and conjugating enzymes of the NEDD8 conjugation pathway. *J Biol Chem.* 274:12036-12042.

Gottesman, S., and M.R. Maurizi. 1992. Regulation by proteolysis: energy-dependent proteases and their targets. *Microbiol Rev.* 56:592-621.

Groll, M., L. Ditzel, J. Lowe, D. Stock, M. Bochtler, H.D. Bartunik, and R. Huber. 1997. Structure of 20S proteasome from yeast at 2.4 A resolution. *Nature.* 386:463-471.

Guarino, L.A., G. Smith, and W. Dong. 1995. Ubiquitin is attached to membranes of baculovirus particles by a novel type of phospholipid anchor. *Cell.* 80:301-309.

Guzman, L.M., D. Belin, M.J. Carson, and J. Beckwith. 1995. Tight regulation, modulation, and high-level expression by vectors containing the arabinose PBAD promoter. *J Bacteriol.* 177:4121-4130.

Haas, A.L., and T.J. Siepmann. 1997. Pathways of ubiquitin conjugation. *Faseb J.* 11:1257-1268.

Harding, T.M., K.A. Morano, S.V. Scott, and D.J. Klionsky. 1995. Isolation and characterization of yeast mutants in the cytoplasm to vacuole protein targeting pathway. *J Cell Biol.* 131:591-602.

Hershko, A. 1999. Mechanisms and regulation of the degradation of cyclin B. *Philos Trans R Soc Lond B Biol Sci.* 354:1571-1575; discussion 1575-1576.

Hershko, A., and A. Ciechanover. 1998. The ubiquitin system. *Annu Rev Biochem.* 67:425-479.

Hochstrasser, M. 1996. Ubiquitin-dependent protein degradation. *Annu Rev Genet.* 30:405-439.

Hochstrasser, M. 2000. Evolution and function of ubiquitin-like protein-conjugation systems. *Nat Cell Biol.* 2:E153-157.

Huibregtse, J.M., M. Scheffner, S. Beaudenon, and P.M. Howley. 1995. A family of proteins structurally and functionally related to the E6-AP ubiquitin-protein ligase. *Proc Natl Acad Sci U S A.* 92:5249.

Huibregtse, J.M., M. Scheffner, and P.M. Howley. 1991. A cellular protein mediates association of p53 with the E6 oncoprotein of human papillomavirus types 16 or 18. *Embo J.* 10:4129-4135.

Irniger, S., S. Piatti, C. Michaelis, and K. Nasmyth. 1995. Genes involved in sister chromatid separation are needed for B-type cyclin proteolysis in budding yeast. *Cell.* 81:269-278.

Ishihara, N., M. Hamasaki, S. Yokota, K. Suzuki, Y. Kamada, A. Kihara, T. Yoshimori, T. Noda, and Y. Ohsumi. 2001. Autophagosome Requires Specific Early Sec Proteins for Its Formation and NSF/SNARE for Vacuolar Fusion. *Mol Biol Cell.* 12:3690-3702.

Ito, T., K. Tashiro, S. Muta, R. Ozawa, T. Chiba, M. Nishizawa, K. Yamamoto, S. Kuhara, and Y. Sakaki. 2000. Toward a protein-protein interaction map of the budding yeast: A comprehensive system to examine two-hybrid interactions in all possible combinations between the yeast proteins. *Proc Natl Acad Sci U S A.* 97:1143-1147.

Johnson, E.S., and G. Blobel. 1997. Ubc9p is the conjugating enzyme for the ubiquitin-like protein Smt3p. *J Biol Chem.* 272:26799-26802.

Johnson, E.S., I. Schwienhorst, R.J. Dohmen, and G. Blobel. 1997. The ubiquitin-like protein Smt3p is activated for conjugation to other proteins by an Aos1p/Uba2p heterodimer. *Embo J.* 16:5509-5519.

Kabeya, Y., N. Mizushima, T. Ueno, A. Yamamoto, T. Kirisako, T. Noda, E. Kominami, Y. Ohsumi, and T. Yoshimori. 2000. LC3, a mammalian homologue of yeast Apg8p, is localized in autophagosome membranes after processing. *Embo J.* 19:5720-5728.

Kamada, Y., T. Funakoshi, T. Shintani, K. Nagano, M. Ohsumi, and Y. Ohsumi. 2000. Tor-mediated induction of autophagy via an Apg1 protein kinase complex. *J Cell Biol.* 150:1507-1513.

Kametaka, S., T. Okano, M. Ohsumi, and Y. Ohsumi. 1998. Apg14p and Apg6/Vps30p form a protein complex essential for autophagy in the yeast, Saccharomyces cerevisiae. *J Biol Chem.* 273:22284-22291.

Kamizono, S., T. Hanada, H. Yasukawa, S. Minoguchi, R. Kato, M. Minoguchi, K. Hattori, S. Hatakeyama, M. Yada, S. Morita, T. Kitamura, H. Kato, K. Nakayama, and A. Yoshimura. 2001. The SOCS box of SOCS-1 accelerates ubiquitin-dependent proteolysis of TEL-JAK2. *J Biol Chem.* 276:12530-12538.

Kamura, T., D.M. Koepp, M.N. Conrad, D. Skowyra, R.J. Moreland, O. Iliopoulos, W.S. Lane, W.G. Kaelin, Jr., S.J. Elledge, R.C. Conaway, J.W. Harper, and J.W. Conaway. 1999. Rbx1, a component of the VHL tumor suppressor complex and SCF ubiquitin ligase. *Science.* 284:657-661.

Kamura, T., S. Sato, D. Haque, L. Liu, W.G. Kaelin, Jr., R.C. Conaway, and J.W. Conaway. 1998. The Elongin BC complex interacts with the conserved SOCS-box motif present in members of the SOCS, ras, WD-40 repeat, and ankyrin repeat families. *Genes Dev.* 12:3872-3881.

Kihara, A., Y. Kabeya, Y. Ohsumi, and T. Yoshimori. 2001a. Beclin-phosphatidylinositol 3-kinase complex functions at the trans- Golgi network. *EMBO Rep.* 2:330-335.

Kihara, A., T. Noda, N. Ishihara, and Y. Ohsumi. 2001b. Two distinct Vps34 phosphatidylinositol 3-kinase complexes function in autophagy and carboxypeptidase Y sorting in Saccharomyces cerevisiae. *J Cell Biol.* 152:519-530.

Kikuchi, S., I. Shibuya, and K. Matsumoto. 2000. Viability of an Escherichia coli pgsA null mutant lacking detectable phosphatidylglycerol and cardiolipin. *J Bacteriol.* 182:371-376.

Kim, J., V.M. Dalton, K.P. Eggerton, S.V. Scott, and D.J. Klionsky. 1999. Apg7p/Cvt2p is required for the cytoplasm-to-vacuole targeting, macroautophagy, and peroxisome degradation pathways. *Mol. Biol. Cell.* 10:1337-1351.

Kim, J., W.P. Huang, and D.J. Klionsky. 2001. Membrane recruitment of Aut7p in the autophagy and cytoplasm to vacuole targeting pathways requires Aut1p, Aut2p, and the autophagy conjugation complex. *J Cell Biol.* 152:51-64.

Kim, J., and D.J. Klionsky. 2000. Autophagy, cytoplasm-to-vacuole targeting pathway, and pexophagy in yeast and mammalian cells. *Annu Rev Biochem.* 69:303-342.

Kim, J., S.V. Scott, M.N. Oda, and D.J. Klionsky. 1997. Transport of a large oligomeric protein by the cytoplasm to vacuole protein targeting pathway. *J Cell Biol.* 137:609-618.

King, R.W., J.M. Peters, S. Tugendreich, M. Rolfe, P. Hieter, and M.W. Kirschner. 1995. A 20S complex containing CDC27 and CDC16 catalyzes the mitosis-specific conjugation of ubiquitin to cyclin B. *Cell.* 81:279-288.

Kirisako, T., M. Baba, N. Ishihara, K. Miyazawa, M. Ohsumi, T. Yoshimori, T. Noda, and Y. Ohsumi. 1999. Formation process of autophagosome is traced with Apg8/Aut7p in yeast. *J. Cell Biol.* 147:435-446.

Kirisako, T., Y. Ichimura, H. Okada, Y. Kabeya, N. Mizushima, T. Yoshimori, M. Ohsumi, T. Takao, T. Noda, and Y. Ohsumi. 2000. The reversible modification regulates the membrane-binding state of Apg8/Aut7 essential for autophagy and the cytoplasm to vacuole targeting pathway. *J Cell Biol.* 151:263-276.

Kisselev, A.F., T.N. Akopian, K.M. Woo, and A.L. Goldberg. 1999. The sizes of peptides generated from protein by mammalian 26 and 20 S proteasomes. Implications for understanding the degradative mechanism and antigen presentation. *J Biol Chem.* 274:3363-3371.

Klionsky, D.J., and S.D. Emr. 2000. Autophagy as a regulated pathway of cellular degradation. *Science.* 290:1717-1721.

Klionsky, D.J., and Y. Ohsumi. 1999. Vacuolar import of proteins and organelles from the cytoplasm. *Annu Rev Cell Dev Biol.* 15:1-32.

Komatsu, M., I. Tanida, T. Ueno, M. Ohsumi, Y. Ohsumi, and E. Kominami. 2001. The C-terminal region of an Apg7p/Cvt2p is required for homodimerization and is essential for its E1 activity and E1-E2 complex formation. *J Biol Chem.* 276:9846-9854.

Kopitz, J., G.O. Kisen, P.B. Gordon, P. Bohley, and P.O. Seglen. 1990. Nonselective autophagy of cytosolic enzymes by isolated rat hepatocytes. *J Cell Biol.* 111:941-953.

Kornitzer, D., and A. Ciechanover. 2000. Modes of regulation of ubiquitin-mediated protein degradation. *J Cell Physiol.* 182:1-11.

Kretz-Remy, C., and R.M. Tanguay. 1999. SUMO/sentrin: protein modifiers regulating important cellular functions. *Biochem Cell Biol.* 77:299-309.

Kwon, Y.T., Y. Reiss, V.A. Fried, A. Hershko, J.K. Yoon, D.K. Gonda, P. Sangan, N.G. Copeland, N.A. Jenkins, and A. Varshavsky. 1998. The mouse and human genes encoding the recognition component of the N- end rule pathway. *Proc Natl Acad Sci U S A.* 95:7898-7903.

Lake, M.W., M.M. Wuebbens, K.V. Rajagopalan, and H. Schindelin. 2001. Mechanism of ubiquitin activation revealed by the structure of a bacterial MoeB-MoaD complex. *Nature.* 414:325-329.

Lang, T., E. Schaeffeler, D. Bernreuther, M. Bredschneider, D.H. Wolf, and M. Thumm. 1998. Aut2p and Aut7p, two novel microtubule-associated proteins are essential for delivery of autophagic vesicles to the vacuole. *Embo J.* 17:3597-3607.

Legesse-Miller, A., Y. Sagiv, R. Gluzman, and Z. Elazar. 2000. Aut7p, a Soluble Autophagic Factor, Participates in Multiple Membrane Trafficking Processes. *J Biol Chem.* 275:32966-32973.

Li, S.J., and M. Hochstrasser. 2000. The yeast ULP2 (SMT4) gene encodes a novel protease specific for the ubiquitin-like Smt3 protein. *Mol Cell Biol.* 20:2367-2377.

Matsuura, A., M. Tsukada, Y. Wada, and Y. Ohsumi. 1997. Apg1p, a novel protein kinase required for the autophagic process in Saccharomyces cerevisiae. *Gene.* 192:245-250.

McGrath, JP., S. Jentsch, and A. Varshavsky. 1991. UBA 1: an essential yeast gene encoding ubiquitin-activating enzyme. *Embo J.* 10:227-236.

Michel, J.J., and Y. Xiong. 1998. Human CUL-1, but not other cullin family members, selectively interacts with SKP1 to form a complex with SKP2 and cyclin A. *Cell Growth Differ.* 9:435-449.

Mizushima, N., T. Noda, and Y. Ohsumi. 1999. Apg16p is required for the function of the Apg12p-Apg5p conjugate in the yeast autophagy pathway. *Embo J.* 18:3888-3896.

Mizushima, N., T. Noda, T. Yoshimori, Y. Tanaka, T. Ishii, M.D. George, D.J. Klionsky, M. Ohsumi, and Y. Ohsumi. 1998a. A protein conjugation system essential for autophagy. *Nature*. 395:395-398.

Mizushima, N., H. Sugita, T. Yoshimori, and Y. Ohsumi. 1998b. A new protein conjugation system in human. The counterpart of the yeast Apg12p conjugation system essential for autophagy. *J. Biol. Chem.* 273:33889-33892.

Mizushima, N., A. Yamamoto, M. Hatano, Y. Kobayashi, Y. Kabeya, K. Suzuki, T. Tokuhisa, Y. Ohsumi, and T. Yoshimori. 2001. Dissection of autophagosome formation using Apg5-deficient mouse embryonic stem cells. *J Cell Biol.* 152:657-668.

Nakamura, N., A. Matsuura, Y. Wada, and Y. Ohsumi. 1997. Acidification of vacuoles is required for autophagic degradation in the yeast, Saccharomyces cerevisiae. *J Biochem (Tokyo)*. 121:338-344.

Noda, T., J. Kim, WP. Huang, M. Baba, C. Tokunaga, Y. Ohsumi, and D.J. Klionsky. 2000. Apg9p/Cvt7p is an integral membrane protein required for transport vesicle formation in the Cvt and autophagy pathways. *J Cell Biol.* 148:465-480.

Noda, T., A. Matsuura, Y. Wada, and Y. Ohsumi. 1995. Novel system for monitoring autophagy in the yeast Saccharomyces cerevisiae. *Biochem. Biophys. Res. Commun.* 210:126-132.

Noda, T., and Y. Ohsumi. 1998. Tor, a phosphatidylinositol kinase homologue, controls autophagy in yeast. *J Biol Chem.* 273:3963-3966.

Ohsumi, Y. 2001. Molecular dissection of autophagy: two ubiquitin-like systems. *Nat Rev Mol Cell Biol.* 2:211-216.

Ohta, T., J.J. Michel, A.J. Schottelius, and Y. Xiong. 1999. ROC1, a homolog of APC11, represents a family of cullin partners with an associated ubiquitin ligase activity. *Mol Cell.* 3:535-541.

Osaka, F., H. Kawasaki, N. Aida, M. Saeki, T. Chiba, S. Kawashima, K. Tanaka, and S. Kato. 1998. A new NEDD8-ligating system for cullin-4A. *Genes Dev.* 12:2263-2268.

Paz, Y., Z. Elazar, and D. Fass. 2000. Structure of GATE-16, Membrane Transport Modulator and Mammalian Ortholog of Autophagocytosis Factor Aut7p. *J Biol Chem.* 275:25445-25450.

Pickart, C.M. 1997. Targeting of substrates to the 26S proteasome. *Faseb J.* 11:1055-1066.

Rechsteiner, M., L. Hoffman, and W. Dubiel. 1993. The multicatalytic and 26 S proteases. *J Biol Chem.* 268:6065-6068.

Renkonen, O. 1967. The analysis of individual molecular species of polar lipids. *Adv Lipid Res.* 5:329-351.

Rietveld, A.G., J.A. Killian, W. Dowhan, and B. de Kruijff. 1993. Polymorphic regulation of membrane phospholipid composition in Escherichia coli. *J Biol Chem.* 268:12427-12433.

Rose, M.D., F. Winston, and P. Hieter. 1990. Methods in Yeast Genetics: A laboratory Manual. Cold

Spring Harbor Laboratory Press, Cold Spring Harbor, NY.

Sagiv, Y., A. Legesse-Miller, A. Porat, and Z. Elazar. 2000. GATE-16, a membrane transport modulator, interacts with NSF and the Golgi v-SNARE GOS-28. *Embo J.* 19:1494-1504.

Saha, S.K., S. Nishijima, H. Matsuzaki, I. Shibuya, and K. Matsumoto. 1996. A regulatory mechanism for the balanced synthesis of membrane phospholipid species in Escherichia coli. *Biosci Biotechnol Biochem.* 60:111-116.

Sambrook, J., E.F. Fritsch, and T. Maniatis. 1989. Molecular Cloning: A Laboratory Manual. Cold Spring Harbor Laboratory Press, Cold Spring Harbor, NY.

Saurin, A.J., K.L. Borden, M.N. Boddy, and P.S. Freemont. 1996. Does this have a familiar RING? *Trends Biochem Sci.* 21:208-214.

Scheffner, M., U. Nuber, and J.M. Huibregtse. 1995. Protein ubiquitination involving an E1-E2-E3 enzyme ubiquitin thioester cascade. *Nature.* 373:81-83.

Schlumpberger, M., E. Schaeffeler, M. Straub, M. Bredschneider, D.H. Wolf, and M. Thumm. 1997. AUT1, a gene essential for autophagocytosis in the yeast Saccharomyces cerevisiae. *J. Bacteriol.* 179:1068-1076.

Schuller, C., J.L. Brewster, M.R. Alexander, M.C. Gustin, and H. Ruis. 1994. The HOG pathway controls osmotic regulation of transcription via the stress response element (STRE) of the Saccharomyces cerevisiae CTT1 gene. *Embo J.* 13:4382-4389.

Schworer, C.M., and G.E. Mortimore. 1979. Glucagon-induced autophagy and proteolysis in rat liver: mediation by selective deprivation of intracellular amino acids. *Proc Natl Acad Sci U S A.* 76:3169-3173.

Scott, S.V., A. Hefner-Gravink, K.A. Morano, T. Noda, Y. Ohsumi, and D.J. Klionsky. 1996. Cytoplasm-to-vacuole targeting and autophagy employ the same machinery to deliver proteins to the yeast vacuole. *Proc Natl Acad Sci U S A.* 93:12304-12308.

Shintani, T., N. Mizushima, Y. Ogawa, A. Matsuura, T. Noda, and Y. Ohsumi. 1999. Apg10p, a novel protein-conjugating enzyme essential for autophagy in yeast. *EMBO J.* 18:5234-5241.

Shintani, T., K. Suzuki, Y. Kamada, T. Noda, and Y. Ohsumi. 2001. Apg2p functions in autophagosome formation on the perivacuolar structure. *J Biol Chem.* 276:30452-30460.

Shteinberg, M., Y. Protopopov, T. Listovsky, M. Brandeis, and A. Hershko. 1999. Phosphorylation of the cyclosome is required for its stimulation by Fizzy/cdc20. *Biochem Biophys Res Commun.* 260:193-198.

Skowyra, D., K.L. Craig, M. Tyers, S.J. Elledge, and J.W. Harper. 1997. F-box proteins are receptors that recruit phosphorylated substrates to the SCF ubiquitin-ligase complex. *Cell.* 91:209-219.

Skowyra, D., D.M. Koepp, T. Kamura, M.N. Conrad, R.C. Conaway, J.W. Conaway, S.J. Elledge, and J.W. Harper. 1999. Reconstitution of G1 cyclin ubiquitination with complexes containing SCFGrr1 and

Rbx1. *Science*. 284:662-665.

Stromhaug, P.E., and D.J. Klionsky. 2001. Approaching the molecular mechanism of autophagy. *Traffic*. 2:524-531.

Sudakin, V., D. Ganoth, A. Dahan, H. Heller, J. Hershko, F.C. Luca, J.V. Ruderman, and A. Hershko. 1995. The cyclosome, a large complex containing cyclin-selective ubiquitin ligase activity, targets cyclins for destruction at the end of mitosis. *Mol Biol Cell*. 6:185-197.

Suzuki, K., T. Kirisako, Y. Kamada, N. Mizushima, T. Noda, and Y. Ohsumi. 2001. The pre-autophagosomal structure organized by concerted functions of APG genes is essential for autophagosome formation. *Embo J*. 20:5971-5981.

Takahashi, Y., J. Mizoi, E.A. Toh, and Y. Kikuchi. 2000. Yeast Ulp1, an Smt3-specific protease, associates with nucleoporins. *J Biochem (Tokyo)*. 128:723-725.

Takeshige, K., M. Baba, S. Tsuboi, T. Noda, and Y. Ohsumi. 1992. Autophagy in yeast demonstrated with proteinase-deficient mutants and conditions for its induction. *J Cell Biol*. 119:301-311.

Tan; P., S.Y. Fuchs, A. Chen, K. Wu, C. Gomez, Z. Ronai, and Z.Q. Pan. 1999. Recruitment of a ROC1-CUL1 ubiquitin ligase by Skp1 and HOS to catalyze the ubiquitination of I kappa B alpha. *Mol Cell*. 3:527-533.

Tanida, I., N. Mizushima, M. Kiyooka, M. Ohsumi, T. Ueno, Y. Ohsumi, and E. Kominami. 1999. Apg7p/Cvt2p: A novel protein-activating enzyme essential for autophagy. *Mol. Biol. Cell*. 10:1367-1379.

Tanida, I., E. Tanida-Miyake, T. Ueno, and E. Kominami. 2001. The human homolog of Saccharomyces cerevisiae Apg7p is a Protein- activating enzyme for multiple substrates including human Apg12p, GATE- 16, GABARAP, and MAP-LC3. *J Biol Chem*. 276:1701-1706.

Thumm, M., R. Egner, B. Koch, M. Schlumpberger, M. Straub, M. Veenhuis, and D.H. Wolf. 1994. Isolation of autophagocytosis mutants of Saccharomyces cerevisiae. *FEBS Lett*. 349:275-280.

Tsukada, M., and Y. Ohsumi. 1993. Isolation and characterization of autophagy-defective mutants of Saccharomyces cerevisiae. *FEBS Lett*. 333:169-174.

Varshavsky, A. 1996. The N-end rule: functions, mysteries, uses. *Proc Natl Acad Sci U S A*. 93:12142-12149.

Wang, C.W., J. Kim, W.P. Huang, H. Abeliovich, P.E. Stromhaug, W.A. Dunn, Jr., and D.J. Klionsky. 2001. Apg2 is a novel protein required for the cytoplasm to vacuole targeting, autophagy, and pexophagy pathways. *J Biol Chem*. 276:30442-30451.

Wang, H., F.K. Bedford, N.J. Brandon, S.J. Moss, and R.W. Olsen. 1999. GABA(A)-receptor-associated protein links GABA(A) receptors and the cytoskeleton. *Nature*. 397:69-72.

Wilkinson, K.D., M.K. Urban, and A.L. Haas. 1980. Ubiquitin is the ATP-dependent proteolysis factor I

of rabbit reticulocytes. *J Biol Chem*. 255:7529-7532.

Yamamoto, A., R. Masaki, and Y. Tashiro. 1990. Characterization of the isolation membranes and the limiting membranes of autophagosomes in rat hepatocytes by lectin cytochemistry. *J Histochem Cytochem*. 38:573-580.

Yamano, H., J. Gannon, and T. Hunt. 1996. The role of proteolysis in cell cycle progression in Schizosaccharomyces pombe. *Embo J*. 15:5268-5279.

Yeh, E.T., L. Gong, and T. Kamitani. 2000. Ubiquitin-like proteins: new wines in new bottles. *Gene*. 248:1-14.

Acknowledgements

I wish to express my deepest appreciation to Professor Yoshinori Ohsumi for constant supervision and encouragement through this study. I also wish to express my gratitude to Dr. Takeshi Noda for his extensive advice and profound discussion on my study. I am grateful to Professor Tamotsu Yoshimori for constructive advice and encouragement. I am also grateful to Drs. Yoshiaki Kamada and Noboru Mizushima for their proper advice and technical guidance. I thank to Drs. Takayoshi Kirisako and Naotada Ishihara for their technical advice and helpful discussion, and Professor Masato Umeda and Dr. Kazuo Emoto for their helpful suggestions and technical assistance.

I wish to express my appreciation to other members (and past members) of Ohsumi laboratory, Drs. Takahiro Shintani, Akio Kihara, Tkayuki Sekitho, Mitsuki Yoshimoto, Messrs. Kuninori Suzuki, Atsuki Nara, Hideki Hanaoka, Yoshinori Kobayashi, Jun Onodera, Hisashi Okada, Misses Yukiko Kabeya, Akiko Kuma, Maho Hamasaki, Shisako Shyoji, Fumi Yamagata, Mio Ito, Kumi Tsukeshiba, and Satsuki Okamoto,

I also thank to Professor Mariko Ohsumi and members of her laboratory.